UNIVERSITY OF PADOVA

Faculty of Engineering

Master Degree Course in Product Innovation Engineering

Master Thesis

Investigation of the influence from the manufacturing process and the resulting microstructures on the mechanical properties of biocomposites

Supervisors: Ch.mo. Prof. Marino Quaresimin

Prof. Bo Madsen

Author: Luca Pegoraro

Academic Year 2010-2011

SUMMARY

The interest in plant fibers as reinforcement for composites have been keeping on increasing thanks to the attractive mechanical properties that they exhibit, and the possibility of making more eco-friendly materials. At present several alternatives are coming out for commercial applications since fibers such as flax, hemp and jute show properties that make them suitable for load-bearing composite components, especially as substitute for glass-fibers. Several previous studies have demonstrated that the fully reinforcement potential of plant fibers can be exploited in bio-composites if an aligned fiber orientation is chosen. Based on these findings, flax yarn composites with an unidirectional fiber orientation were investigated in the present work. Mechanical tests were carried out to investigate the different tensile properties at different off-axis angles (0°, 30° and 90°) for composites with different fibre contents (30, 40, 50, 60 w%), different types yarn pre-forms (twisted and blended yarns), and different types of thermoplastic matrix (PET and PLA).

The influence of fiber content was investigated. Four different neat flax yarn composites with a matrix of PET were made with increasing fiber weight fraction. The experimental results have been compared with the results of a volumetric interaction model and a rules-of-mixture model. Data exhibit a good agreement with the model predictions. It was found that, with an off-axis angle of 0°, for composites with fiber volume fractions in the range 0.28-0.48, stiffness is in the range 16-21 GPa and ultimate strength is in the range 150-220 MPa. As the off-axis angle increases, the tensile properties decrease. With an off-axis angle of 90°, stiffness is in the range 2-3 GPa while ultimate strength is in the range 6-16 MPa.

Nowadays no plant fiber yarns are specifically made for reinforcement of composites, thus it was decided to study the effect of two types of pre-forms to investigate the influence of changing the composite microstructure. Therefore, in addition to neat flax yarns, two pre-forms (twisted yarns and blended yarns) were used in composite manufacturing to evaluate if the idea of mixing together plant fibers and matrix polymer in one single yarn is promising. The twisted is obtained by winding a flax yarn around a polymer matrix yarn, while the blended yarn is made up mixing intimately the flax fibers and the polymer fibers and then making a yarn. Referring to the twisted yarns, the yarn twisting angles with PET and PLA matrix are 10° and 8°, respectively. Referring to the blended yarns, the fiber twisting angles with PET and PLA matrix are 20° and 22°, respectively. For flax yarns the fiber twisting angle is 16°.

Observing the general trend of tensile test results, it can be stated that the blended yarns lead to lower composite mechanical properties. Referring to an off-axis angle of 0°, for composites with blended yarns stiffness is in the range 10-12 GPa and ultimate strength is in the range 90-110 MPa. The corresponding values of stiffness and ultimate strength for the neat flax composites, are in the range 18-19 GPa and 160-180MPa.It is believed that properties are lower than composites with neat flax yarns because of the poor fiber orientation in the blended yarn.

It cannot be stated that the twisted yarns provide a significant improvement of composite properties, since no marked differences have been observed with respect to corresponding composites with neat yarns. Referring to an off-axis angle of 0°, composites with twisted yarns stiffness is in the range 16-18 GPa and ultimate strength is in the range 150-170 MPa.

In bio-composites the matrix part takes also importance in an ecological point of view, therefore it was decided to use thermoplastic matrices (PET and PLA) thanks to their recycle ability, the absence of toxic byproducts in processing and, in the PLA case, for the possibility to obtain a completely bio degradable composite. Part of the study has consisted in the evaluation of the influence of matrix type on mechanical composites properties. With an off-axis angle of 0°, considering only twisted and neat yarns cases, the PET matrix composite stiffness is in the range 18-19 GPa, while the PLA matrix composite stiffness is in the range of 16-18 GPa, the PET matrix composite ultimate strength is in the range 170-180 MPA, whereas the PLA matrix composite ultimate strength is in the range 150-160 MPA. Altogether, even if PLA composite properties are a little lower than PET composite, the results point towards that the PLA could represent an effective alternative to PET.

The failure behavior of the composites was studied making a qualitative analysis basing on the images of fractured surfaces of the testing samples. It has been observed that most of the specimens show a marked transversal fractured surface with an off-axis angle of 0°. Composites with blended yarns are characterized by a fracture with a straighter edge, whereas the composites with twisted yarns show a fracture profile that is more jagged. The neat flax/PET composite with the higher fiber weight fractions don't show a delineated transversal fracture line because of the formation of several breaking points at different locations. With an off-axis angle of 30°, the fracture is 30° oriented and no notches have been observed. Only in the case of PLA matrix composites it has been observed that the fractured section is a little more irregular, and especially the composites with blended yarns exhibit a sort of concavity in the fractured profile. All the specimens with an off-axis angle of 90° are characterized by a failure that is almost orthogonal to the applied stress direction. Most of the samples didn't break into two separated parts, except the PLA composite with blended yarns

Finally, a micromechanical model has been developed by analyzing the geometrical configuration of the flax fiber in the composites, in order to back-calculate the mechanical properties of the fibers from the results of tensile composite tests. The model considers that the real fiber angle is different with respect to the yarn angle because of the twisting effect. The mean value of the back-calculated flax fiber stiffness was found to be 72 GPa, while the mean value of the back-calculated fiber strength was found to be 1700 MPa. Stiffness result is in agreement with the range obtained in previous studies (50-70 GPa), whereas the calculated ultimate stress seems to be slightly overestimated with respect to the range of 1200-1500 MPa estimated in previous studies. It is believed that more accuracy can be obtained by using the model combined with a FEM simulation.

PREFACE

This work represents a Master thesis carried out within the ERASMUS project for the Product Innovation Engineering Degree in Padua University (Italy). The research activity has been carried out at the Materials Research Division, Risoe National Laboratory for Sustainable Energy, Technical University of Denmark. The work was part of an European project, "Natural aligned fibers and textiles for use in structural composites" (NATEX).

The period of the Master thesis study has been lasting for 6 months, since August 2010 until January 2011.

The study has been supervised by:

Senior Scientist, Ph.D., Bo Madsen	Main supervisor
Professor, Marino Quaresimin	Main supervisor
Senior Scientist, Ph.D., Povl Brøndsted	Co-supervisor

I wish to thank my supervisors for the support given during the study period and for the opportunity of using professional equipment in the laboratories.

Furthermore, I would like to acknowledge Hans Lilholt for assistance in the study of the micromechanical model on the effect of a changed fiber orientation in the flax fibre/polymer yarns, Jacob Christiansen for the determination of the fiber content in twisted and blended yarns and for assistance in density measurement and use of compression moulding equipment, the technicians Frank Adrian, Eric Vogeley and Vagn Jensen for instructions on tensile-test operations, Preben Olesen for helping me with the optical microscope observations, Stergios Goutianos and Mustafa Aslan for helping me with the electron microscope observations, Tom Andersen for the support with the filament- winding operations and Christian Madsen for advices on composite grinding operations.

CONTENTS

1 INTRODUCTION

Today the research of more eco-friendly materials is getting more importance because of a growing environmental awareness, and therefore the interest in natural fiber reinforced composites keeps on increasing and they are beginning to be also seriously considered for industrial applications. Despite the high number of natural fibers in nature, only a few are suitable for industrial use. [1] In fact the natural origin of plant fibers results in a large variation in their properties, and this is conflicting with the constant quality of materials required by industrial production. So far the dominant position in the plant fiber market has been represented by cotton but actually its cultivation is characterized by a considerable environmental impact [2], therefore there are several alternatives that are coming out. The most promising plant fiber yarns commercially available at the moment are jute, flax and hemp yarns. The cultivation of these fibers requires a low consumption of fertilizers and pesticides in contrast to cotton [2], but the most important characteristic is given by their good mechanical properties that make it possible to use them in load-bearing composite components, being a substitute for especially glass-fibers.

Currently, the general industrial trend for biocomposites is giving more importance to a thermoplastic matrix, rather than a thermosetting matrix, because of the recycle ability, the faster processability (no time for curing is required), the more cheapness and the absence of toxic byproducts [3].

There are plenty of thermoplastic polymers derived from renewable raw materials which are available to meet the ecological purpose of biodegradability. The polylactic acid (PLA) is probably the most promising ecological matrix, since it shows properties that are close to the most widespread thermoplastic matrix of polyethylene terephtalate (PET) and polypropylene (PP).

The degree of adhesion between fibers and matrix is also a fundamental aspect that must be always taken account and investigated in biocomposite design, since it determines the stress transfer efficiency at the interface between the fibers and the matrix, which influences the final mechanical properties of composites. In addition, production of good quality natural fibers is strongly dependant on the environmental conditions during growing, as well as the conditions during fiber processing, e.g. harvesting, extraction, separation, refining and surface treatments [1].

At present, commercial available plant fiber yarns are not made for composites, but for textiles. Thus, work is needed to tailor-make the best plant fiber yarn for reinforcement of composites. This includes also to study if it is a good idea to mix the plant fibers and the matrix polymer in one yarn (a composite pre-form), and how to do it (twisted or blended).

2 OBJECTIVES

Basing on the above mentioned considerations in the Introduction, the overall objective of this study is to achieve a better understanding of the relationship between mechanical properties of bio-composites and their microstructure, focusing on the effect of using different types of reinforcement. Therefore composites were made using both neat natural fibers yarns and different composite pre-forms (twisted and blended yarns).

Particular attention has been given to the ecological matter, since a PLA matrix was used in order to be able to realize a completely biodegradable composite material. The investigation has been carried out making a comparison with the performances of PET matrix composites.

In this study flax yarn is chosen as reinforcement material in unidirectional (UD) composites and both PET and PLA were used as thermoplastic matrix, with the purpose of evaluate any differences in material behavior. In addition to the use neat flax fiber yarns, two different composite pre-forms were used: 1) twisted flax fiber/polymer yarn where the yarn was made by twisting the neat flax fiber yarn with polymer filaments, and 2) blended flax fiber/polymer yarn where the flax fibers and the (short) polymer fibers were first blended and then made into a yarn. The evaluation of the potential of these two flax fiber/polymer matrix yarns (twisted and blended) represents one of the main objectives of this study; this includes investigations of the influence of the fiber/matrix microstructure on the composite properties. If it is found that the twisted and blended yarns provide improvement of material behavior, it will represent the starting point for a further development of the fiber yarns pre-forms for composite applications.

A relevant part of this work consists in achieving a better understanding of biocomposite properties, investigating both stiffness and ultimate strength. The attention was focused on composites with an aligned fiber orientation. The experimental data of tensile tests of composites with variable fiber content were analyzed with the use of a volumetric interaction model developed by Madsen et.al (2004). [4] . Furthermore, the results of composites tested with different loading directions were analyzed by a developed micromechanical model which includes the effect of a changed fiber orientation in the flax fiber/polymer yarns. It was attempted to make a direct correlation between composite properties and fiber properties.

Finally, the failure behavior of the composites was studied making a qualitative analysis basing on the images of fractured surfaces of the testing samples to get further indications about the effect of fiber content, fiber/matrix microstructure and matrix type.

3 BACKGROUND

3.1 PLANT FIBERS

Natural fibers are completely or partially recyclable so they are candidates to replace the mineral reinforcement fibers, such as glass. They represent a renewable source and are carbon neutral since carbon dioxide (CO_2) emitted during production is reabsorbed by new plant growth [1]. Natural fiber reinforced thermoplastics are best suited for reuse thanks to the reduction of production waste and to the possibility of use them thermally after use, since the energy stored in the material can be used during combustion and no environmentally onerous pollutants are released [1]. Although natural fibers are fully recyclable by combustion, the same cannot be said for the synthetic polymeric matrix and chemical additives. However at the moment the most relevant drawback is probably represented by the hydrophilic nature of natural fibers. If left unprotected, they can uptake moisture, and swell in the process [5]. Cracking and delamination can also occur in the composite in case of incomplete impregnation of the fibers and wet storage in the material.

3.2 PLANT FIBER STRUCTURE

The term plant fiber refers to the plant cells having an elongated shape and a high aspect ratio (length/diameter ratio). Referring to flax, the fiber length is varying from 9 to 70 mm whereas the diameter range is from 5 to 38 μm. The aspect ratio is around 1750. Data are from Bledski et al. (2002). [6]

The structure of these cells is characterized by the presence of a rigid cell wall that is responsible for structural integrity and provides mechanical stability to the plant. Inside the fiber there is an empty central cavity, the so-called lumen, whose dimension varies considerably both within one fiber type and between different fiber types [3]. The cell wall is made up by three polymers having different molecular composition and structure: 1) cellulose, 2) hemicellulose and 3) lignin. Cellulose is a non branched polysaccharide constituted by several cellobiose units that are giving it a chain structure [3]. These cellulose chains are combined together into a microfibril having both of crystalline regions and amorphous regions whose ratio varies with the type of plant fibers. Hemicellulose is a heterogeneous group of polysaccharides which are non-linear, shorter and more branched than the cellulose. Finally, lignin is a highly branched phenyl based polymer having a very complex 3D structure that make its extraction process rather difficult [3].

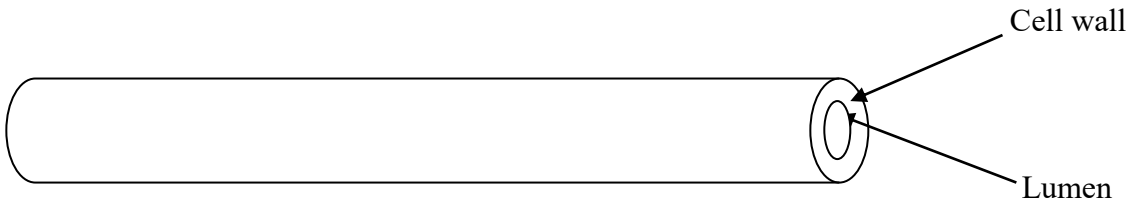

Figure 3.1 Drawing of a plant fiber.

Structure and chemical composition of natural fibers determine their properties. The more parallel the microfibrils are to the fiber axis, the higher is the fiber strength [3]. However it must be considered that there is a large natural variability both within a plant population and even within individual plants due to the location where the fibers are taken from. The most useful bundles are localized in the outer stem layers just beneath the epidermis, because in the inner part several dislocations and discontinuities are present and they can be responsible for degradation of properties. The degree of crystallinity is also an influential factor of the final characteristics [5] .

Figure 3.2 Flax: from plants to products

3.3 PROCESSING OF PLANT FIBERS

One of the aims of this study has been the evaluation of the twisting effect and the blending effect on the fibers properties thus both spinning and blending processes are explained, after having summarized the initial fiber process operations. [7]

3.3.1 Extraction

The further developed harvesting and processing technology now make it possible to adapt flax fibers to the corresponding uses, to obtain them with reproducible quality as well as to get a better cost efficiency production.

Flax fibers are extracted from the stem of the flax plant and are in the form of long fiber bundles called technical fibers. Each stem contains around 700-1400 technical fibers with a length of 0.5-1 m and it has an helical shaped cross section.

3.3.2 Opening

After the extraction further treatments are necessary, since the extracted fiber material is only partially separated into single fibers. The big reduction that needs to be done to the raw material can be clearly noted comparing the number of fibers in a length of yarn with the mass of fibers from which it had been made [7]. The first stage is denoted opening and it works separating the bales into smaller bunches. During opening a cleaning stage is also intrinsically carried out. There exist further treatments both mechanical and chemical to improve fiber separation as defibration and alkalization [8]. The first is achieved by carding, which keeps on the subdivision of tufts until each fiber is separated, while the second one is a chemical process made by means of an alkaline solution in order to degrade the pectins of the middle lamella [3].

3.3.3 Blending process

The blending process is one of the mostly used method to make better the processability, to improve the batch variability and to produce a material having characteristics unattainable from one single component [7]. Under a composite production point of view, the good mixing of matrix and reinforcement fibers might provide an improvement of mechanical properties, but particular attention must be given to the fiber orientation.

One of the distinctive characteristics of blending consists in the possibility of carry it out at different stages during processing. For instance, prior to impurity removal, bale mixing can be carried out, similarly during opening and cleaning, tuft blending can be performed. Further blending types as silver blending and roving blending can be carried out subsequently. The listed blending systems are different to each other depending on the principles involved. The main classification consists in four blending type: 1) stack blending, 2) batch blending, 3) direct continuous blending, and 4) silver blending [7].

The mostly used machineries to achieve a good quality blending process are the hopper blenders, and the in-line blending machinery.

Hopper blenders

In the hopper blenders several lattices are present. On the feed lattice fibers are placed, and by means of an apron lattice they are moved towards the inclined lattice. When they came into contact with the spikes of the inclined lattice, the fibers are lifted up and part of them is also worked by the evener roller. The amount of material allowed to progress is determined setting opportunely the speed of the different lattices. In order to improve the accuracy of material weigh, before the fiber output point a weigh pan associated with a control flap might be used. Another possibility to improve the blending quality consists in using the automated bale opening. In these system it has been tried to preclude the human error removing little clumps from bales of raw material. The installation of weigh pans achieve a further control of blend accuracy [7].

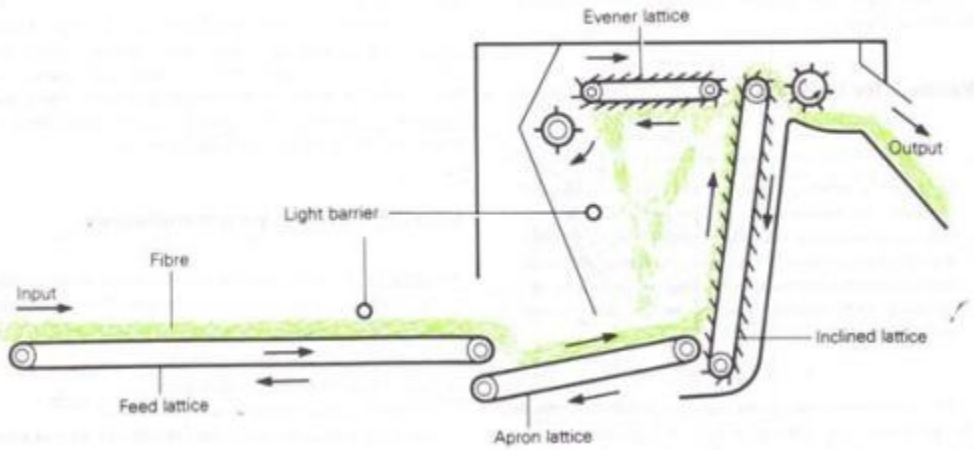

Figure 3.3 Hopper blender [7].

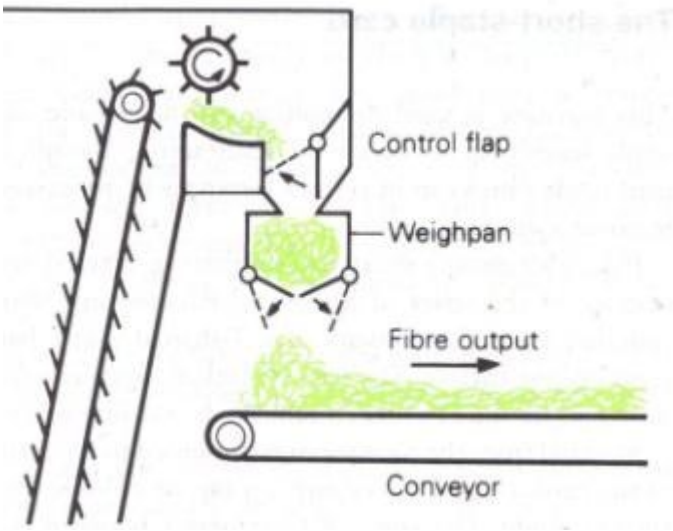

Figure 3.4 Hopper blender with weighpan [7].

In line blending machinery

These blending machines have been designed in order to create a delay during processing. The most common used machine is the multimixer whose blending chamber is divided in six or seven sections which are filled in sequence by the fibers coming from the top. The operation is completely automated in order to empty each compartment at the same rate by means of a roller that control the correct amount of feeding fibers [7] .

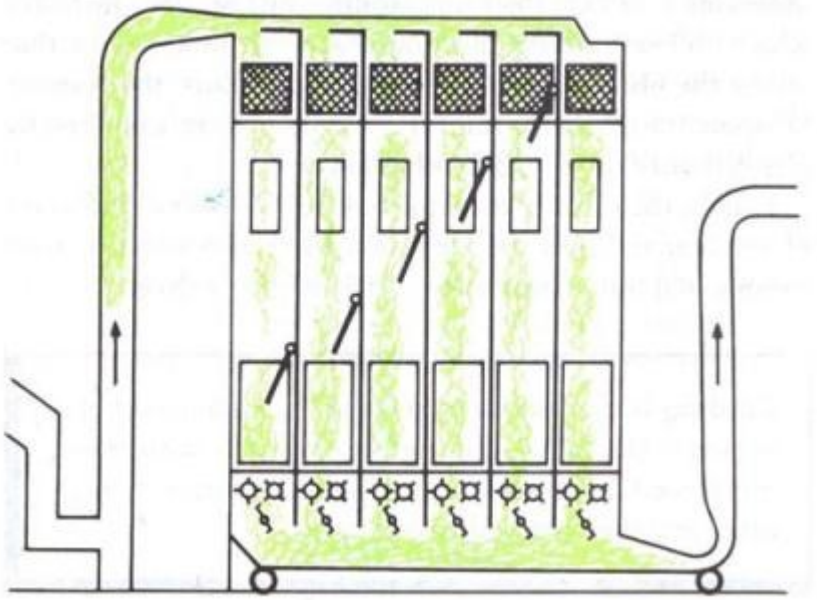

Figure 3.5 Blending chamber or an in-line blending machine [7].

3.3.4 Combing and drafting

With the purpose of improving yarn quality, regularity and fiber order are the most important features that must be investigated and taken in account. Combing and drafting are the two most used processes to improve fiber alignment and to make the fibers straightened [3]. A further effect is given by the reduction of linear density, since the number of fibers in the output material cross-section is lower than the number of fibers in the input material [7]. In both of these two processes there is a series of pinned rollers which provide to comb out the short and tangled fibers, and align the long ones. In drafting the rotational speed of the roller is furthermore increased in the forward direction, drawing apart the filament, so that the fibers move relative to each other, reducing the fiber linear density [3].

If filaments are slightly twisted, the twists are primarily located at thinner positions. When drafting is carried out, the fibers slide apart at locations of low friction (i.e. the thick locations of low twist), redistributing in this way the twists and improving the entire filament regularity [3], [9]. Other commonly applied methods to increase yarn regularity consist in adding a small amount of lubricating agents, as oil, prior the drafting process or soaking the fiber filament in hot water to soften the fibers. After combing it's necessary to reduce the irregularity present in single slivers with a process called drawing. It consists of combining a number of slivers and drafting them to produce a single sliver [7].

3.3.5 Spinning process

Yarn axial strength is correlated with the resistance to fiber slippage, therefore the insertion of twists is expected to be a good way to generate the forces necessary to prevent it [7]. Twists are inserted by rotating one end of a fiber bundle relative to the other end giving a spiral shape to the strand. Obviously the twist level is directly connected with the twisting angle: the smaller the twist level, the smaller the angle. In presence of small angle the fibers slip past each other if an axial tension is exercised, whereas with bigger angle the bundle results to be strengthened. If the tension is increased, the effect will be the breaking of single fibers [7]. Even if the twisting angle is more or less constant, the twist level varies along the axis. In fact it is function of the strand thickness as if the yarn diameter increases, the twist level decreases. The lowered twisting level makes the slippage easier [7]. Finally it can be said that the yarn diameter regularity is directly connected with the failure in case of applied stress, because the greater the variation in thickness along the axis, the greater the number of weak places with low twist level. In these parts, fibers are free to slide [7]. There exist several types of spinning process, the most used are the following:

Bobbin and flyer spinning

This method of twist insertion is based on the rotation of a flyer whose presser guides the material onto the bobbin surface. The flyers is driven at a constant speed to keep the twist level constant, as it inserts one turn of twist for each revolution. The speed is relatively low because of the risk of damaging the bundle and for the structure of the flyer assembly mounted on the spindle. Spindle speed range is between 800 and 1800 rpm [7].

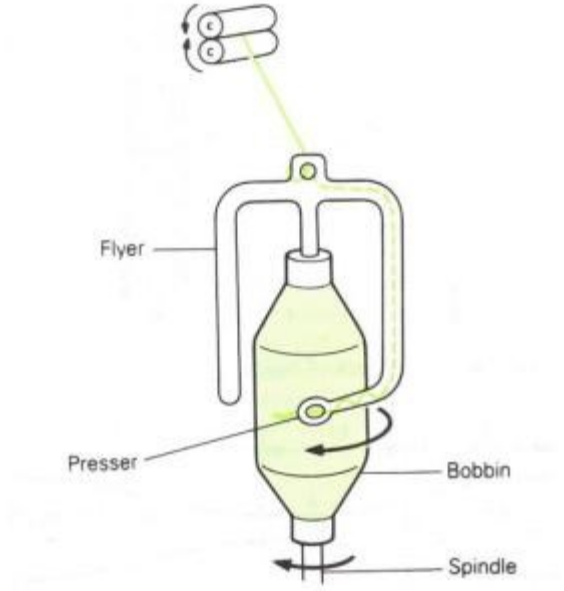

Figure 3.6 Flyer and bobbin method of twist insertion [7].

Ring spinning

In this mechanism a ring is positioned horizontally over a spindle which, during its rotation, drags a traveller (a little C-shaped item clipped to the ring edge) where the yarn passes in. Twisting and winding occur at the same time because the friction between ring and traveller reduces the traveller speed in respect to the spindle and consequently also its number of revolutions [7].

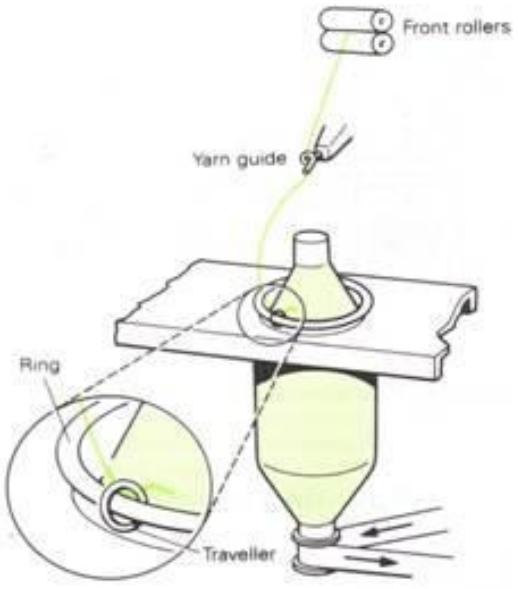

Figure 3.7 Ring twisting [7].

Self-twist spinning

In self-twist spinning two single yarns pass through two rollers that rotate in way to turn them first in one direction, then back in the opposite direction. The two bundles are guided through different paths in order to make the twist cycles in each strand out of phase. As the torque force in the material works to untwist the yarns ,but they are lying next to each other, it acts twisting them together. Since the resulting self-twist yarn can result to be too weak, a further twisting operation can be carried out producing a so called self-twist twisted yarn [7].

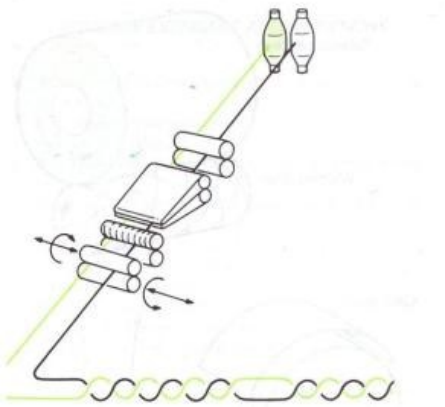

Figure 3.8 Self-twist spinning [7].

Wrap spinning

Wrap spinning method consists in leading the fibers through the centre of a rotating hollow spindle. This rotation causes the yarn wound around the twistless core of drafted fibers whereas a driving and traverse drum wound the bundle onto a cone [7].

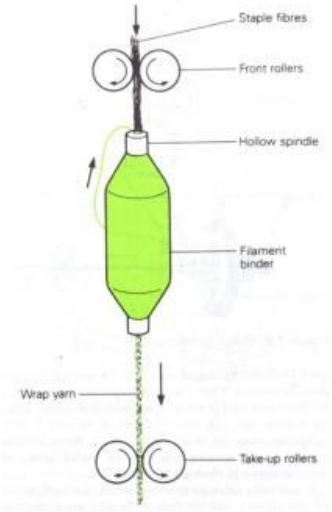

Figure 3.9 Wrap spinning [7].

Rotor spinning

In this process the separated fibers fed into the rotor. It represents the twisting element into of which a length of yarn is introduced in the reverse direction and is made rotate about its own axis by the centrifugal force. Twist is transferred from the yarn to the fibers when they came in contact and the fibers attaches to the rotating end of the yarn when it is withdrawn from the centre of the rotor. In order to succeed in setting up a stable continuous spinning system, the fibers speed in the output is as high as their fed rate [7].

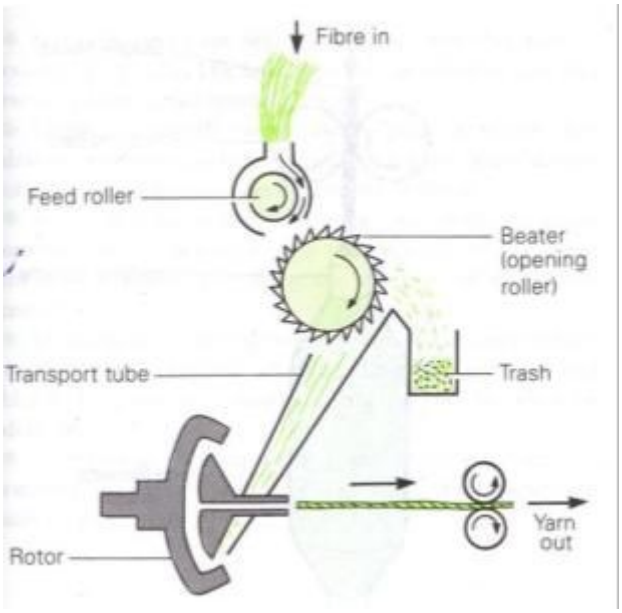

Figure 3.10 Rotor spinning [7].

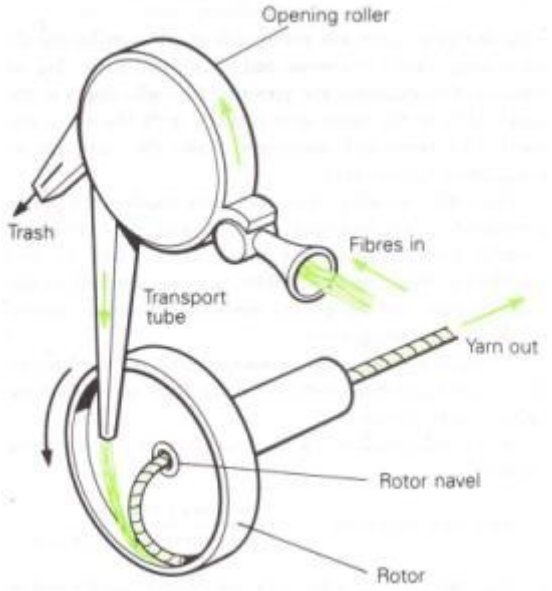

Figure 3.11 Rotor spinning unit [7].

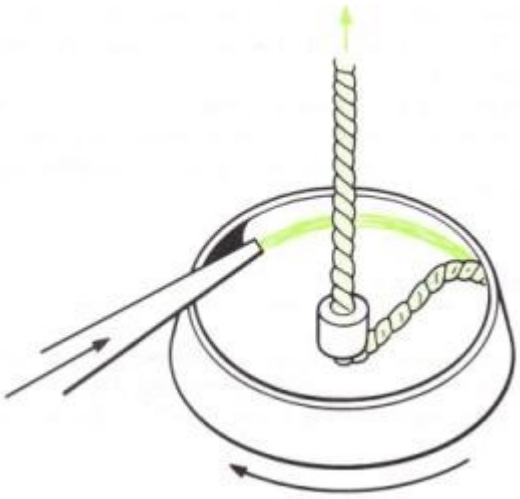

Figure 3.12 Yarn formation in the rotor [7].

Friction spinning

This method is similar to rotor spinning since the twisting element is common to both. In this case a pair of perforated rollers that rotate in the same direction insert twist. Fibers are sucked on their surface and rolled in their nip forming the yarn which is taken off and wound on to a bobbin [7].

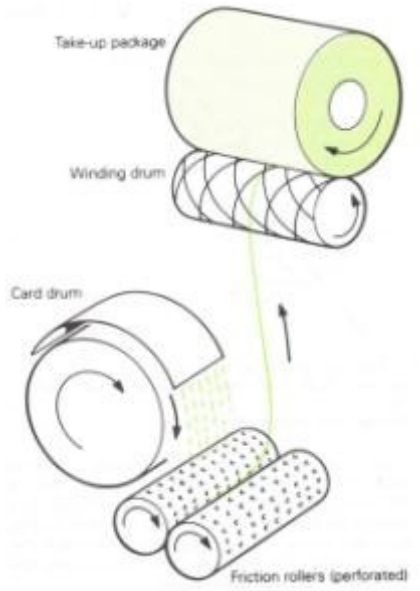

Figure 3.13 Friction spinning [7].

3.3.6 Mechanical properties of plant fibers

It is fundamental to underline that, for a given plant fiber type, both stiffness and strength values show large variations [1]. Each plant fiber can in fact be thought as a complex composite material made up of two-phases matrix and cell wall layers, and this complicate furthermore the study of mechanical properties [3]. The upper limits in the tensile performance of plant fibers are highly influenced by the level of bond energies between cellulose atoms, but there are several structural aspects that can influence both the stiffness and ultimate stress of fibers. The most important are: the cellulose content and its degree of crystallinity, the microfibril angle, and the presence of fiber defects, that affects the failure mechanisms [3].

In Table 3.1 typical reported tensile properties and microfibril angles are illustrated. It can be seen that flax is characterized by the higher stiffness value as well as the higher ultimate stress, besides it shows a small microfibril angle.

Plant fiber	Stiffness	Ultimate Stress	Microfibril angle
	(GPa)	(MPa)	(degrees)
Hemp	30-60	300-800	6
Flax	50-70	500-900	6-10
Jute	20-55	200-500	8
Sisal	10-25	100-800	6-25
Cotton	-	300-600	-
Softwood	3-50	100-170	3-50

Table 3.1 Microfibril angle and tensile properties of different plant fibers. Data for microfibril angles are from Gassan et.al.(2001), except data on softwood that are from Anaghnost et.al.(2002). Data for tensile properties are form Lilholt and Lawther(2000) [10] [11] [12] [3].

A further important consideration that must be done for the assessment of plant fibers properties is regarding the test length. It was found that the higher the test length, the lower the strength of the fibers, because of the raise of weak spots and imperfections within a single fiber [1] .

3.4 MATRIX MATERIALS

In this study polyethylene teraphthalate (PET) and polylactic acid (PLA) were used as composite matrix therefore their main characteristics and fields of use are briefly described.

3.4.1 PET (polyehthylene terephtalate)

Within the engineering thermoplastics, polyesters constitute one of the most relevant category thank to their particular properties that make them a very suitable material for industrial applications. PET is probably the most important representative of the group. It belongs to the polyesters since its structure is characterized by the presence of one polyester functional group. This group has a polar carbon-oxygen double bond but it gives a very small polar component, considering that it is only a little percentage of the whole molecule, hence moisture absorptivity is low giving good electrical properties that have led to several applications such as electrical switches and connectors.

The excellent PET mechanical properties are to a great extent due to orientation effect obtained from stretching during the processing. Afterwards the orientation is locked in place by the crystallinity, even if crystallization is slow and it can reach difficultly values higher than 50%. However cristallinity slowness doesn’t represent a drawback since it is well compensated by the

medium viscosity that helps processing. PET stiffness is around 2.7 GPa and it shows very good dimensional stability over a wide range of moisture, but however it needs to be dried before molding because small amounts of moisture could react with the melt degrading mechanical properties.

At the moment the success is due in large part to the acceptance of PET as best resin in the market of soft-drink container and high-performance films, thank to its low cost and the low permeability to carbon dioxide. It is also used as insulative material for winter coats and as fiber reinforcement in tyres since it is used as nylon substitute when water is likely to be present during material exercise. Because of its high operation temperature capability, PET is also used as sterilizable packaging for medical applications.

3.4.2 PLA (polylactic acid)

One of the more noteworthy material suited to biocomposites manufacturing is certainly polylactic acid. It is obtained by the fermentation of lactic acid, which can be extracted from acrylonitrile as well as with biotechnical production. Polylactides are fully biodegradable since the material disappears within 3 to 4 weeks if composted with other biomass that can achieve hydrolysis to lactic acid [1]. Despite their advantages however there are considerable drawbacks which still need to be overcome, as high price and moisture sensitivity.

Generally polylactic acid needs to be reinforced with fibers to enhance termal stability, but processing temperature must not exceed 200°C to avoid thermal degradation [1] . The drawback of the thermal properties can therefore be overcome by mean of the addition of flax fibers [1].

It can be said that polylactide polymer is stiff but brittle, in fact the tensile strength exceeds 60 MPa but plasticizers are needed to improve elongation and impact properties. It was demonstrated that the use of plasticizers as triacetin can increase the elongation to over 300% with a tensile strength of 40 MPa even if it might decrease strength and stiffness of pure PLA and PLA/flax composites because of the consequent change of fiber structure [1].

PLA has many promising markets thanks to its biodegradability that makes it one of the best candidates for substitution of PET. At the moment the typical utilizations are represented by plastic bags for household bio waste, barriers for sanitary products and diapers, planting cups, disposable cups, plates, and several items for orthopedics and medicine as sutures, screws, nails, and plate for bone fracture fixation [1]. PLA based composites could also be a possibility for automotives interior panels. [1]

3.5 FIBER/MATRIX INTERFACE

The matrix/fiber compatibility gives indications about how much the fiber and matrix parts are close each other. This represents a fundamental point for stress transfer and thus, for the mechanical properties of composite. In the case of plant fibers (hydrophilic) and thermoplastic matrix (hydrophobic) the compatibility is low so the adhesion is restricted, confirming that the surface polarity of the two parts governs their interactions [3].

Several methods based on chemical or physical treatments are available to enhance matrix/fibers interaction. By means of acetylation, for example, it's possible to make the fibers less hydrophilic promoting interatomic fiber/matrix adhesion by van der Waals forces [3]. In contrast, coupling agents as maleic anhydride can improve the mechanical properties creating stronger bonds between fibers and matrix [13].

It has been demonstrated that with aligned fibers, the tensile properties are much higher and the obtainable fiber volume fraction is also increased. Furthermore in this way the use of chemical additives is avoided [3]. From the opposite point of view it can be stated that reducing the fiber/matrix bond strength, the load transfer between fibers and matrix drops notably, therefore the lower is the bond strength, the lower is the matrix deformation since it's easier that failure occurs at the interface [14].

3.6 COMPOSITE POROSITY

The properties of natural fibers reinforced composites are highly dependent on porosity since it can act as a local weakness with a deleterious effect on mechanical properties, especially on tensile stiffness. It is accepted that the porosity of a component should not exceed 1% for high performance laminates but levels up to 5% can be tolerated for modest performance applications [14].

Several factors can increase the amount of porosity. The complexity of the surface chemistry and the irregularity of both form and dimensions of plant fibers is one of the most important aspects in addition to the presence of luminal cavities. Furthermore porosity is also affected by the applied processing techniques [4].

3.7 COMPARISON BETWEEN PLANT FIBERS AND GLASS FIBERS

In the fiber composite design, using a materials selection criteria based on weight, it has been pointed towards that there exist two main competing candidates: glass fibers and plant fibers. It has been demonstrated that mechanical properties of vegetable fibers may successfully compete with the glass fibers ones and, furthermore, they show higher elongation to break than glass and even of carbon fibers. Another advantage of natural fiber is correlated to their thermal properties in fact their low thermal conductivity (0.29-0.32 W/mK), allow them to be used also as thermal barrier.

One of the most important parameter among the selection criteria is obviously the fibers strength. The absolute value for natural fibers is notably below the level of glass fiber (as it can be seen in Table 3.2) so the ultimate stress needs to be somehow improved. Things change thinking in terms of specific fiber strength, considering that the mean natural fibers density (1.5 g/cm^3) is about 40% lower than the glass fibers density (2.6 g/cm^3) [3]. In this case comparison is possible and in some instances natural fibers properties could exceed fiber glass ones. Basing on the experimental values obtained so far, it seems that the stiffness of glass fibers is slightly higher than the highest plant fibers one, in fact the values are respectively about 75 GPa and 65 GPa [3].

In a study of Madsen [3] it was shown that if a composite component compliance is fixed, its thickness will be the largest for plant fibers composite (see Figure 3.14 A for details) but its weight will be below the glass fibers one, beyond a given threshold. It is possible to see in Figure 3.14 B that the threshold is V_f= 0.10 with random fibers orientation and V_f=0.14 with unidirectional fibers orientation, and that the weight component reduction is more emphasized in composites with a random fibers orientation. To go into more depth the ratio between material stiffness and material density could be used. It's denoted the specific stiffness and it's usable for components loaded in pure tension. It has been found that calculating specific stiffness with a plant fiber stiffness of 50 GPa instead of 65 GPa, the threshold above of which plant fiber composites are superior to glass fiber composite in respect of component weight, changes from 0.14 to 0.55 [3]. This demonstrates that if the plant fiber stiffness decreases, that is more probably in respect with keeping on the maximum value, the threshold V_f increases. Figure 3.15 shows the relationship between plant fibers stiffness and threshold V_f of composites with random and unidirectional fiber orientation, demonstrating how the lower limit of stiffness for random fiber orientation is higher (55 GPa) than the aligned composite one. In Figure 3.16 the trends of glass fiber composite stiffness and cellulose fiber composites stiffness are shown. [15]

Because of it, the percentage of natural fibers must be higher than that of glass fibers in order to achieve comparable properties. However the weight of natural fiber reinforced parts remains still lower than glass fiber reinforced parts [5].

Regarding the impact strength, glass fiber composites are better than vegetable fiber ones, in fact the natural reinforced plastics value lies below the typical limits of glass fiber materials.

Furthermore there are interesting issues for natural fibers regarding the advantages of not causing allergies and skin irritation [1], differently from glass fiber dusts. In fact it has been observed that when fiber particles are inhaled, there's no risk to human health [5].

The cost of raw fibers is lower for the flax fibers (more or less half of the glass chopped strands), whereas in the semi-products market, glass is more convenient since a glass roving costs about 4/5 times less than a flax yarn. This is due to the high quality required by textile products. However it must be said that a composite reinforcement purpose required an adjustment of the processing method, and probably it can result in reduction of the semi-product cost [3]. Market prices are referring to the following suppliers: Owens Corning (CA), for glass chopped strands and glass roving, Bio-7-Fibers (DK) for flax raw fibers, and Linificio e Canapificio (I) for flax yarns.

From an ecological point of view there exist also additional advantages since the energy consumption to produce a natural fiber mat (9.7 MJ/kg) amounts to just less than one-fourth of the energy required to produce a glass fiber mat(54,8 MJ/kg) and at end of life the material is biodegradable [16].

Finally it must be said that actually only little experience has been accumulated in regard to the recyclability of plant fiber composites. In fact the risk of deteriorate their mechanical properties with repeated thermal exposure must be treated differently from glass fiber composites, which can be recycled simply by remoulding used parts .

Fiber type	Fiber orientation	V_f	Stiffness	Ultimate stress	Reference
			(GPa)	(MPa)	
Hemp	Random	(W_f=0.4)	2.7	33	Mishra et al.(2000)
	Aligned	0.48	27.6	277	Madsen (2004)
Flax	Random	0.14	3.4	36	Hornsby et al.(1997b)
	Aligned	0.51	28.7	288	Madsen (2004)
Jute	Random	0.30	5.2	40	Andersen and Plackett (2002)
	Aligned	0.50	27.2	225	Roe and Ansell (1985)
Wood	Random	0.27	4.2	28	Clemons (2000)
	Aligned	0.27	4.2	52	Clemons (2000)
Glass	Random	0.20	5.4	77	Oksman (2000)
	Aligned	0.60	45.0	1020	Gamstedt et al. (1999)

Table 3.2 Typical reported tensile properties of most important biocomposites. For means of comparison also properties of glass fiber composites are reported. From Madsen (2004) [3].

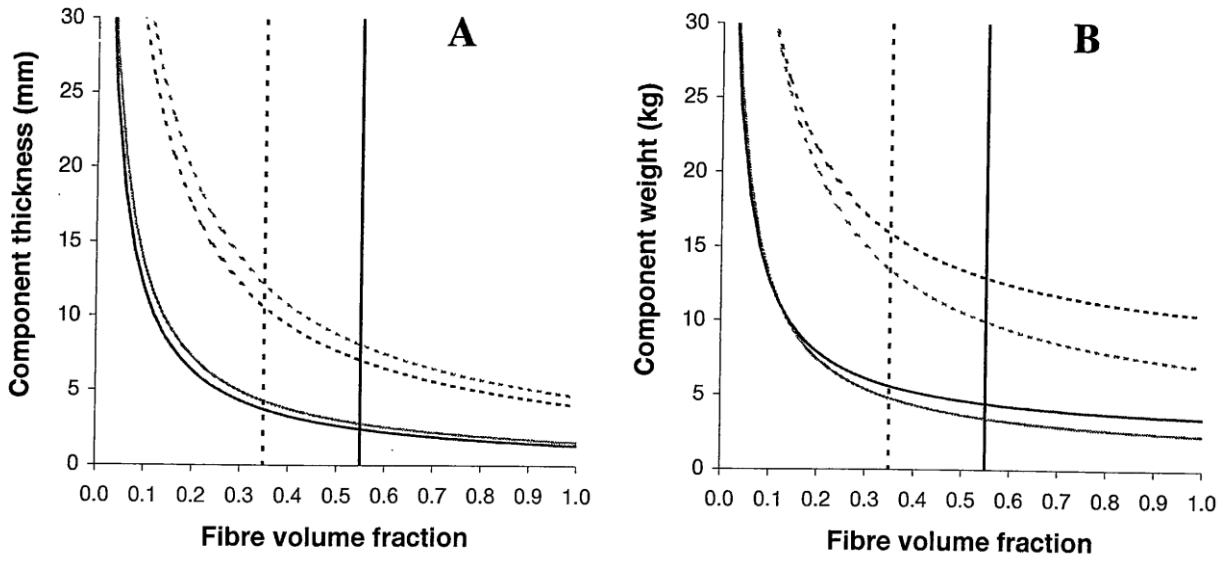

Figure 3.14 The required thickness (A) and weight (B) as a function of V_f for a square composite component having 1x1 m^2 dimensions and with a compliance of 0.01 m/GN. The full lines indicate an UD fiber orientation whereas the dotted lines are referred to a random fiber orientation. In the thickness char the line above represents the plant fiber composite, while the line below represents the glass fiber composite. Because of the lower natural fiber stiffness, it can be seen that the required component thickness is largest. The reciprocal position of the two lines in the char B is the opposite, showing the advantage of using plant fiber composites under the weight point of view. From Madsen (2004) [3].

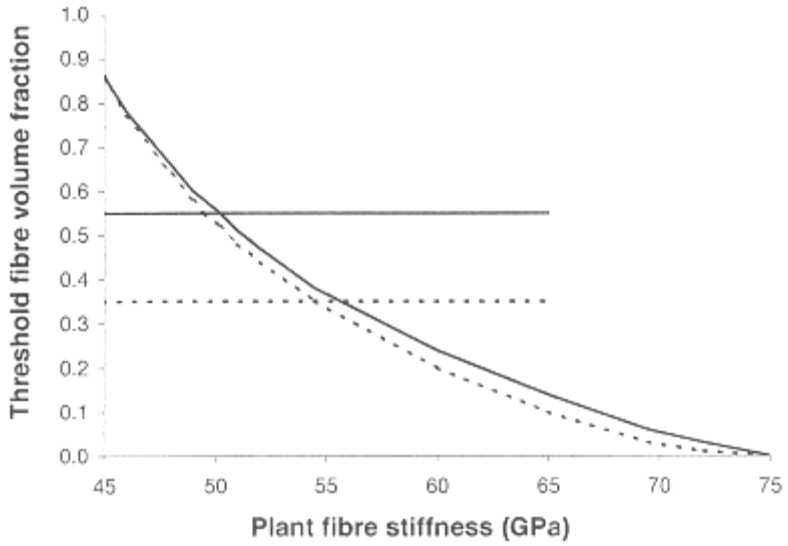

Figure 3.15 Relationship between plant fiber stiffness and threshold Vf of composites with random (dotted line) and unidirectional(full line) fiber orientation. Horizontal lines represent the maximum obtainable Vf in composites with the two fiber orientations. From Madsen (2004) [3].

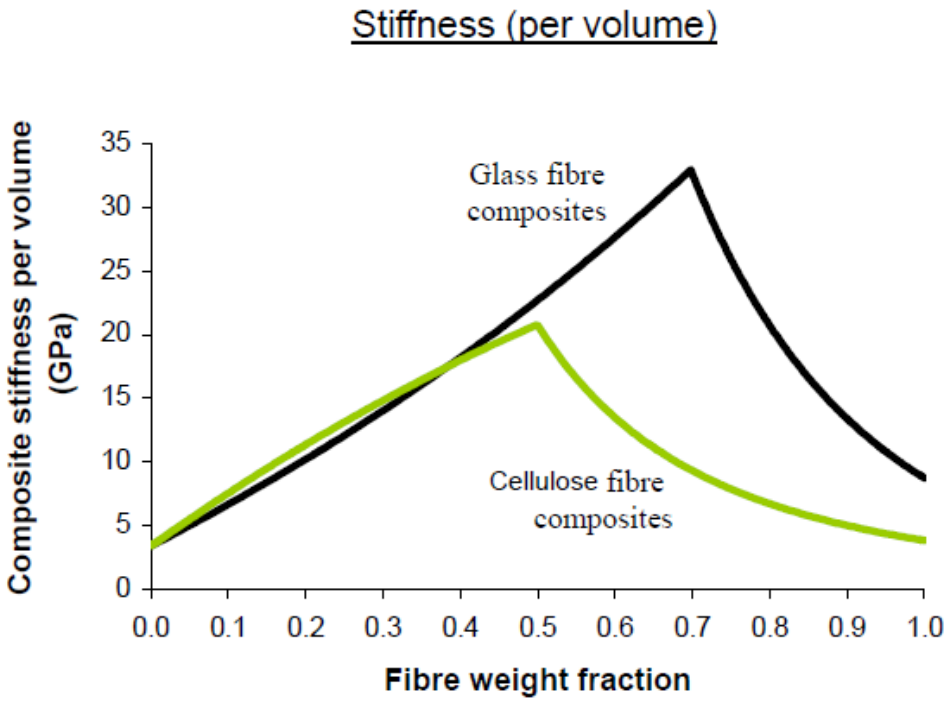

Figure 3.16 Trends of stiffness per volume values referred to both glass fiber composites and cellulose fiber composites [5].

3.8 APPLICATIONS

At the moment the interest in natural fiber composites, especially with flax fibers, is growing , especially regarding sportive applications. Some articles are already available on the market, whereas other products are still in a prototype phase to evaluate the effective improvement offered by this type of material. Some interesting examples of biocomposite applications are reported in the following figures and tables.

Figure 3.17 "World first formula 3 car" represents one of the most interesting application of biocomposite and recycled materials [17].

Component	Material
Frame	Vegetable fibers
Steering wheel	Resin derived from carrots
Front wing	Flax fibers.
Seat	Flax fibers, foam soybean oil and recycled polyester fabric
Aerodynamic element of the suspension	Woven natural fiber composite
Tyres	Elimination of polycyclic aromatic compounds
Shell mirrors	Potato starch and flax fibers
Engine cover	Carbon Fiber Recycled
Shock adsorbers	Carbon fiber recycled

Table 3.3 List of ecological components used in "World first" formula 3 car. Performances of this prototype are absolutely comparable with the characteristics of "normal" formula 3 car used so far, demonstrating how the vegetable fibers, and other recycled materials can be used as substitutes of less eco friendly materials [17].

Figure 3.18 Example of future design from the French society DCS (Design Composites Solution). These chairs and table are obtained by a particular molding process for thermosetting resins that allow to use flax fibers as composite material [18]

Figure 3.19 The Belgian framemaker Museeuw has been creating a new carbon hybrid composite made up by flax fibers and ultramodern carbon fibers. The new material is thought to have exceptional shock adsorbing capabilities, demonstrating how flax fibers can be useful also as further reinforcement in already existing high performance composites [19].

Figure 3.20 Rossignol made the first flax fiber ski called "Attraxion 3 Echo" to exploit the lightness and the handiness offered by this material [20].

Figure 3.21 A collaboration of Canadian car manufacturers (Now Project Eve), is developing a prototype for an electric car with a hemp body called the Kestrel. With the exception of the structural frame, all the traditionally metal components will be replaced with a hemp-fiber composite [21].

Component	Material
Glove box	Flax/sisal, wood/cotton fibers molded
Door panels	Flax/sisal/wood fibers with epoxy resin/UP matrix
Instrument panel support	Wood fiber molded material
Seat coverings	Leather/wool backing
Seat surface/backrest	Rubber hair (coconut fiber/natural rubber)
Seat backrest panel	Cotton fiber
Trunk panel	Cotton with PP/PET fibers
Trunk floor Kombi	Laminated wood
Insulation	Cotton fiber
Molding rod/apertures	Wood
Floor panels	Flax

Table 3.4 List of Mercedes-Benz auto motive parts containing plant fibers [1].

Car model	No. of plant fiber parts	Weight
		(kg)
Mercedes-Benz C Class (2000)	33	22.0
Mercedes-Benz S Class	32	24.6
Mercedes-Benz E Class	21	20.5
Mercedes-Benz A Class	27	11.9
Mercedes-Benz C Class (1992)	30	18.3
Travego	3	12.3
TopClass	3	14.1
BMW Series 3		12.0
Audi A4		10.0
VW Passat		2.0
Audi A4		1.5

Table 3.5 Vehicular use of plant fibers reinforced materials [1].

4 MATERIALS

4.1 YARNS USED

Two special kinds of yarn were used in composite manufacturing in order to evaluate the effect of microstructure changes on the mechanical properties of composites. They are two composite pre-forms, indicated as twisted yarns and blended yarns. The twisted is obtained by winding a flax yarn around a polymer matrix yarn, while the blended yarn is made up mixing intimately the flax fibers and the polymer fibers and then making a yarn. Images of the two pre-form are shown in Figure 4.2 and 4.3. Blended yarns and twisted yarns were supplied respectively by EKOTEX (PL) and BRIERLY (UK). The two companies are partners in the EU project called NATEX. Since the nominal weight ratio of both the composite pre-forms was fixed to 50 %, but composites with a fiber weight fraction different from 50% were required for this study, it was also necessary to use additional neat polymer yarns (PET and PLA) in composite manufacturing. In addition to the two pre-forms, neat flax yarns were used (see Figure 4.1). They were supplied by EKOTEX (PL).

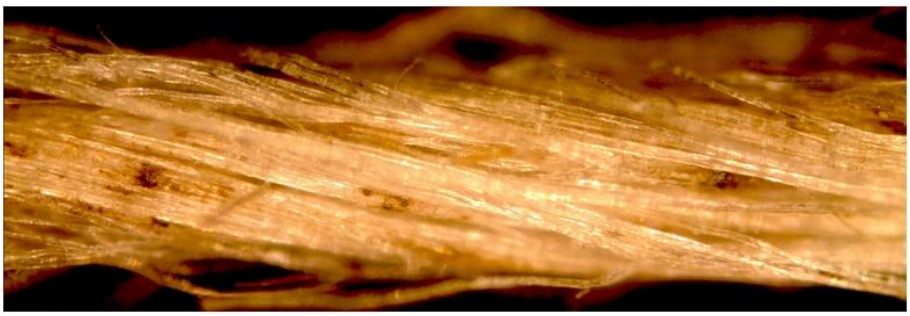

Figure 4.1 Example of neat flax yarn.

The pre-form that were used are the following:

Type of composite pre-form
Twisted flax/PET yarn
Twisted flax/PLA yarn
Blended flax/PET yarn
Blended flax/PLA yarn

Table 4.1 List of pre-forms used

The twisted flax/PET yarn is constituted by a flax yarn winded around two PET filaments having 56 tex as linear density (see Figure 4.2), whereas the twisted flax/PLA yarn is made up of 3 PLA filaments having a linear density of 22.5 tex and 2 PLA filaments having a linear density of 15 tex.

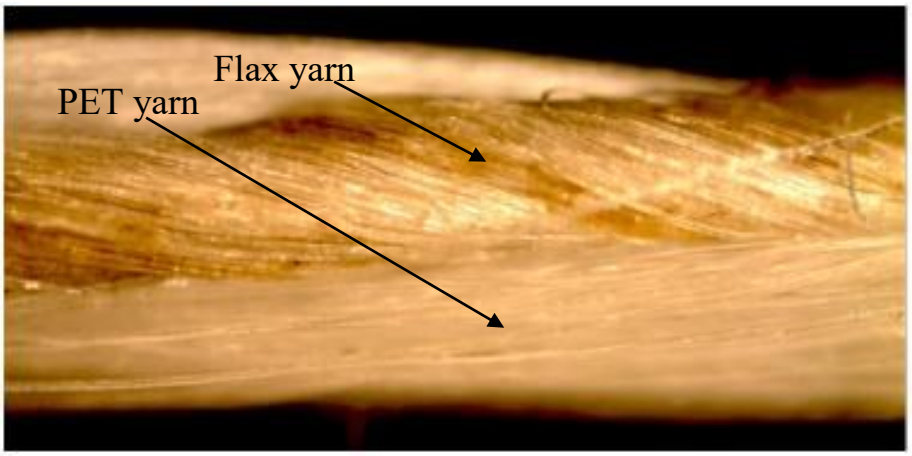

Figure 4.2 Example of twisted flax/PET yarn. Visible are the two different wounded yarns. Close up there is the flax yarn, whereas on the background the PET filament can be seen.

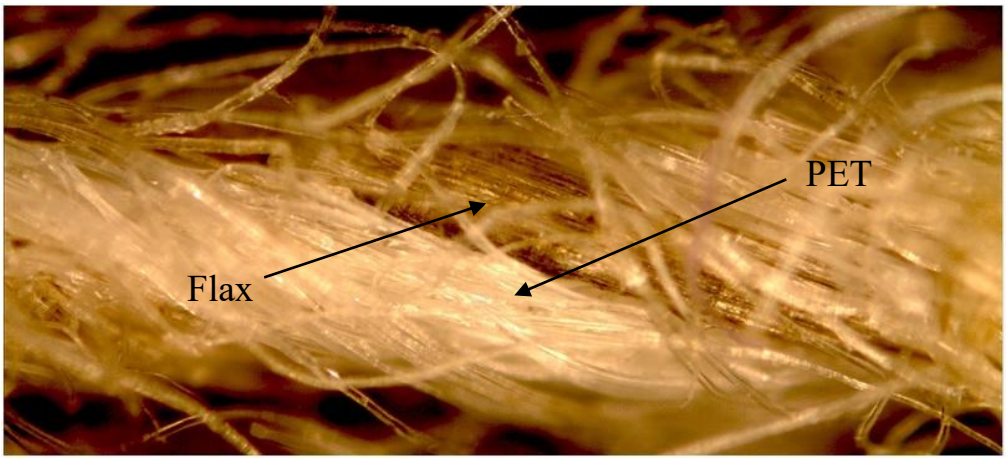

Figure 4.3 Example of blended flax/PET yarns. Visible are the two constituents (the dark one is flax, the white one is polymer) and their high level of mixing.

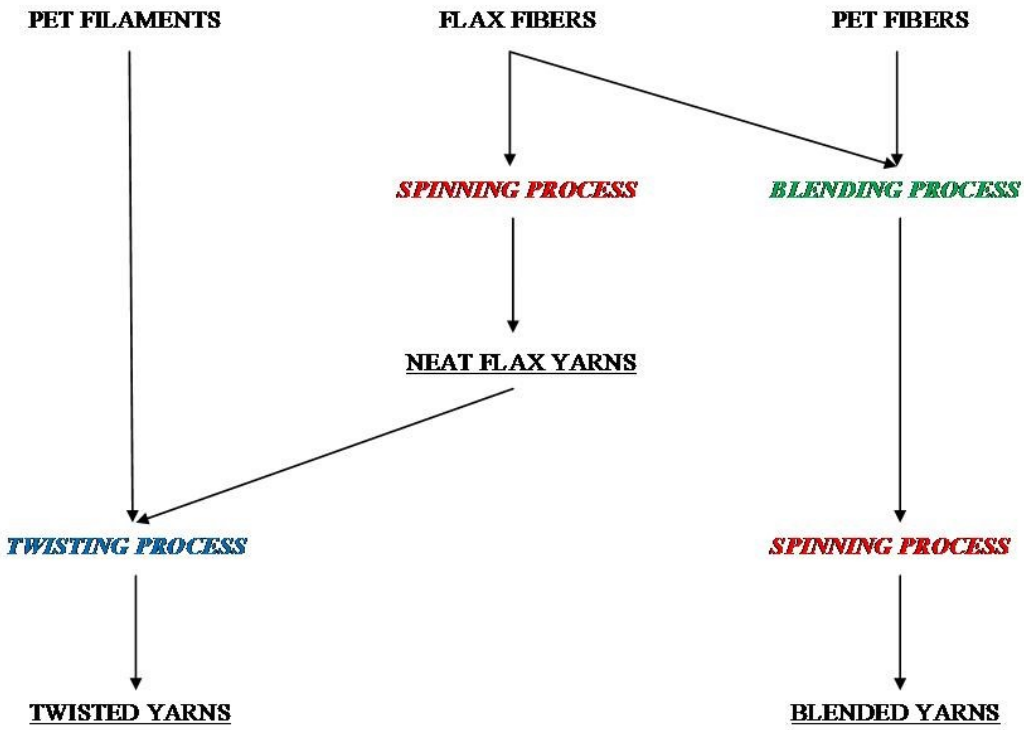

Figure 4.4 Methods for fabrication of the used yarns.

It should be considered that the real linear densities of the pre-forms yarns and the neat flax yarn are slightly deviated from the nominal values given by the suppliers. Therefore, the real values were measured to achieve a more correct evaluation of weight fiber fraction in the composites. Yarn samples having a length of 10 m were cut for each type of yarns, were weighed and put in vacuum chamber (0.9 mbar, 20°C) for 24 hours so that the measured tex values are closer to the dry yarn linear density in the composite. This analysis was not carried out for neat polymer yarns since their nominal linear densities have been considered correct. Nominal linear densities, and measured linear densities for the different yarns, before and after the vacuum chamber treatment, are reported in Table 4.2.

It was considered that the real values of the fiber content could be somehow different in respect to the indicated value of 50%. Thus it was decided to carry out a chemical analysis where the matrix part was dissolved by a organic solvent (chloroform for PLA and hexafluoropropanol for PET) in order to obtain a more accurate value of weight ratio. As expected, the experimental results prove this disagreement since the nominal weight content of 50% is slightly overestimated for PLA composites, both with twisted and blended yarns, whereas it is slightly underestimated for the corresponding PET composites. Measured weight content of the two types of yarn are reported in Table 4.2

Type of yarn	Supplier linear density	Measured linear density before vacuum treatment	Measured linear density after vacuum treatment	Supplier fiber weight content	Measured fiber weight content
	(tex)	(tex)	(tex)	(%)	(%)
Twisted flax/PET	220	227	222	50.0	51.5
Blended flax/PET	200	174	170	50.0	54.4
Twisted flax/PLA	220	220	215	50.0	47.9
Blended flax/PLA	200	195	190	50.0	45.9
Neat flax	110	109	104	100.0	
Neat PET	56				
Neat PLA	23				

Table 4.2 Theoretical tex values are furnished by suppliers, while experimental tex values are obtained from 10m of yarn weighed by a balance having an accuracy of 0.0001g. Experimental weight fiber fractions were experimentally obtained my means of a chemical analysis.

4.2 MANUFACTURING OF COMPOSITES

All the produced composites in this study were made by means of commingled filament-winding to make fiber/matrix unidirectional yarn assemblies, followed by vacuum heating, and press consolidation.

4.2.1 Filament winding

To mix properly the fibers and the thermoplastic matrix before they are processed into composites by compression moulding, the commingled filament winding process was chosen since it presents several advantages in respect with other technologies as film stacking. Indeed the uniformity of the spatial distribution of fibers in composite cross section is excellent, and the impregnation distance of the matrix is reduced thanks to the intimate mixing, reducing the amount of porosity that would be created during the process. Furthermore there no exists a lower limit regarding the fiber volume fraction and the time consuming is low since only one operation is required to make the panel. All composites has been made using a custom built filament winding

machine in order to produce unidirectional fiber configurations. The bundle of filament fibers is fastened on a rectangular frame (300 mm x 490 mm) that is fixed on a rotating mandrel. The bundle is pulled through a pulleys-path in order to get the right tension. The mandrel rotates while the carriage with the pulleys moves horizontally, laying down fibers in the desired pattern. The tension of the filament can directly affect the void content and fiber volume so it has to be carefully controlled. The amount of applied tension depends also on the fiber material, part size and the pattern that is being wound [22].

The four required filament-winding control parameters are the start and end positions for each layer, the numbers of turns required for each layer, and the number of layers. These parameters were calculated by mean of the ratio between the width of the frame and the parameter s. This parameter indicates the sideward movement mm/turn. The number of layers L and the value of sideward movement per rotation s, represent the controlling parameters in order to have a thickness of the panels as close as possible to 2.5mm. Based on the desired volume fractions, and by knowing the fiber and matrix densities, the total composite density can be estimated by using the rule of mixture (see equation 4.1). Since this density has been obtained, it is possible to calculate the total area, so that the panel thickness can be predicted by means of equation 4.3.

$$\rho_c = V_f\rho_f + V_m\rho_m \qquad 4.1$$

$$A = \frac{(tex_f + tex_m)}{\rho_c} \qquad 4.2$$

$$t = \frac{2AL}{s} \qquad 4.3$$

where ρ_c is the composite density and A represents the area of the panel.

Both the number and the type of made composites had to be chosen with the purpose to be able to make comparisons between properties of PLA composites and PET composites, and to evaluate the effect of using either twisted yarns or blended yarns. Moreover it was decided to carry out an analysis focusing on mechanical behaviour of neat flax yarns reinforced PET composites with variable fiber content. Therefore it was chosen to produce 9 different types of composites, whose specifications are presented in Table 4.3. At the beginning the fiber weight fraction (W_f) to investigate was chosen to be 0.50 (since this is the W_f of the pre-form yarns), but by means of simple observations of the manufactured composite panels using the light table, it was seen that the porosity content was too high, so it was decided to focus on composites with a lower fiber weight fraction (of about 0.4), except for the case of neat flax fiber yarn with PET where the effect of fiber content was studied by making four different composite panels with 4 different nominal fiber

weight fractions (0.3, 0.4, 0.5, 0.6). In all the work, reference will be made to these nominal fiber weight fractions, to identify easily the different composite types. All composites have a unidirectional (UD) fiber orientation.

To determine the nominal value of the fiber weight fraction (W_f) and the nominal value of the fiber volume fraction (V_f) of composites, the following equations were used:

$$W_f = \frac{no_f \, tex_f}{no_f \, tex_f + no_m \, tex_m} \qquad 4.4$$

$$V_f = \frac{no_f \frac{tex_f}{\rho_f}}{no_f \frac{tex_f}{\rho_f} + no_m \frac{tex_m}{\rho_m}} \qquad 4.5$$

where no is the number of yarn threads in winding process, ρ is the density, and the subscripts m and f denote respectively matrix and fibers. It must be observed that these two formulas provides "nominal" values of W_f and V_f that probably are different with respect to the measured values (see section 6) since no porosity effect is considered in the calculation of the nominal values.

Concentrating first on PET composites, for a given type of them, the linear densities are known parameters, while the numbers of yarn threads must be chosen subsequently in order to make the fiber weight fraction as close as possible as 40%. In this way the value of fiber volume fraction is consequently calculated by means of densities. Once the PET composite variables have been fixed, to manage to compare the corresponding PLA composites, the variables no_m and no_f must be investigated focusing on V_f instead of W_f, since the composite properties are governed by the fiber volume fraction. Therefore, for a given PET composite type, they have to be chosen in way of make the value of volume fraction of the corresponding PLA composite as close as possible to the PET composite one previously calculated.

To simplify the fiber volume fraction and fiber weight fraction calculations, when equation 4.4 and 4.5 were used for the twisted and blended yarns, the number of yarn threads was set equal to 1, both for the fiber yarn and for the matrix yarn, while the corresponding yarn tex values were modified in the following way: the total tex value of the yarn obtained experimentally, was multiplied by the weight fiber content in order to get the tex value of fibers; differently, the matrix tex value has been worked out as sum of the contribution of the neat polymer yarns used (with the nominal tex values reported above) and the difference between the total tex value of the yarn and the corresponding fiber tex value previously calculated. Results are shown in Table 4.4.

Composite	Number	Matrix type	Reinforment type	Additional polymer yarns	W_f
Twisted flax/PET	1	PET	2 twisted yarns	2 neat PET yarns	0.41
Blended flax/PET	2	PET	1 blended yarn	1 neat PET yarn	0.41
Neat flax/PET 30%	3	PET	1 neat flax yarn	4 neat PET yarns	0.32
Neat flax/PET 40%	4	PET	1 neat flax yarn	3 neat PET yarns	0.38
Neat flax/PET 50%	5	PET	1 neat flax yarn	2 neat PET yarns	0.48
Neat flax/PET 60%	6	PET	2 neat flax yarns	3 neat PET yarns	0.55
Twisted flax/PLA	7	PLA	1 twisted yarn	3 neat PLA yarns	0.36
Blended flax/PLA	8	PLA	1 blended yarn	3 neat PLA yarns	0.34
Neat flax/PLA 40%	9	PLA	1 neat flax yarn	7 neat PLA yarns	0.40

Table 4.3 Specifications of 9 types of made composites with respective fiber weight fractions.

Figure 4.5 Example of filament winding operations.

Composite type	Fiber linear density	Matrix linear density	Fiber density	Matrix density	s	L	V_f	W_f	ρ_c	Area	Predicted thickness
	(g/km)	(g/km)	(g/cm^3)	(g/cm^3)	(mm/turn)	layers number			(g/cm^3)	(mm^2)	(mm)
Twisted flax/PET	228.74	327.25	1.55	1.34	0.65	2	0.38	0.41	1.42	0.39	2.41
Blended flax/PET	92.95	133.85	1.55	1.34	0.60	4	0.38	0.41	1.42	0.16	2.13
Neat flax/PET 30%	104.30	224.00	1.55	1.34	0.55	3	0.29	0.32	1.39	0.24	2.58
Neat flax/PET 40%	104.30	168.00	1.55	1.34	0.65	4	0.36	0.38	1.40	0.19	2.40
Neat flax/PET 50%	104.30	112.00	1.55	1.34	0.50	4	0.45	0.48	1.41	0.15	2.45
Neat flax/PET 60%	208.60	168.00	1.55	1.34	0.65	3	0.53	0.55	1.42	0.26	2.44
Twisted flax/PLA	103.32	179.78	1.55	1.24	0.50	3	0.31	0.36	1.34	0.21	2.54
Blended flax/PLA	87.58	170.82	1.55	1.24	0.65	4	0.30	0.34	1.32	0.20	2.41
Neat flax/PLA 40%	104.30	157.50	1.55	1.24	0.65	4	0.35	0.40	1.33	0.20	2.42

Table 4.4 Filament winding processing data. The values of fiber volume fractions are calculated in order to have the possibility to set the data for comparing the different composite type. The effective fiber volume fractions are calculated in section 7 basing on the composite density measurements.

4.2.2 Drying of fiber/matrix assemblies

Once the filament-winded fiber/matrix assemblies had been made, they have been put in vacuum chamber (0,9 mbar; 20°C) for at least 18 hours to be dried before the compression moulding.

4.2.3 Vacuum heating and press consolidation

Composite laminates were obtained by means of a specially designed compression moulding system constituted by three units: a loading unit, a heating unit, and a press unit. The procedure of making composite starts fixing the frame into another bigger frame and covering itself with two pairs of polymer foils, two per each side, in order to avoid damaging the material in the subsequent working steps. After placement of the assembly in the loading unit, it is conveyed first to the heating unit where it will be contact heated under vacuum, and afterwards to the press unit where it will be consolidated by compression at high pressure. Key parameters that must be controlled in order to carry out a good quality laminates production are temperature, time and pressure of the treatment. Values for vacuum heating have been set respectively to 200 °C, 15 minutes and 4 mbar, while for press consolidation they are respectively 30°C, 1 minute and 2.2 MPa. The established vacuum condition during heating of the assembly is essential to remove water vapour and limit oxidative chemical reactions. The first effect make the drying of the fibers more efficient, whereas the latter effect might reduce the potential thermal degradation of the natural fibers. The temperature of 200°C has been chosen in order to succeed in casting the polymer matrix without damaging the fibers in fact melting PLA temperature is about 170°C, melting PET temperature is about 180°C while flax fibers have a decomposition temperature of about 220°C.

4.3 PREPARATION OF TESTS SPECIMENS

The dimensions of the samples were chosen to be able to obtain 15 specimens for each panel: 5 with the yarns oriented with 0° direction, 5 with 90° and 5 with 30°. After pressing, the width and the height of panels are respectively 300 mm and 400 mm. It was decided to cut out a frame having a width of 10 mm on the edge of each panel because of the lower material quality at the edges. Considering the corrected dimensions (280mm and 380mm), a specimen width of 25 mm and a specimen height of 150 mm were selected to get the correct number of specimens. During the making of the cutting plan the thickness of the buzz saw was considered to be 3 mm . The specimen layout that was used is depicted in Figure 4.6. It can be seen that specimens having the same fiber angle have been located in the same panel part, to make the cutting operation easier. For each panel, first a cut at half height was made, then, in the order, the 90 and 0 degrees specimens from the top part of the frame and 30 degrees specimens from the bottom part were cut. Finally each specimen was numbered. Some further finishing operations were made manually in order to eliminate any edge specimen splinters improving the measuring accuracy of specimen dimensions.

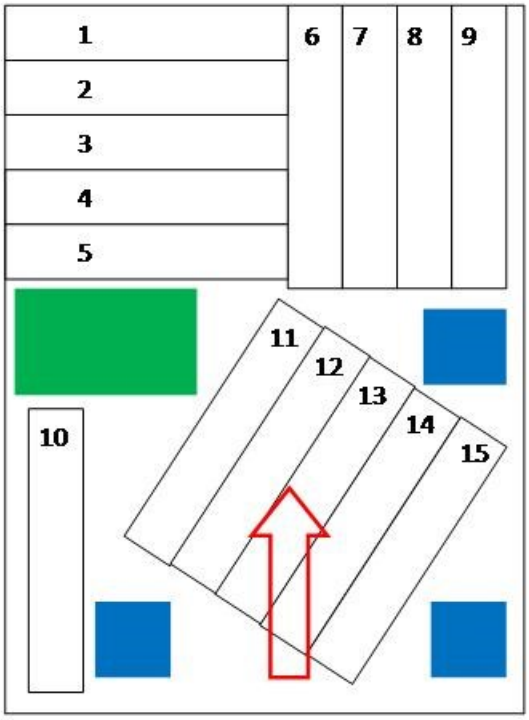

Figure 4.6 Specimens cutting layout. The red arrow indicated the orientation of the yarns. The green area and the blue areas indicate respectively where the sample for density measurements and the samples for microscopy analysis were taken from..

5 METHODS

5.1 STRUCTURE OF YARNS

The external structure of yarns was analyzed by means of environmental scanning electron microscope images (ESEM). A short sample of about 2 cm was cut for each type of yarn used, subsequently each sample was fixed on a slide. Before using the microscope a gold sputtering treatment had to be applied to the fibers. The set parameters were 100 s sputtering time and 30 mA intensity current. Figure 5.1 shows that this setting provides a film thickness of about 35 µm.

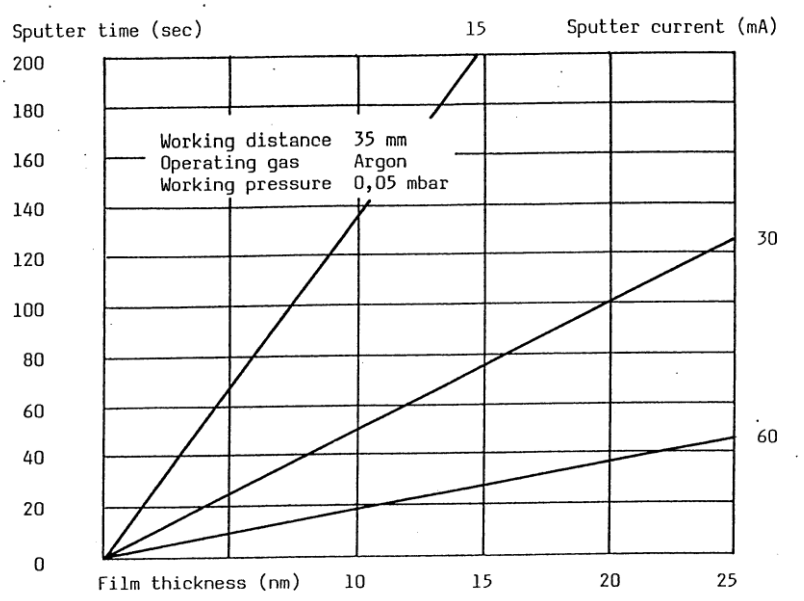

Figure 5.1 Relationship between sputter time, sputter current and film thickness

5.2 FIBER TWISTING ANGLE OF YARNS

Fiber twisting angle and yarn diameter were measured from optical microscope images (OM). Short yarn samples were mounted on glass slides and placed under the microscope to measure yarn diameter and fiber twisting angle. In order to get representative measures of real yarn characteristics

three samples were used for each yarn. The length of the samples is around 70 mm and each sample was taken 2 m distant to each other in the same yarn.

5.3 MEASUREMENT OF COMPOSITE DENSITY

Composite density is one of the fundamental parameters that must be evaluated in order to assess the volumetric composition. In this study it was experimentally determined using the Buoyancy method, by means of which the measurements of weights are converted to volume. Archimedes principle states that the buoyancy force acting to a submerged object is equal to the weight of the liquid displaced by the object so it's possible to determine the volume of the object by submerging it in a liquid of known density. Setting the equilibrium between the buoyancy force and the gravity force the object volume is calculated. For each composite type, 4 specimens with 15x15 mm dimensions were cut and polished by grinding. Afterward they were put in vacuum chamber and have been left in it for 36 hours to take out moisture. Finally they were precisely weighted in the air. Before the specimens were immersed in water they had been covered by a varnish containing paraffin to avoid water absorption during immersion. After that they were dried and subsequently they were weighted in air. A sample holder was weighted. In order to have very accurate measurements, water density had to been constantly controlled therefore water temperature was checked each time a specimen was changed. No temperature water changes were registered since measured temperature had been constant at 23.4 °C so the liquid density used in the calculations was unchanging. One by one the specimens were immersed in water handling with care and trying to avoid bubbles formation that would have distorted the sample weight. Finally specimen weights in water were measured. The precision of the weigh and temperature measurements was respectively ± 0.0001 g and ± 0.1 °C. The density of the composites was calculated by means of the following formula obtained from force equilibrium:

$$\rho_c = \frac{M_1 \rho_w}{M_2 - (M_4 - M_3) - \frac{\rho_w}{\rho_v}(M_2 - M_1)} \qquad 5.1$$

where M_1, M_2, M_3 and M_4 indicate respectively the weight of uncoated sample in air, the weight of coated sample in air, the weight of sample holder in water and the weight of coated sample in water. The density of water, the density of varnish and the density of sample are indicated respectively with ρ_w, ρ_v and ρ_s.

5.4 CALCULATIONS OF VOLUME FRACTIONS

The value of V_f can be estimated analyzing the polished composite cross-sections but this procedure required a lot of assumptions to manage to distinguish the different phases in the material. Indeed the colour threshold to discriminate matrix parts from fiber parts could be difficult to be individuated therefore the results can be too much approximated and less reliable.

Probably the most precise way to estimate V_f is based on the measurement of density composite ρ_c. In this study composite densities were measured by means of the Buoyancy method and W_f was determined from the yarn linear densities of fibers and matrix, as filament winding was used for fiber/matrix mixing.

Experimental volume fractions of fiber, matrix and porosity have been calculated by means of the following equations from the model [4] :

$$V_f = \frac{\rho_c}{\rho_f} W_f \qquad 5.2$$

$$V_m = \frac{\rho_c}{\rho_m}(1 - W_f) \qquad 5.3$$

$$V_p = 1 - (V_f + V_m) \qquad 5.4$$

These volumetric fractions might not represent true values since they are estimated basing on the W_f of the whole composite panel, whereas the densities are evaluated from small sample measurements. The fiber weight fraction of the small sample (here indicated as W_f' for simplicity) used for the density measurement, could be calculated by dissolving the matrix. However also this measure is affected by an experimental error, since it might be that some fibers are dissolved too. Therefore, by basing on previous studies of Madsen [3] that demonstrated the reasonableness of assuming the equality of W_f and W_f', the used method for volume fractions calculation has been considered reliable. Flax fiber density was assumed to be 1.55 g/cm^3 [4], PET and PLA fiber densities were assumed to be, respectively, 1.34 g/cm^3 [4] and 1.25 g/cm^3 [1].

5.5 MICROSTRUCTURE OF COMPOSITES

The spatial distribution of fiber and matrix parts was assessed by observing the composite cross sections oriented perpendicular to the fibers by means of both the electron microscope (ESEM) and the optical microscope (OM).

For electron microscope analysis of cross sectional composite areas, small samples (25x15 mm^2) were cut, one for each different composite, and thereafter they were grinded and polished in multiple steps in succession:

- 1 minute grinding with #500 silicon carbide paper 500

- 5 minute grinding with #4000 silicon carbide paper

- 5 minute polishing with 1 μm diamond powder

The specimens were fixed on a holder that was pressed on the turning plate with a force of about 70 N. The rotational speed was kept around at 150 RPM. When the surface quality of each sample appeared to be good, the specimens were put in oven for 5 minutes at 40 °C to be dried and afterwards a gold sputtering treatment was applied to them. The same samples that had been already prepared for electron microscope analysis were also used for the optical microscope analysis

5.6 MECHANICAL PROPERTIES OF COMPOSITES

5.6.1 Conditioning in climate chamber

To make certain that the equilibrium condition of the specimens was attained before starting mechanical tests, a conditioning treatment was applied putting the samples into a climate chamber at humidity of 50% RH and 23°C. These values were chosen as they represent a standard condition for plastic materials and it was assumed that they are also suitable for plant fiber composites. During this conditioning in the climate chamber, the weights of 27 specimens (one for each composite type, with 0°, 30° and 90° yarn orientation) were measured with an interval of about one day so that it could be possible to plot the moisture adsorption trends and make a comparison with the theoretical curve predicted with the Fickian model. See appendix B for details.

5.6.2 Tensile tests

Once the conditioning treatment had been finished the specimens were ready to be tested since their weight were stabilised. To avoid weight changes outside the climate chamber, all handling of the conditioned samples was carried out within 30 min, therefore a group of max 3 or 4 specimens was taken out, put in a plastic bag and tested.

Tensile tests were carried out using a testing machine with a load cell of 25 kN and crosshead speed of 1mm/min. To compensate for any possible bending and obtain a more accurate strain evaluation, two extensometers having a gauge length of 25 mm were centred on each side of the specimen.

The stiffness of all specimens were measured by means of linear regression between strain of 0.0001 and 0.0010. This range was selected based on the stress-strain curve of the 90° specimens since they are characterized by having the shortest linear zone as compared to the 30° and 0° off axis specimens, as it is shown in Figure 5.2. Stress-strain curves were corrected to make sure that they pass at the origin of reference system. Stress-strain curves were plotted for all the sample tests and in addition to the stiffness, also ultimate stress and strain at ultimate stress were determined from them.

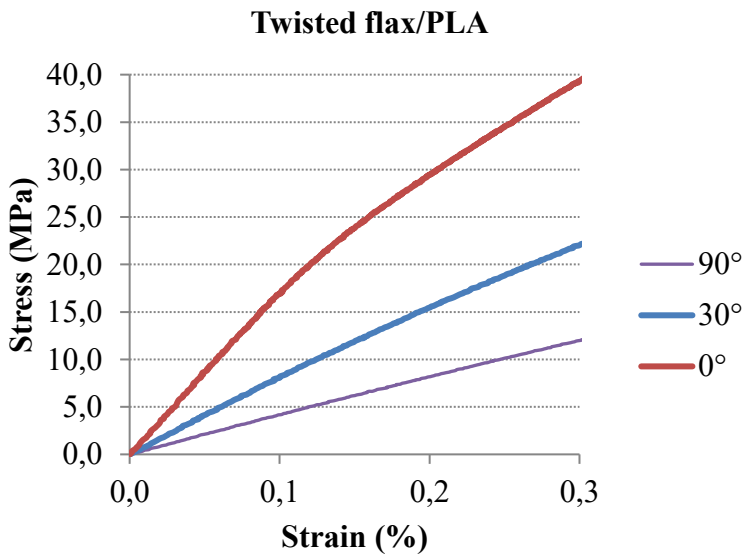

Figure 5.2 Stress-strain curves for twisted flax/PLA composite. It can clearly noted that the higher is the off-axis angle, the lower is the stiffness.

Figure 5.3 Tensile specimen mounted for testing with the two extensometers centred at the gauge section.

6 RESULTS AND DISCUSSIONS

6.1 STRUCTURE OF YARNS

Observations from both the electron microscope and the optical microscope confirm that the neat flax yarn is constituted by several fibers that are twisted with a right-handed angle to the yarn axis (a so-called Z-twist) (see Figures 4.1 and 6.2). The mean flax twisting angle resulting from the measures is 16±3° whereas the average diameter is 389±92 μm (Table 6.1). There exists a significant spread of data especially for the diameter, as demonstrated by the relatively high standard deviation. This is due both to the experimental intrinsic error of measurements, and to the natural irregularity of the fibers.

Focusing on the twisted yarns it clearly appears that the twisting angle is opposite to the flax yarn one (see Figure 4.2, 6.7 and 6.8). Indeed the images show that the different filaments are twisted with a left-handed angle (a so-called S-twist) both in twisted flax/PET and twisted flax/PLA yarns. The twisted measured angles for flax/PET and flax/PLA are respectively 10±2° and 8±3°, while the average diameters are, respectively, 799±134 μm and 840±132 μm (Table 6.1). Probably the filaments are twisted in the opposite direction to the fibers to make the yarn more bulky, but with a lower breaking load [23].

The fiber twisting angle of the flax yarns in the twisted yarns was also analyzed. Comparing the flax fiber twisting angle of the two twisted yarns with the twisting angle of the neat flax yarn, it has been observed that the value in the twisted yarns with PLA (16±3°) seems to be a little closer to the neat flax yarn value than the twisted PET yarn (17±3°), but probably this effect is due to the measurement approximations, since considering the standard deviations it can be inferred that the angle is the same in all three yarns.

The neat PET yarn and the neat PLA yarn diameters were also measured giving respectively 620±23 μm and 330±20 μm whereas the neat polymer yarn twisting angle is measured to be approximately equal to zero in both of cases. Observing the PLA yarn images (Figure 6.1), it has been seen that the yarn is made up by two smaller filament types confirming the supplier indications.

Things change radically referring to the blended yarns since the twisting angle type is Z-twist instead of S-twist (Figures 4.3, 6.5 and 6.6). The angle values also are different in fact they are shown to be higher than the twisted yarn ones. The angle measures are 20±3° and 22±3° respectively for blended flax/PET and blended flax/PLA. The diameter values are 608±61 μm for

the blended flax/PET yarns and 640±61 μm for the blended flax/PLA yarns, which are lower than the diameters of the twisted yarns.

Observing the external structure of the various yarns it can be see that there are some typical characteristics in each yarn type:

- the fibers are not homogeneous, but are varying in diameters

- several surface defects are present, especially on the flax fibers, whereas the polymer fibers appear to be much smoother

- the twisting angle varies slightly for groups of fibers

Figure 6.1 and Figure 6.2 demonstrate respectively the smoothness difference between the PLA fibers surface and the flax fiber surface, whereas in Figure 6.3 a typical defect of the flax fibers in the twisted yarns is shown. Likewise many imperfections has been found in the blended yarns as it can be seen in Figure 6.4. However it has been observed that the presence of entangled up fibers within several messy yarn parts is probably the main characteristic of the blended yarns. Figure 6.5 and Figure 6.6 show some fiber tangled areas respectively in the flax/PET blended yarns and in the flax/PLA blended yarns. In Table 6.1 values of all the measurements of twisting angles and diameters are reported.

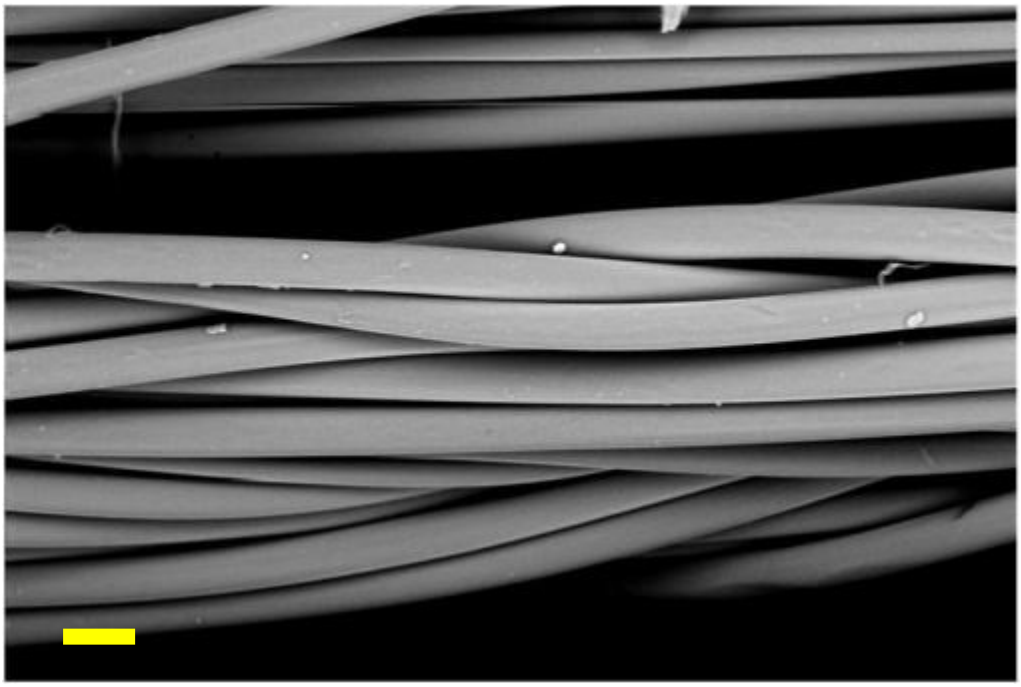

Figure 6.1 ESEM image of neat PLA. Scale bar is 20 μm.

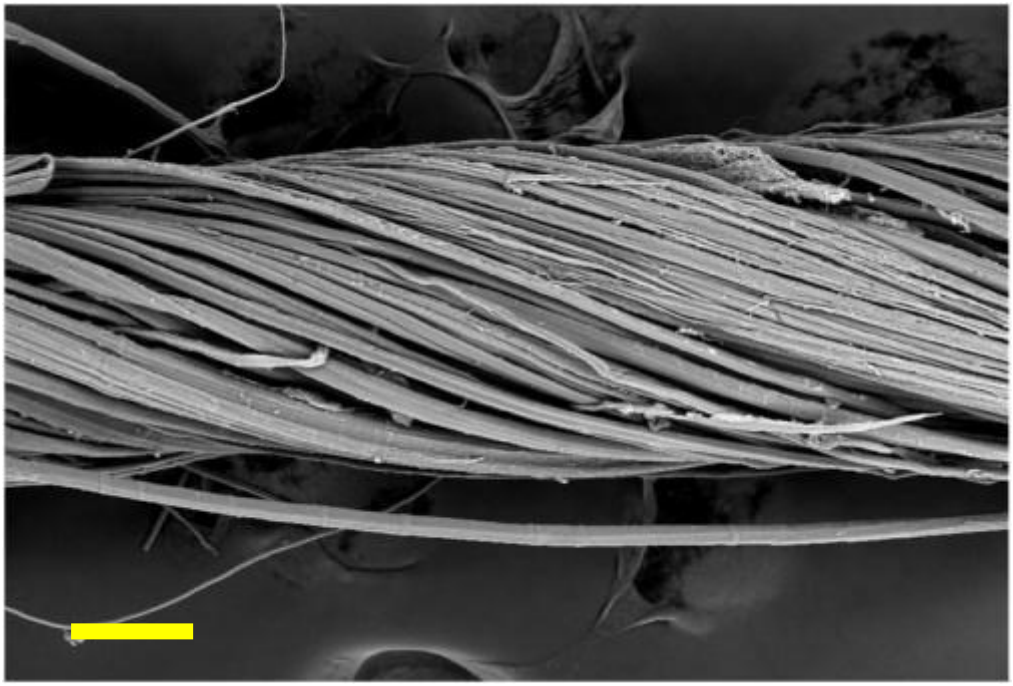

Figure 6.2 ESEM image of neat flax yarn. Scale bar is 100 µm.

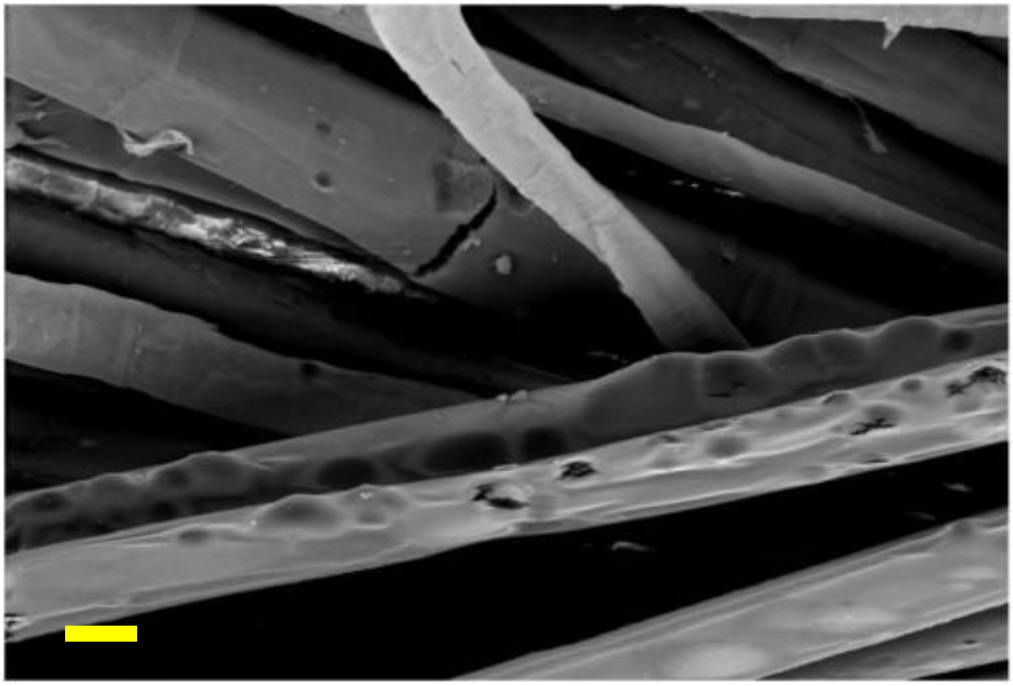

Figure 6.3 ESEM image of typical defects within flax fibers. Scale bar is 20 µm.

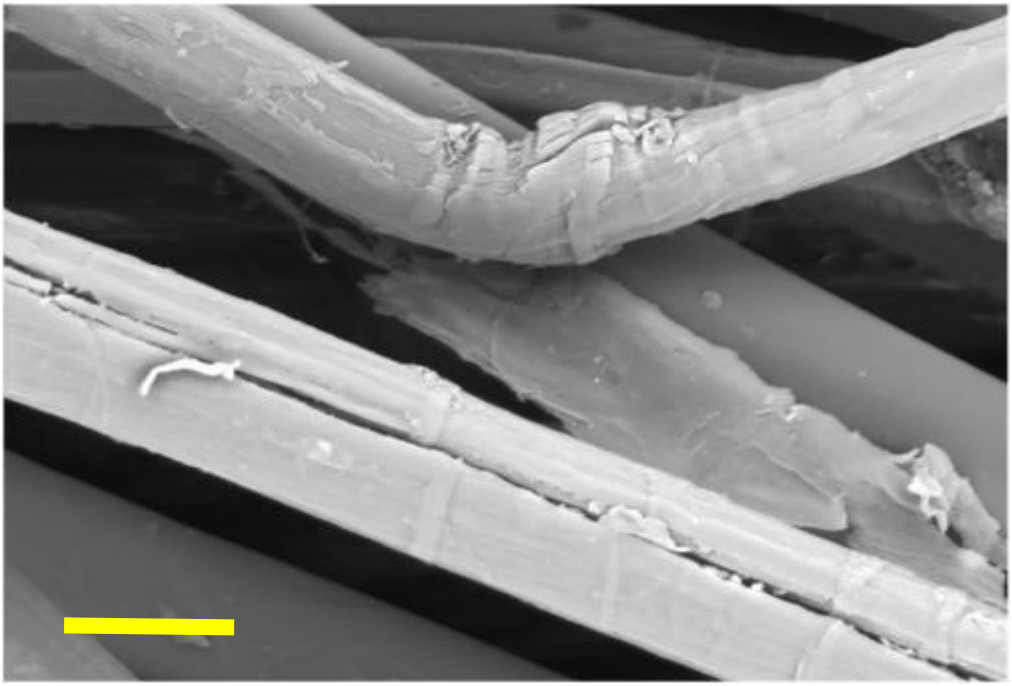

Figure 6.4 ESEM image of flax fibers in a blended yarn. Scale bar is 20 µm.

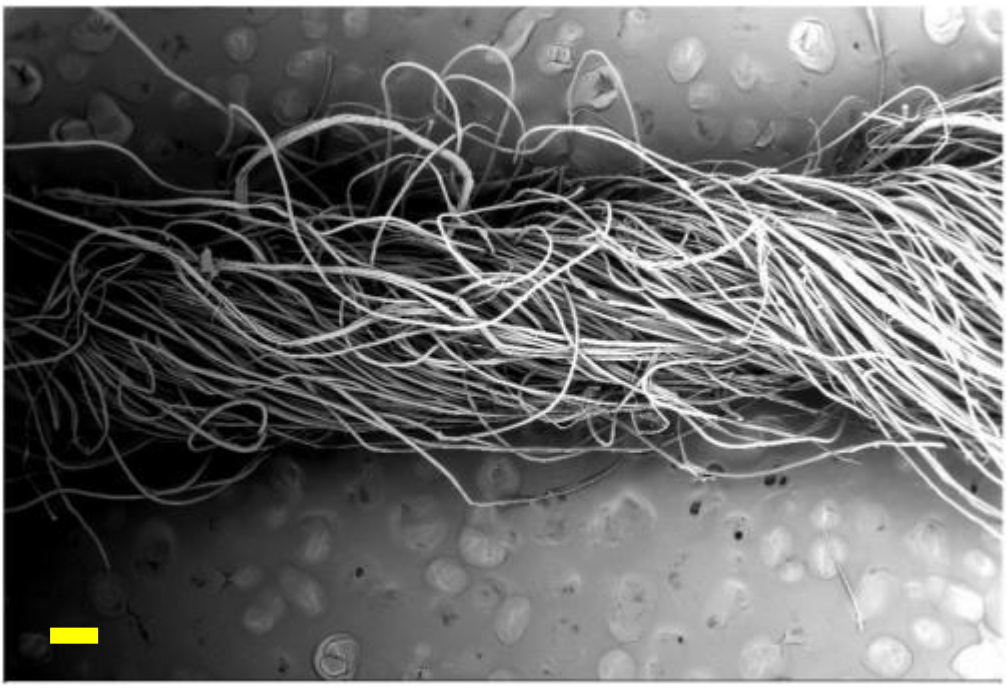

Figure 6.5 ESEM image of messy zone of a blended flax fiber PET yarn. Scale bar is 200µm.

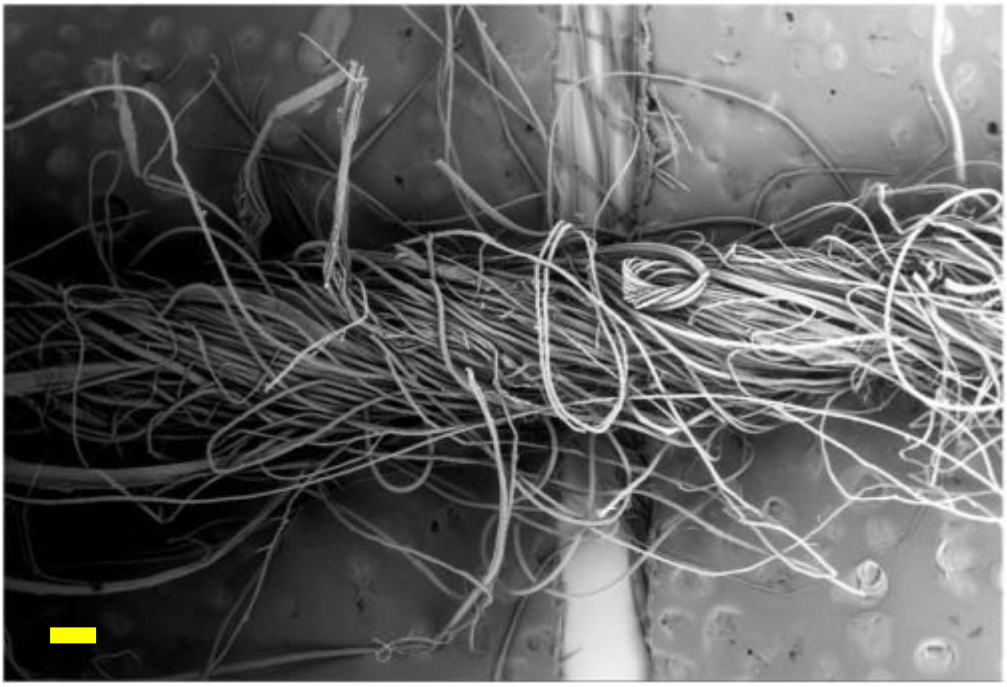

Figure 6.6 ESEM image of messy zone of a blended flax fiber PLA yarn. Scale bar is 200µm.

Figure 6.7 ESEM image of a twisted flax fiber PET yarn. Scale bar is 200µm.

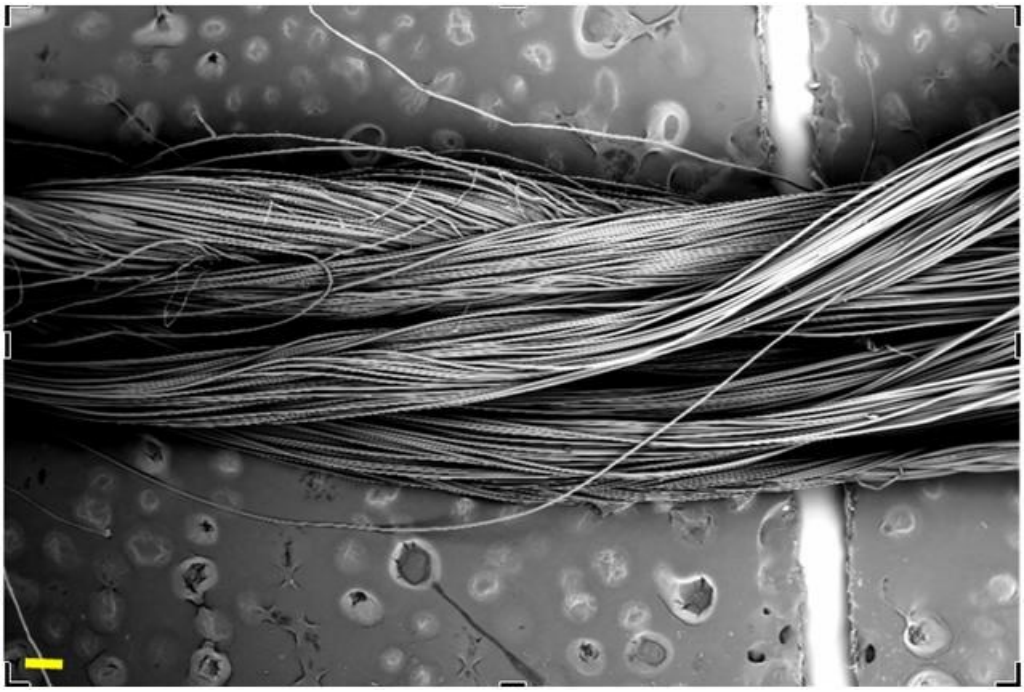

Figure 6.8 ESEM image of a twisted flax fiber PLA yarn. Scale bar is 200μm.

Yarn type	Yarn twisting angle	Yarn diameter	Flax fiber twisting angle
	(degrees)	(μm)	(degrees)
Neat flax		389±92	16±3
Twisted flax/PET	10±2	799±134	17±3
Twisted flax/PLA	8±3	840±142	16±3
Blended flax/PET		608±61	20±3
Blended flax/PLA		640±61	22±3
Neat PET		620±23	
Neat PLA		330±20	

Table 6.1 Angle and yarn diameter measurements. Data of flax fibers were obtained by means of observations of neat fibers and fibers that are present in twisted and blended yarns. No angles are reported for the polymer fibers since no twisting effect has been observed.

6.1.1 Fiber twisting angle in composites

The fiber orientation in aligned plant fiber yarn composites cannot be considered perfectly unidirectional because of the fiber twisted structure. In respect to the vertical sample axis, in fact, fiber direction is a bit skewed. This angle is equal to plus-minus the fiber twisting angle for both the neat and the blended yarns, but it's more complicated for the twisted yarns since the actual twisting arrangement depends on two contributes. Indeed in this case the final flax fiber angle value is given by the sum of the twisting yarn angle and the twisting flax angle. Differently, it can be noted that in the twisted yarn case there are 4 different fiber angles instead of 2. It has been calculated that for the twisted flax/PET yarns the values are 27°, 7°, -7° and - 27° while for the twisted flax/PLA yarns they are 24°, 8°, -8° and -24°. For more details see section 6.3.

6.2 COMPOSITE PROPERTIES

In this section volumetric composition, mechanical properties, microstructure and failure characteristics of all composites have been analyzed trying to evaluate:

1) the effect of fiber content (30, 40, 50, 60 %)
2) the effect of type of composite pre-forms (twisted and blended yarns)
3) the effect of matrix type (PET and PLA)

Results of the tensile tests of all the composites are reported in this section. The results will also be used in section 6.3 for the estimation of the mechanical properties of the flax fibers.

The microstructure of the different composite is analyzed and both electron microscope images and optical microscope images are reported to illustrate the found main characteristics.

A investigation of the failure characteristics is carried out to attempt to spot any dissimilarity between the different composites. A qualitative analysis has been conducted confronting the fracture surface images of all tested specimens. Attention has been focused especially on the profile of fracture edges, in addition to the localization and the orientation of the cracks.

6.2.1 Influence of fiber content

In this section the influence of fiber content has been studied, using the results from the neat flax/PET composites.

a) Volumetric composition

In order to analyze the influence of fiber content the volume fractions of flax/PET composites were determined. The results are reported in Table 6.2.

Type of composite	Wf	Density (g/cm^3)	Vf	Vm	Vp
Neat flax/PET 30%	0.318	1.360±0.002	0.279	0.693	0.028
Neat flax/PET 40%	0.383	1.342±0.004	0.332	0.618	0.050
Neat flax/PET 50%	0.482	1.354±0.011	0.421	0.524	0.055
Neat flax/PET 60%	0.554	1.344±0.010	0.480	0.447	0.072

Table 6.2 List of volume fraction values, densities and fiber weight fractions for neat flax/PET composites.

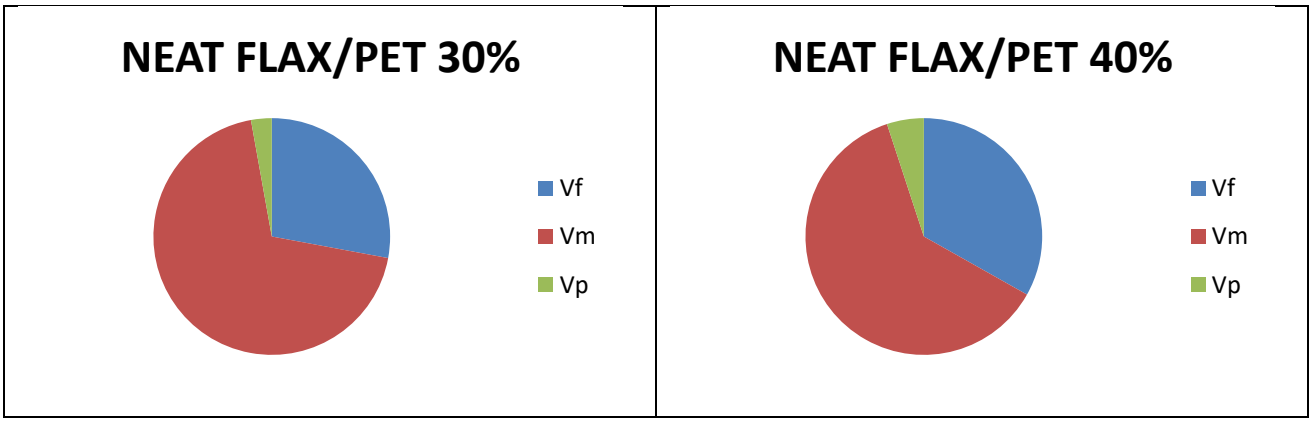

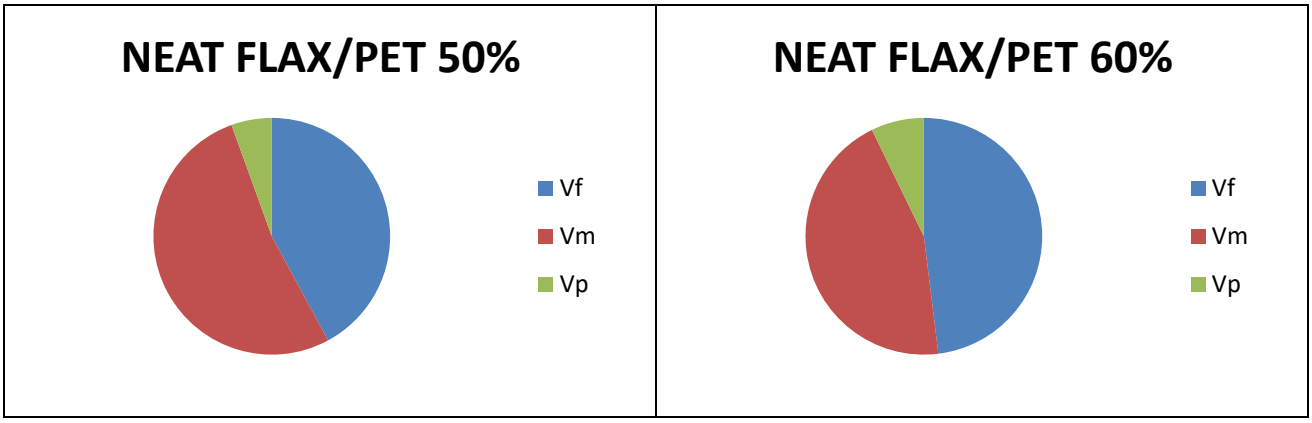

Figure 6.9 Schematic representation of volume fractions of neat flax/PET composites.

Observing the results in Table 6.2 and Figure 6.9 it is possible to see that the higher the fiber volume fraction, the higher the amount of porosity.

In order to enquire further this matter, an analysis was carried out using the experimental data and the predictions of the volumetric interaction model [4].

Volumetric composition has been investigated by means of the volumetric interaction model [4]. In plant fiber composites, the influence of porosity on composite mechanical properties cannot be neglected, therefore the amount of porosity has a fundamental role in the conversion of weight fractions into volume fractions of both the fibers and the matrix parts. The model calculates the porosity fraction (V_p), and the fiber and matrix volume fractions (V_f and V_m) as a function of the fiber weight fraction (W_f). The interaction between the three volume parts is called volumetric interaction. It has been observed that it can be very difficult to control the fiber and matrix volume contents during composite manufacturing, because of the amount of porosity, and therefore W_f was used as the independent variable.

The model is based on the following base relationships:

$$w_c = w_f + w_m \Rightarrow 1 = \frac{w_f}{w_c} + \frac{w_m}{w_c} = W_f + W_m \qquad 6.1$$

$$v_c = v_f + v_m + v_p \Rightarrow 1 = \frac{v_f}{v_c} + \frac{v_m}{v_c} + \frac{v_p}{v_c} = V_f + V_m + V_p \qquad 6.2$$

where w and v are absolute weight and volume respectively, W and V are weight fractions and volume fractions respectively, and the subscripts c, f, m and p are composite, fibers, matrix and porosity respectively. For the analysis of the influence of fiber content (i.e neat flax/PET composites) it was necessary also to determine the transition point, since this point of volumetric

composition is characterized by an optimal combination of high fiber volume fraction and low porosity which lead to high density and stiffness of composites.

It is possible to define a maximum obtainable fiber volume fraction V_{fmax} that gives the transition point [4]:

$$V_{f\,max} = \frac{v_f}{v_{c\,min}} \qquad 6.3$$

The transition fiber weight fraction was then determined by means of the following equation [4]:

$$W_{ftrans} = \frac{V_{f\,max}\rho_f(1+\alpha_{pm})}{V_{f\,max}\rho_f(1+\alpha_{pm}) - V_{f\,max}\rho_m(1+\alpha_{pf}) + \rho_m} \qquad 6.4$$

In the modeling calculations a fiber density of 1.55 g/cm^3 and a matrix density of 1.34 g/cm^3 are used, whereas the fiber porosity constant has been calculated from the slope of the fitted regression line with a fixed intercept in the experimental V_p vs. experimental V_f plot.

$$V_p = \frac{\alpha_{pf} - \alpha_{pm}}{1+\alpha_{pm}} V_f + \frac{\alpha_{pm}}{1+\alpha_{pm}} \qquad 6.5$$

Based on findings in former studies about hemp/PET and flax/PP composites the matrix porosity constant $\alpha_{pm(1)}$ is fixed equal to zero due to the absence of porosity in PET, which has been showed with density measurements and microscope observations.

The determined value of α_{pf} from equation 6.5 is 0.14, which is in the typical range between 0 and 0.5, as indicated by previous work of Madsen et al. [4].

The calculated value of the impregnation porosity is 0.0996.

The maximum fiber volume fraction V_{fmax} could not be determined from the experimental data since the transition point where not reached. Instead, V_{fmax} was set equal to 0.51 [4].

Probably, the making of composites with higher fiber contents above the transition point would have helped the determination of V_{fmax}.

The calculated value of W_{ftrans} by equation 6.4 is 0.58.

Figure 6.10 shows the experimental data of the volume fractions as a function of the fiber weight fraction, together with the model predictions. It can be observed that there is a good agreement between the experimental data points and the model lines. This confirms the substantial effect of the porosity.

It can be observed in Figure 6.10 that for all composites the highest W_f value is still below W_{ftrans}. This indicates that the fiber assembly is not fully compacted and the matrix is able to fill the free space within the fibers [4].

In Figure 6.10, to get a better understanding of the porosity effect, the volume fractions of fibers and matrix under the assumptions of no porosity were also calculated. The expressions used to calculate the fiber and matrix volume fractions assuming no porosity effect are the following:

$$V_f^* = \frac{W_f \rho_m}{W_f \rho_m + (1 - W_f)\rho_f} \qquad 6.6$$

$$V_m^* = 1 - V_f^* \qquad 6.7$$

It can be noted in Figure 6.10 that if the porosity effect was neglected, the fiber and matrix volume fractions would be overestimated, making the prediction of mechanical properties less reliable.

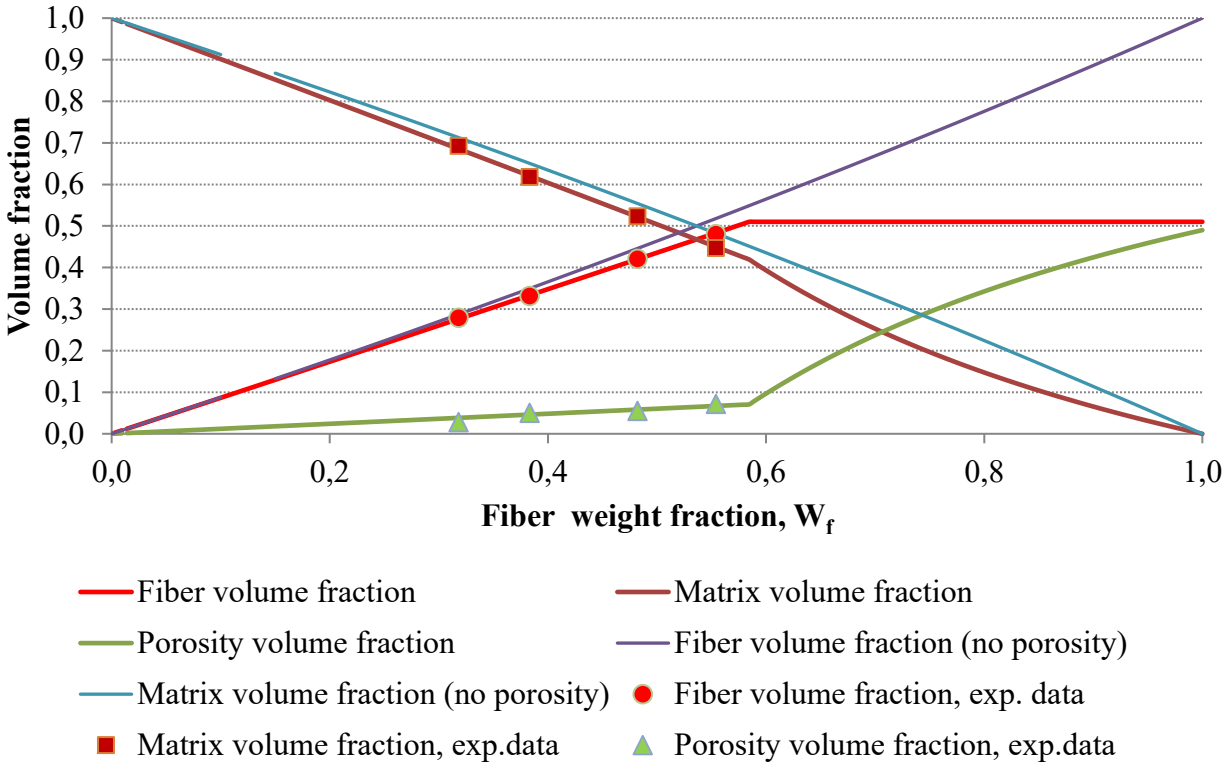

Figure 6.10 Volumetric fractions trends.

Density

The developed model framework of volumetric model interaction can be used to predict the composite density making it possible to compare the model results with the experimental density values. The modeling density equation is the following:

$$\rho_c = V_f\rho_f + V_m\rho_m \qquad 6.8$$

To evaluate the porosity effect also composite density with no porosity (ρ_c^*) was determined. This density is calculated in the same way but referring to V_f^* and V_m^* instead of V_f and V_m. The model predicts a transition maximum ρ_c of 1.352 g/cm^3. As it is depicted in Figure 6.11 the experimental points are overlapped with the model prediction line, demonstrating the good agreement with the model.

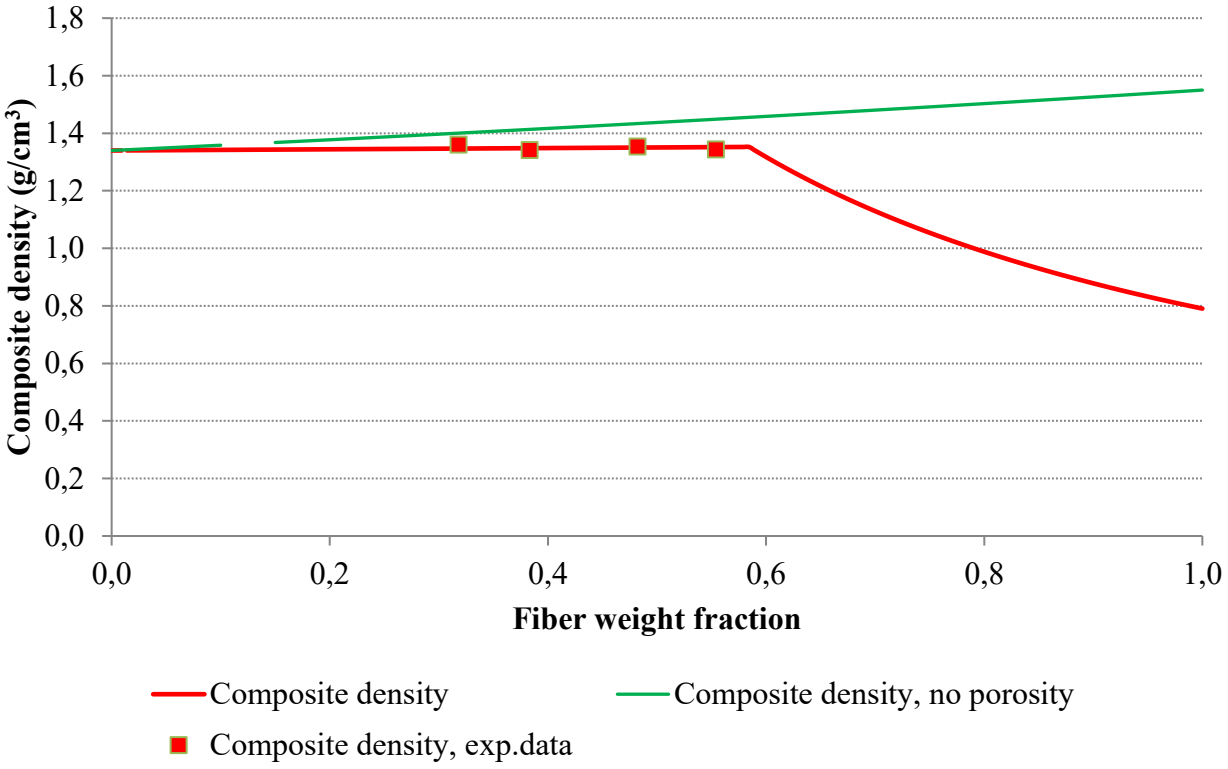

Figure 6.11 Densities trends with and without considering the porosity effect.

Stiffness

The combined rule of mixtures model [24] is a widely accepted micromechanical model for calculating the stiffness of composites with unidirectional fiber orientation therefore it represents the framework of the used volumetric interaction model . It has been observed that it is possible to get a substantial improvement of prediction accuracy including porosity effect and two efficiency factors.

Basing on the previous considerations, the starting point to calculate the stiffness of composites taking in account the volumetric interaction effect is represented by the combined rule of mixture: [3] [25] [26] [27] [28]

$$E_c = \left(\eta_0 \eta_l V_f E_f + V_m E_m\right)\left(1 - V_p\right)^n \qquad 6.9$$

where η_0 is the fiber orientation efficiency factor, n is the porosity efficiency exponent that controls the porosity effect due to stress concentrations in the composite, and η_l is the fiber length efficiency factor that can be calculated by the shear lag model developed by Cox(1958):

$$\eta_l = 2\frac{L}{D}\sqrt{\frac{G_m}{E_f \ln\left(\frac{k}{V_f}\right)}} \qquad 6.10$$

where L represents the fiber length, G_m is shear stiffness of the matrix, D is fiber diameter, and k represents a constant which is controlled by the geometrical packing pattern of the fibers [29]. L and D were assumed to be 20mm and 20μm, respectively therefore L/D is 1000. As it was demonstrated [30] that for L/D ratio above 50, μ_l is asymptotically approaching 1, therefore η_l was set equal to 1.0

Finally the matrix shear stress is obtained by the equation:

$$G_m = \frac{E_m}{2(1+v_m)} \qquad 6.11$$

By using the predicted values of fiber, matrix and porosity volume fractions shown in Figure 6.10, it is possible to predict composite stiffness as a function of W_f.

In the model predictions using equation 6.5, matrix PET stiffness were assumed to be 2.7GPa, while the fiber orientation efficiency factor was set equal to 1, which is the most common value for unidirectional fibers. For the porosity efficiency exponent it was chosen to use the value 2, since it has been shown to give a good prediction of experimental data [3]. The model requires also the fiber stiffness as input. The average of all the back-calculated stiffness values that were obtained from the sixteen elements method (see section 6.3.2) was determined to be 72 GPa in the model. The experimental data points together with the model lines are shown in Figure 6.12.

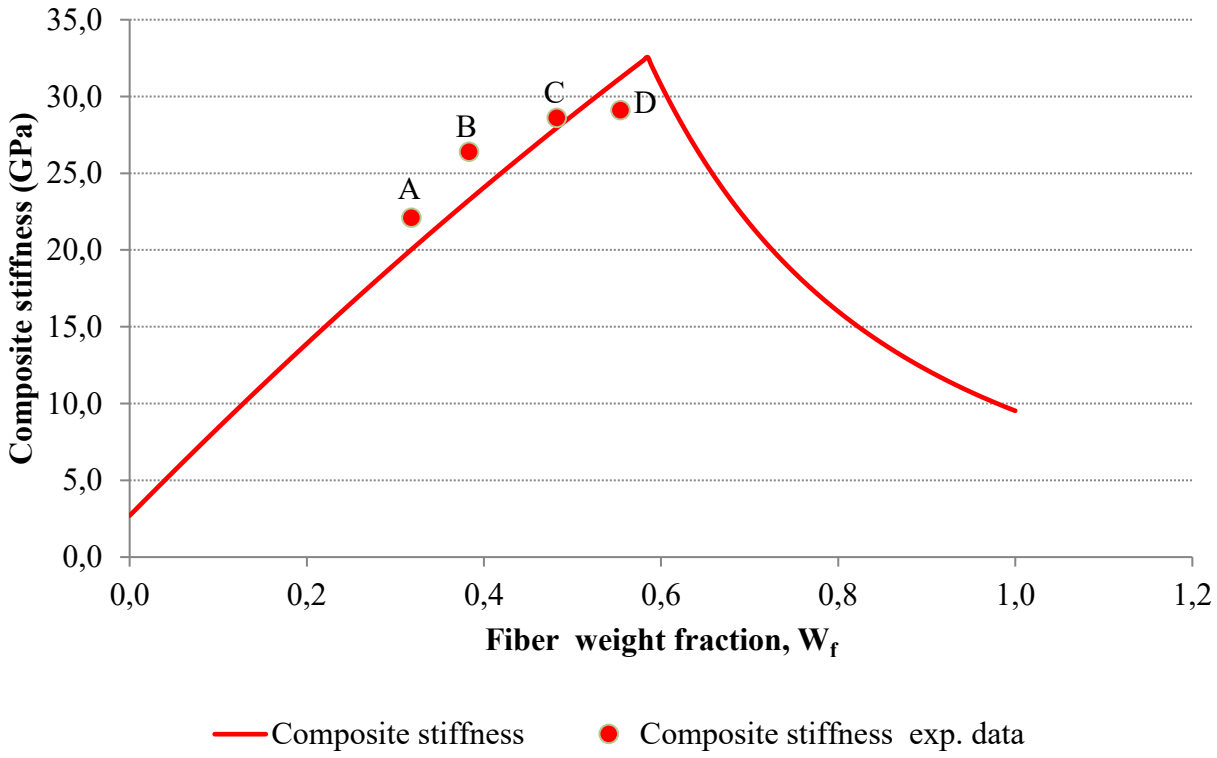

Figure 6.12 Stiffness trend predicted by the volumetric interaction model. Points A,B,C and D are the composite stiffness values back-calculated by means of the sixteen elements model (see section 6.3).

As mentioned earlier, due to the limited available experimental data of volumetric composition, the correct value of V_{fmax} can be determined from Figure 6.10. Instead, in order to find the transition point, it has been tried to fit the experimental stiffness points in Figure 6.12 by changing V_{fmax}. It was observed that with a V_{fmax} of 0.48 (instead 0.51) which corresponds to a W_{fmax} of 0.55 the point D seemed to be closer to the decreasing curve, whereas with the used V_{fmax} of 0.51 the point D is closer to the left branch. However, altogether it was considered that model predictions of Figure 6.12 is more representative for the monotonous trend of the stiffness values.

b) Mechanical properties

The axial properties of all the fabricated composites are illustrated in Table 6.3, 6.4, and 6.5 where each measure represents an average of the five samples tests.

Off axis angle 0°			
Composite type	**Stiffness**	**Ultimate stress**	**Strain at ultimate stress**
	(GPa)	(MPa)	
Neat flax/PET 30%	16.2±0.5	152±5	1.507±0.0849
Neat flax/PET 40%	18.6±0.5	183±3	1.636±0.0383
Neat flax/PET 50%	20.7±0.7	203±6	1.691±0.0845
Neat flax/PET 60%	21.1±2.7	216±18	1.759±0.1746

Table 6.3 List of tensile test results for 0° off-axis angle neat flax/PET specimens. Stiffness, ultimate strength and strain at ultimate strength were measured.

Off axis angle 30°			
Composite type	**Stiffness**	**Ultimate stress**	**Strain at ultimate stress**
Neat flax/PET 30%	6.1±0.3	50±3	1.157±0.0613
Neat flax/PET 40%	6.9±0.2	49±1	1.036±0.0649
Neat flax/PET 50%	7.3±0.3	39±1	0.781±0.1207
Neat flax/PET 60%	7.2±0.7	26±6	0.499±0.1538

Table 6.4 List of tensile test results for 30° off-axis angle neat flax/PET specimens. Stiffness, ultimate strength and strain at ultimate strength were measured.

Off axis angle 90°			
Composite type	**Stiffness**	**Ultimate stress**	**Strain at ultimate stress**
Neat flax/PET 30%	3.3±0.1	16±1	0.735±0.1163
Neat flax/PET 40%	3.1±0.3	12±1	0.463±0.0722
Neat flax/PET 50%	3.2±0.2	13±1	0.657±0.0809
Neat flax/PET 60%	2.0±0.2	6±1	0.468±0.0953

Table 6.5 List of tensile test results for 90° off-axis angle neat flax/PET specimens. Stiffness, ultimate strength and strain at ultimate strength were measured.

It has been observed that the effect of increasing the fiber content provides generally an improvement of mechanical properties of composites, as expected. This trend is particularly marked in the 0° off-axis sample tests, for the effect of alignment of yarns along the tensile direction. If the off-axis angle is increased, the fiber reinforcement effect is attenuated since the composite behavior is more affected by the matrix properties. However it must be considered that after a transition point the fiber volume fraction cannot be further increased since the fiber assembly has a limited packing ability. Therefore an additional porosity phase called structural porosity would be developed, deteriorating the mechanical properties of composite [30]. In the present study all the composites probably have a fiber content which is below the transition point, (see previous section for details) so no decay of stiffness and ultimate strength have been observed.

c) Microstructure

Some OM images of the different neat flax/PET composite cross sections are shown in the following figures.

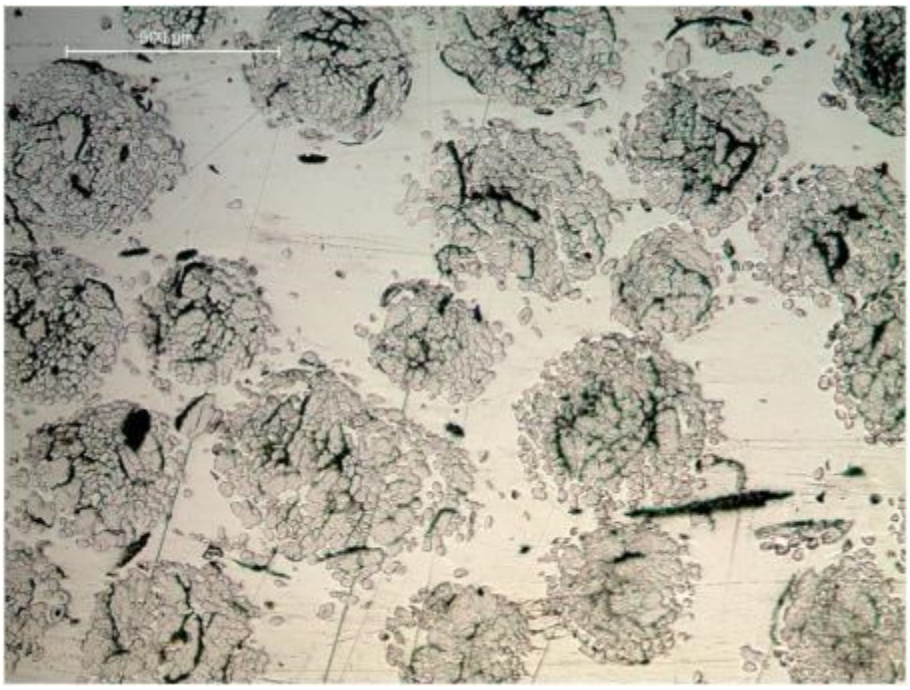

Figure 6.13 OM image of neat flax/PET 30% composite cross section. Scale bar is 500 µm.

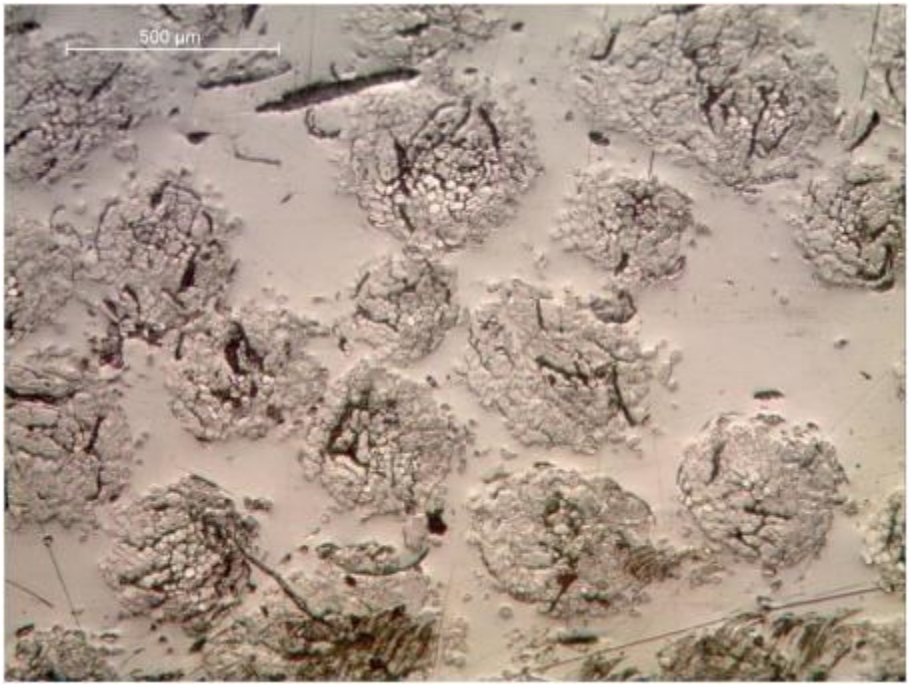

Figure 6.14 OM image of neat flax/PET 40% composite cross section. Scale bar is 500 µm.

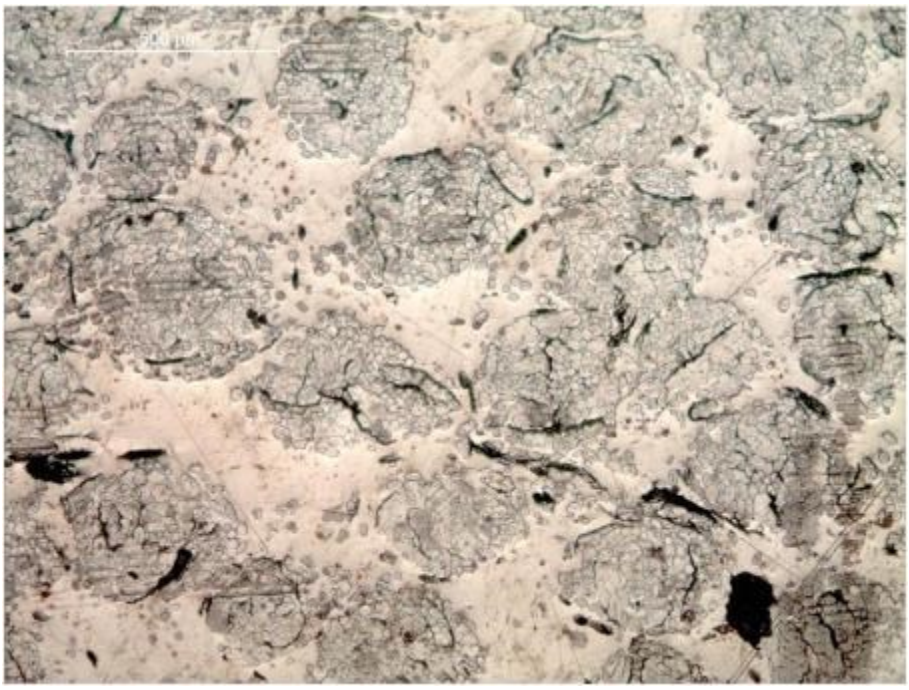

Figure 6.15 OM image of neat flax/PET 50% composite cross section. Scale bar is 500 µm.

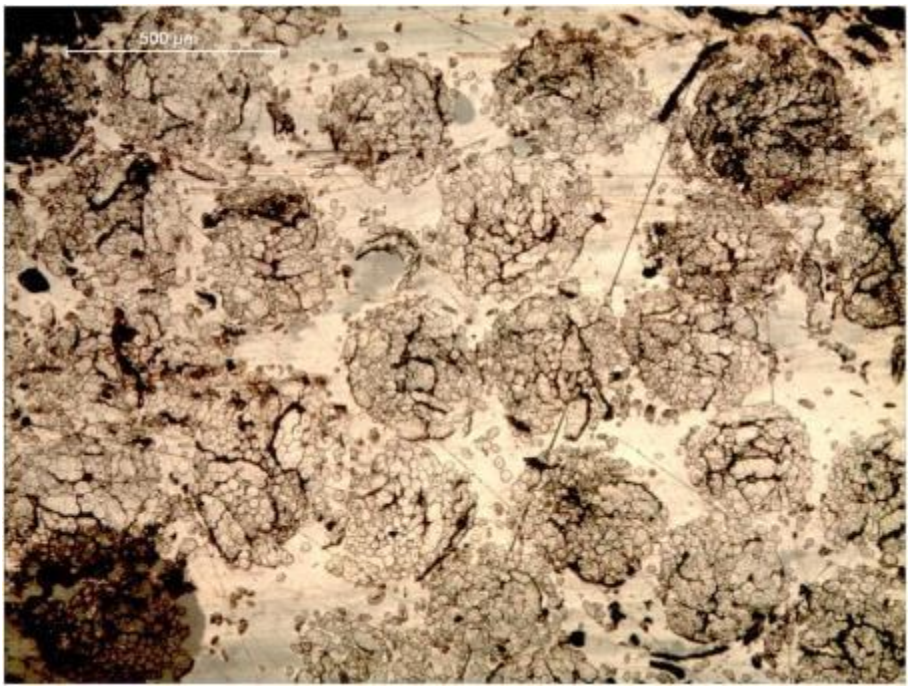

Figure 6.16 OM image of neat flax/PET 60% composite cross section. Scale bar is 500 µm.

From the images it can be observed the relatively uniform distribution of flax yarn bundles within the matrix. The increasing fiber content in the 4 composites is depicted by the growing number of

flax fiber bundles. In the neat flax/PET 60% composite it can be observed how the fiber amount is high in respect with the matrix part.

d) Failure characteristics

0° tests

Almost all the samples with 0° off-axis angle exhibit a neat fracture surface, with the formation of two separated parts. Things change referring to the two PET composites with the higher fiber weight fractions (50% and 60 %, respectively), because they do not show a delineated transversal fracture line. Specially the composite with the highest amount of fibers exhibit a series of failures located in different positions along the sample height. It has been attempted to explain this feature considering the reduced effect of matrix in the sample stress redistribution. Concentrating on a sample section it can be said that the higher is the amount of fibers, the lower is the matrix capacity for leveling the applied load, therefore there exist a larger number of inhomogeneities, due for example to unavoidable diameter fiber variations. In this way the fracture can be started in several points localized in different sections as it can been observed from the images. Another important observation regarding the sample with the highest amount of fibers is the swelling of samples in the middle zone. In fact it can be observed that in the clamping zone the sample width is kept constant owing to the impossibility of expansion, while out of the clamping zone the width of the sample slightly increases towards the middle zone because of the spaces created by cracking in longitudinal direction when fracture occurred.

30° tests

It has been observed that all the neat flax/PET samples broke in two pieces along a 30° direction when fracture occurred, except the PET specimens with the highest amount of flax fibers (50% and 60%, respectively). In these two cases several clear lines with 30° orientation have been observed. It has been hypothesize that they are connected with the crazing phenomenon.

90° tests

The most relevant observation consists in the presence of crazes that lie normal to the stress direction.. The trend seems to be that the more is the amount of fibers, the higher is the number of crazes. In some cases, especially with high fiber weight fractions, craze identification is difficult because of the presence of clear matrix stripes that can be interpreted as craze.

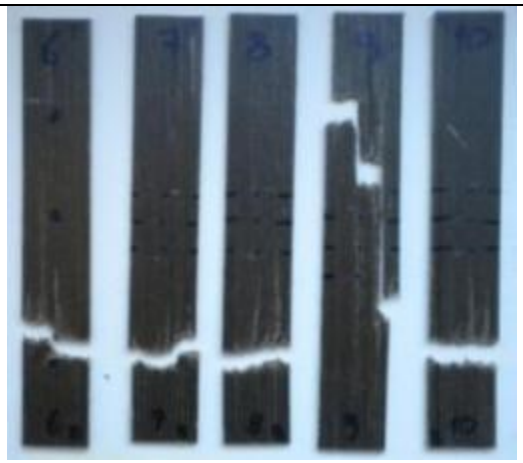

Neat flax/PET 30%,off-axis angle 0°

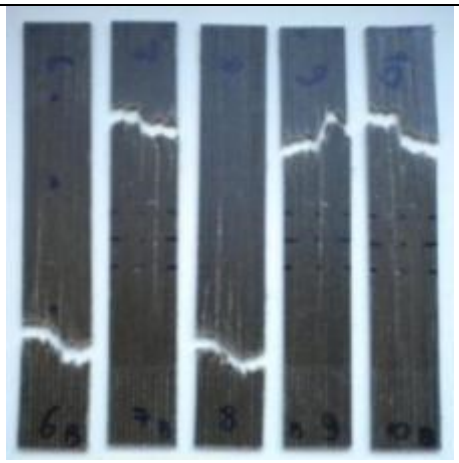

Neat flax/PET 40%, off-axis angle 0°

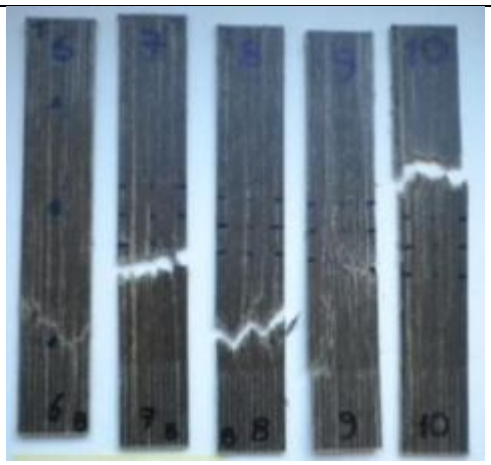

Neat flax/PET 50%, off-axis angle 0°

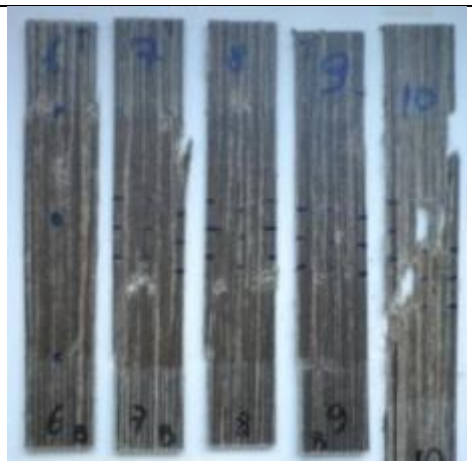

Neat flax/PET 60%, off-axis angle 0°

Neat flax/PET 30%, off-axis angle 30°

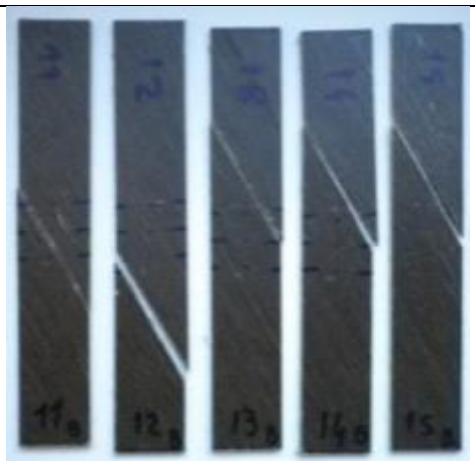

Neat flax/PET 40%, off-axis angle 30°

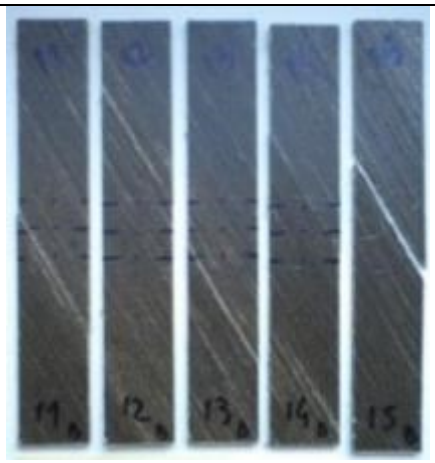

Neat flax/PET 50%, off-axis angle 30°

Neat flax/PET 60%, off-axis angle 30°

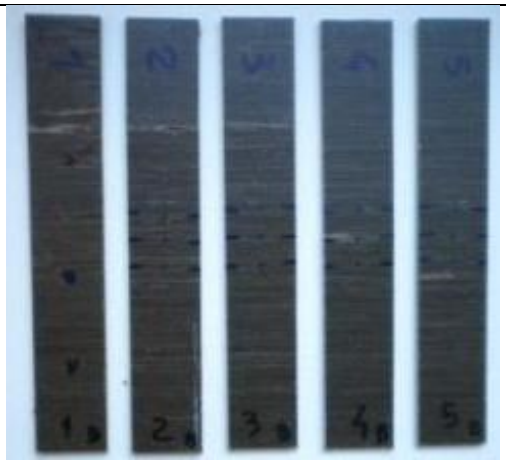

Neat flax/PET 30%, off-axis angle 90°

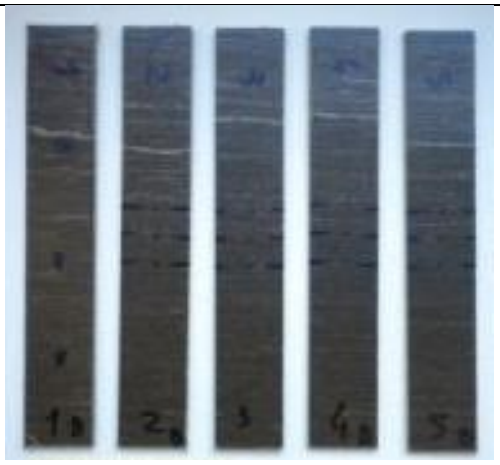

Neat flax/PET 40%, off-axis angle 90°

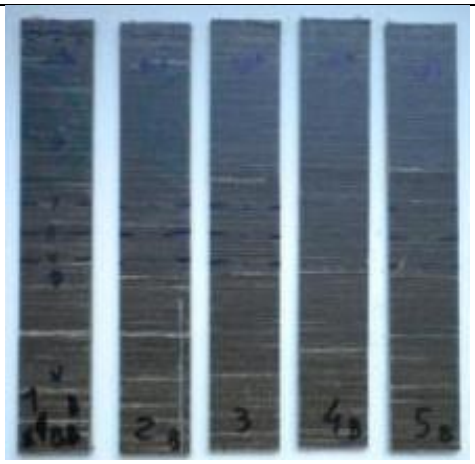

Neat flax/PET 50%, off-axis angle 90°

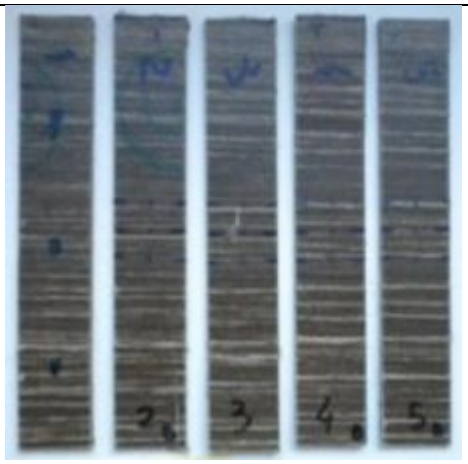

Neat flax/PET 60%, off-axis angle 90°

6.2.2 Influence of using composite pre-forms (twisted and blended yarns

a) Volumetric composition

Use of pre-forms results in a variation of composite microstructure, and in a consequent alteration of volumetric composition, as it can be noted observing Table 6.6.

Type of composite	Theorical Wf	Density (g/cm^3)	Vf	Vm	Vp
Twisted flax/PET	0.411	1.289±0.015	0.342	0.567	0.092
Blended flax/PET	0.410	1.174±0.013	0.311	0.517	0.172
Neat flax/PET 40%	0.383	1.342±0.004	0.332	0.618	0.050
Twisted flax/PLA	0.365	1.313±0.004	0.309	0.673	0.018
Blended flax/PLA	0.339	1.296±0.002	0.283	0.691	0.026
Neat flax/PLA 40%	0.398	1.303±0.003	0.335	0.633	0.033

Table 6.6 List of volume fraction values, densities and estimated fiber weight fraction for composites mad up using pre-forms (twisted yarns and blended yarns). Volumetric composition of neat flax/polymer matrix are reported as term of comparison.

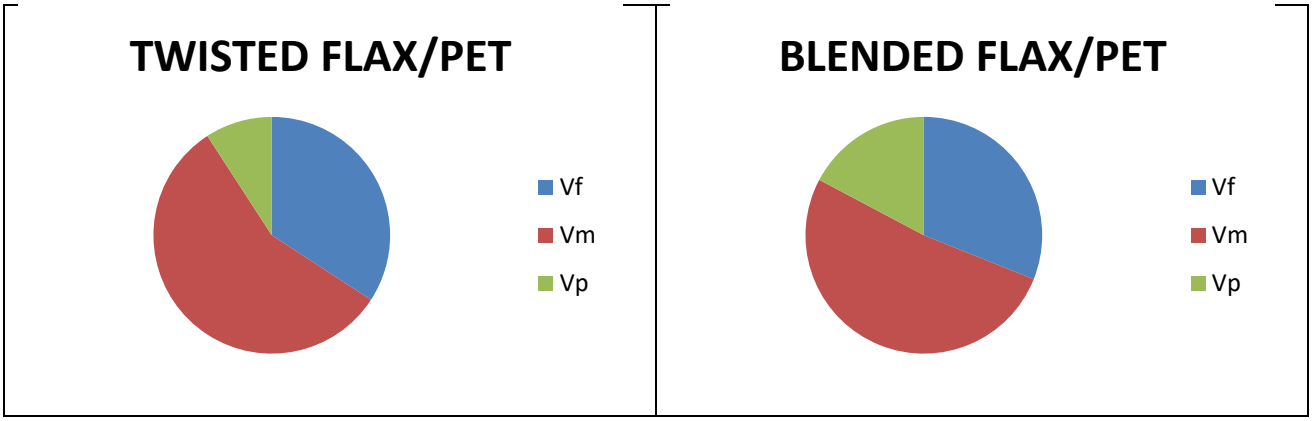

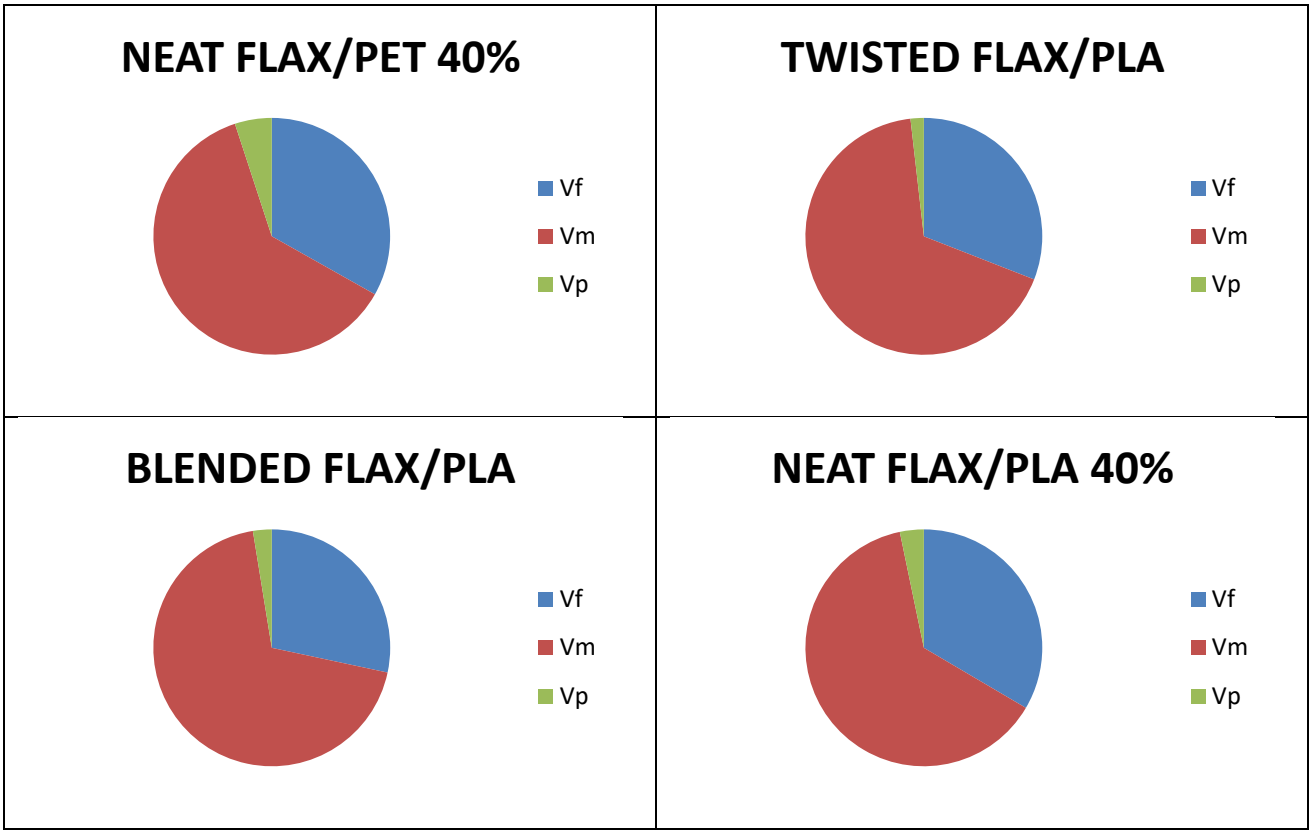

Figure 6.17 Schematic representation of volume fractions of composites made by using pre-forms Neat flax/polymer matrix are reported as term of comparison.

The charts show the effect of using pre-forms in composite manufacturing. However observing the results it cannot be said for a certainty that the effect on volumetric composition is good or not, since it is to a great extent affected by the matrix polymer type. In fact it seems that with PET matrix, the use of twisted yarns causes an increase of the porosity amount in respect with the neat flax/PET composite. However it must be considered that the fiber volume fraction of the composite having twisted yarns is slightly higher than the neat flax/PET composite, so this might explain the increased amount of porosity. Things change referring to the blended case, since the porosity fraction is higher than the neat flax/PET composite, even if the fiber volume fraction is lower. In fact the blended flax/PET composite shows the higher percentage of porosity of all made composites. With PLA matrix the differences between the three type of composites seem to be less evident, as depicted in Figure 6.17. Observing the amount of porosity there is not a great variation, but it must be considered that the fiber volume fraction of the composite with blended yarns is slightly lower than the other two composites.

b) Mechanical properties

List of tensile test results for a comparison between composite made up with pre-forms are reported in the following tables.

Off axis angle 0°			
Composite type	**Stiffness**	**Ultimate stress**	**Strain at ultimate stress**
	(GPa)	(MPa)	
Twisted flax/PET	18.4±1.0	171±12	1.512±0.1620
Blended flax/PET	10.6±0.8	94±7	2.140±0.1437
Neat flax/PET 40%	18.6±0.5	183±3	1.636±0.0383
Twisted flax/PLA	15.5±1.6	147±14	1.648±0.1426
Blended flax/PLA	12.2±0.4	109±4	2.063±0.0611
Neat flax/PLA 40%	18.2±0.3	164±12	1.602±0.1436

Table 6.7 List of tensile test results for 0° off-axis angle specimens with pre-forms and neat yarns as term of comparison. Stiffness, ultimate strength and strain at ultimate strength were measured.

Off axis angle 30°			
Composite type	**Stiffness**	**Ultimate stress**	**Strain at ultimate stress**
Twisted flax/PET	7.5±0.3	53±2	1.197±0.1305
Blended flax/PET	5.3±0.3	27±2	1.262±0.1328
Neat flax/PET 40%	6.9±0.2	49±1	1.036±0.0649
Twisted flax/PLA	7.9±0.4	47±3	1.033±0.0523
Blended flax/PLA	8.0±1.4	47±3	
Neat flax/PLA 40%	7.7±0.5	41±3	0.799±0.0577

Table 6.8 List of tensile test results for 30° off-axis angle specimens with pre-forms and neat yarns as term of comparison. Stiffness, ultimate strength and strain at ultimate strength were measured.

Off axis angle 90°			
Composite type	**Stiffness**	**Ultimate stress**	**Strain at ultimate stress**
Twisted flax/PET	3.2±0.2	16±1	1.123±0.1862
Blended flax/PET	1.9±0.1	10±0	1.339±0.1205
Neat flax/PET 40%	3.1±0.3	12±1	0.463±0.0722
Twisted flax/PLA	4.2±0.0	19±1	0.598±0.0347
Blended flax/PLA	4.2±0.1	19±1	0.665±0.0591
Neat flax/PLA 40%	3.8±0.1	13±1	0.478±0.0542

Table 6.9 List of tensile test results for 90° off-axis angle specimens with pre-forms and neat yarns as term of comparison. Stiffness, ultimate strength and strain at ultimate strength were measured.

Blended yarn effect

Observing the stiffness and ultimate strength data, the results point towards that the blended yarns deteriorate the composite properties. In fact it can be observed that in both the stiffness and the ultimate strength cases the blended values are the lowest. All the data show the same trend, except the experimental tests of PLA in 30° and 90° off-axis directions. Surprisingly they show a little improvement of properties by using blended yarns. However it has been considered that this alteration is not representative of the composites overall behavior because is more restricted in respect to the properties variation of the 0° off-axis samples, and it is referred only to PLA. All the PET data seem to confirm the damaging effect of blending.

The main characteristic observed is the increase of strain at ultimate stress for all the composites with blended yarns. The data of strain at ultimate stress referred to blended flax/PET composite is missing because a problem with one extensometer occurred during the tensile test.

The initial idea that a great number of weak places along the yarns might was present, with the subsequent formation of weak places along the yarn length with low twist level where fibers are free to slide, has been excluded. In fact the standard deviation of the measured blended yarn diameter is not higher than the other yarn cases since considering the ratio between standard deviation and mean diameter, all the results are approximately in the same range around 10-15%.

Instead it is believed that this properties deterioration is due to the messy areas which have been observed with the optical microscope. In fact even if the mixing between fibers and matrix, and the fibers distribution among the polymer are good using the blended yarns, probably they are not enough to allow a good mechanical behavior.

It can be inferred that the fiber alignment is much more important for elevate composite performance and with the blended yarns it is too low, because of the presence of disordered zones in which of them the single fibers seem to be too much deviated from the optimal direction. It might also be that the measured properties are low owing to a poor quality processing, therefore further experiments could be carried out to make blended yarns having a more regular fiber alignment.

Twisted yarn effect

It has been observed that the composite behavior changes slightly depending on the type of polymer used as matrix, especially in the stiffness results. This difference is supposed to be generated during the composite manufacturing, since it might be that the diverse matrix influences the flax fibers diffusion throughout the moulding phase. The PET composites show a restrict variation passing from neat flax fibers to twisted yarns, since the variation is below 8% for any off-axis angle. Differently referring to the PLA composites the percentage difference is higher since the 0° tests show a worsening up to 15%, whereas the 30° and 90° tests show a little improvement, below 8%. Focusing on the ultimate strength the discrepancy between PLA and PET results is somehow attenuated since both the composites with twisted pre-forms show higher properties in the 30° and 90° tests (about 10% and 27% more, respectively), while observing the data of the 0° case it can be inferred that the resistance is made less strong (about 8%).

The inspection of experimental data doesn’t allow to state that the twisted yarns are a good alternative to improve of composite mechanical properties. In fact it can be said neither that the use of twisted yarn provides a neat improvement of composite properties, nor that it clearly deteriorates performances. Therefore the use of twisted yarns in composite manufacturing might represent a good option in that cases where it is preferred to obtain the yarns already containing both reinforcement fibers and matrix, without having to mix them. This possibility could be interesting if the optimal fiber weight fraction was known, in order to make the suppliers produce directly the yarns that will be used in the final composite.

Another idea could be to twist the PET fibers around flax yarns, instead of twisting flax around polymer yarns. In this way the reinforcement fibers in the composite could be kept more aligned, whereas the twisted orientation of the polymer fibers would be lost as it is melted during the moulding process.

c) Microstructure

In this section some ESEM and OM images of composites are reported to illustrate different examples of porosities in composites made with pre-forms and the main differences with respect to the neat flax/polymer composites.

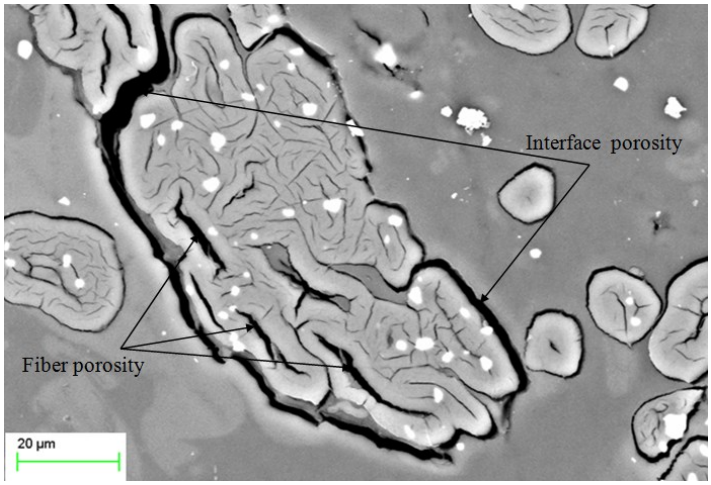

Figure 6.18 ESEM image of twisted flax/PLA composite cross-section. Scale bar is 30 µm. Different types of porosity are shown.

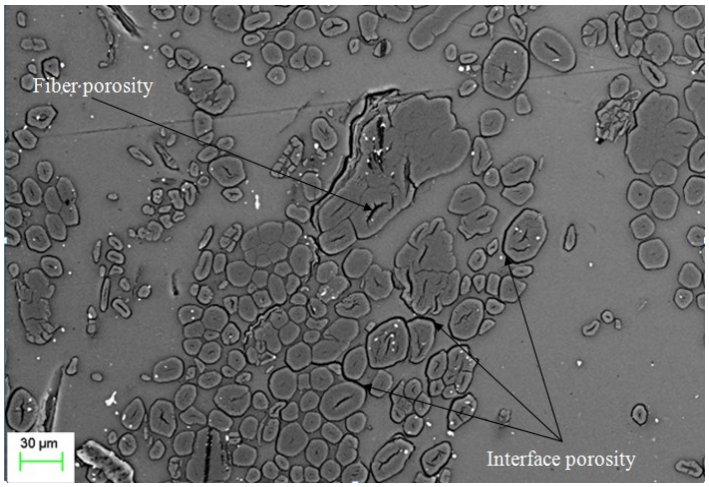

Figure 6.19 ESEM image of blended flax/PET composite cross-section. Scale bar is 20 µm. Different types of porosity are shown. The irregular shaped white flecks are probably impurities induced during the polishing process.

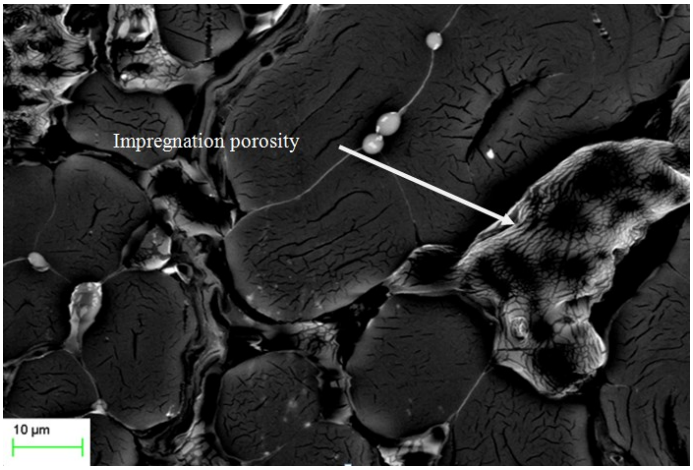

Figure 6.20 ESEM image of twisted flax/PLA composite cross section. Scale bar is 10 µm. Typical example of impregnation porosity is shown.

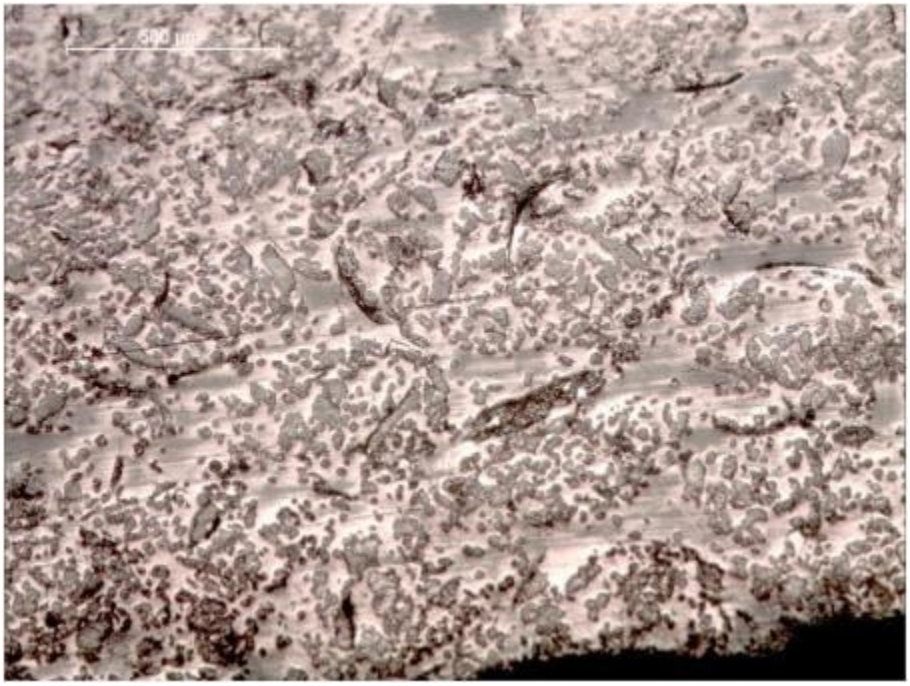

Figure 6.21 OM image of blended flax/PLA composite cross section. Scale bar is 500 µm.

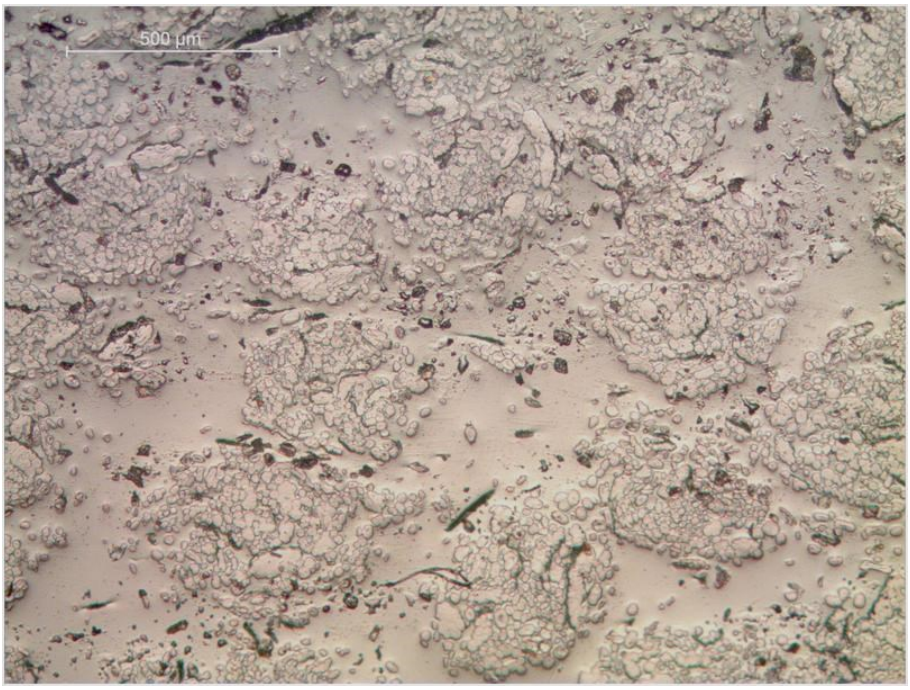

Figure 6.22 OM image of twisted flax/PLA composite cross section. Scale bar is 500 µm

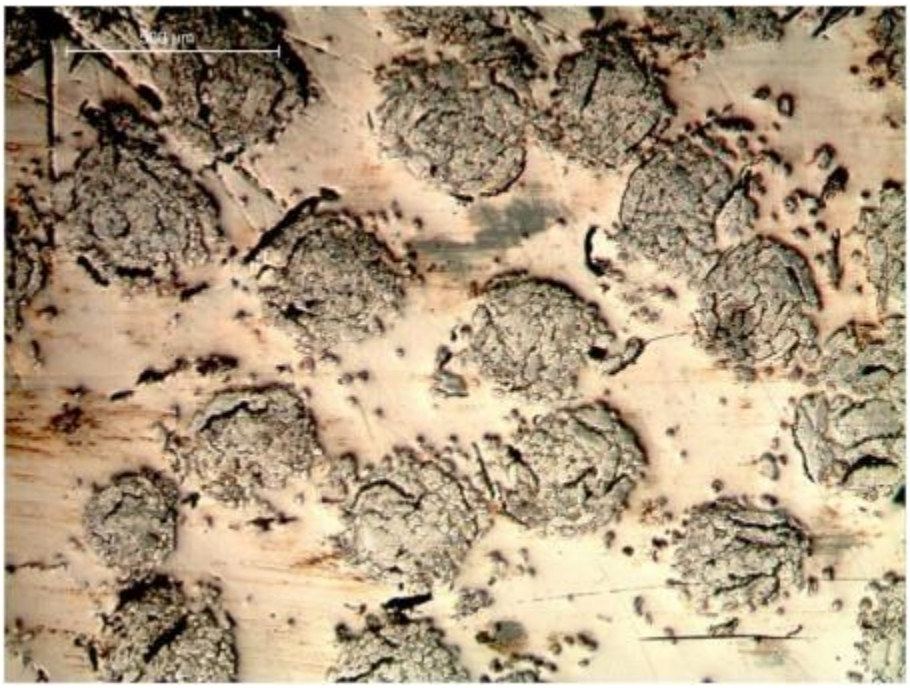

Figure 6.23 OM image of neat flax/PLA 40% composite cross section. Scale bar is 500 µm.

The first three images show typical examples of porosities in composites with twisted and blended yarns. The porosity sub-components (fiber porosity, interface porosity, and impregnation porosity [4]) are the same observed in neat plant yarn composites.

The second group of images demonstrates how different the yarn bundle contours are, if the type of pre-form is changed. PLA composites have been taken as reference, since no substantial variations were observed with PET composites. In the composite with neat yarns, the fiber bundles among the matrix part are very defined, whereas with twisted yarns the contours get a little more confused for the higher dispersion of single fiber parts. Differently in the blended case no bundles are visible and the distribution of fiber in the polymer part seems to be very uniform.

d) Failure characteristics

0° tests

Images of fractured surfaces of composites with twisted and blended yarns were observed, in order to find some possible similarities. It has been noted that all the specimens having 0° off-axis angle show a marked fracture edge, since two broken parts were made in all of cases when fracture occurred. No noteworthy differences have been found between the two composite types except for the location of the fracture and the shape of fracture edges. The composites with blended yarns (both with PLA matrix and PET matrix) are characterized by a fracture which is close to the middle of the sample and with a straighter edge, whereas the composites with twisted yarns show a breaking very close to the clamping zones and their fracture profile is more jagged.

30° tests

Almost all the fractured surfaces are oriented at 30° and no noteworthy differences have been noticed between composites with twisted and blended yarns. The only observation refers to a sort of concavity exhibited in the blended flax/PLA breaking profile.

90° tests

The most relevant observation regards composite with blended yarns since it is the only one case in which two separated parts were not formed when fracture occurred, similarly to what has been observed with the respective 30° samples. No noteworthy differences have been found between the two composites with twisted yarns.

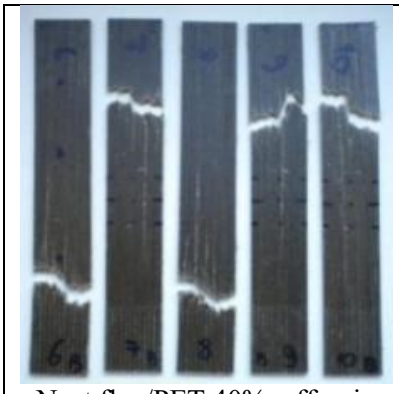

Neat flax/PET 40%, off-axis angle 0°

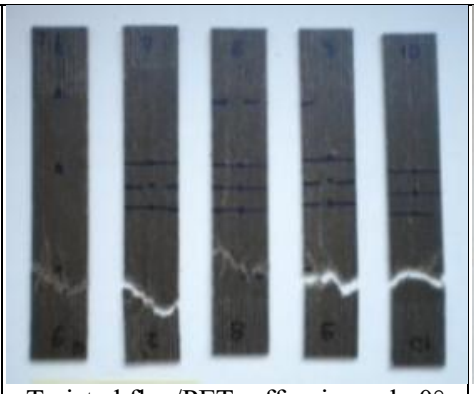

Twisted flax/PET, off-axis angle 0°

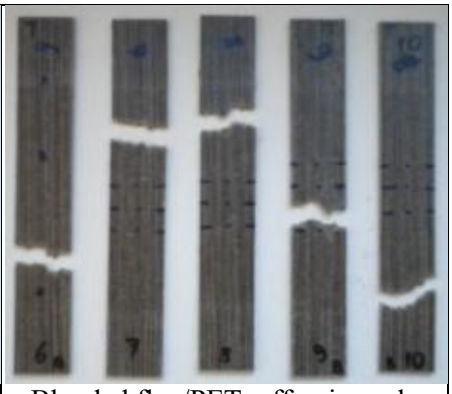

Blended flax/PET, off-axis angle 0°

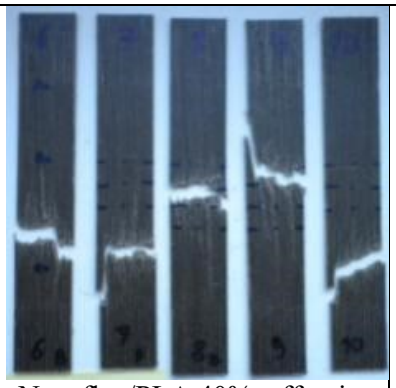

Neat flax/PLA 40%, off-axis angle 0°

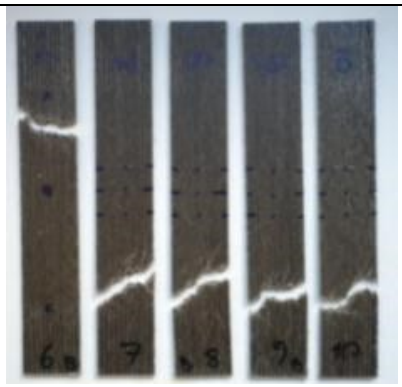

Twisted flax/PLA, off-axis angle 0°

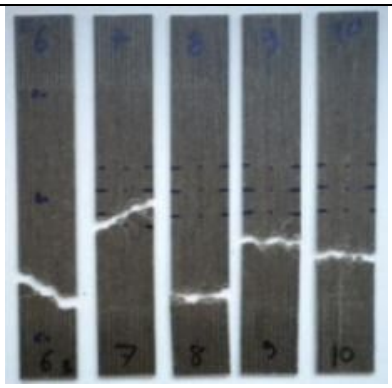

Blended flax/PLA, off-axis angle 0°

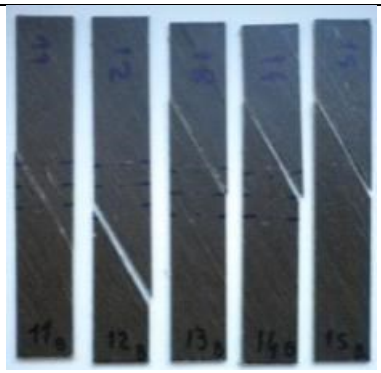

Neat flax/PET 40%, off-axis angle 30°

Twisted flax/PET, off-axis angle 30°

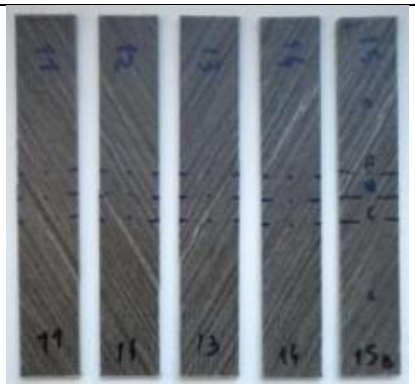

Blended flax/PET, off-axis angle 30°

Neat flax/PLA 40%, off-axis angle 30°

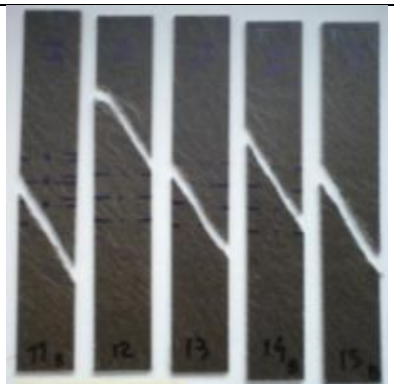

Twisted flax/PLA, off-axis angle 30°

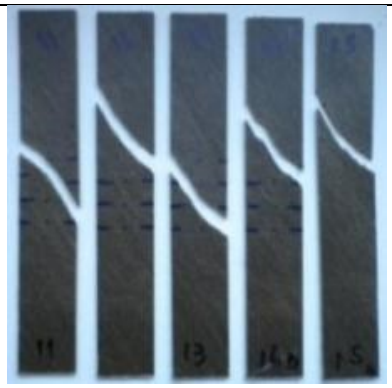

Blended flax/PLA, off-axis angle 30°

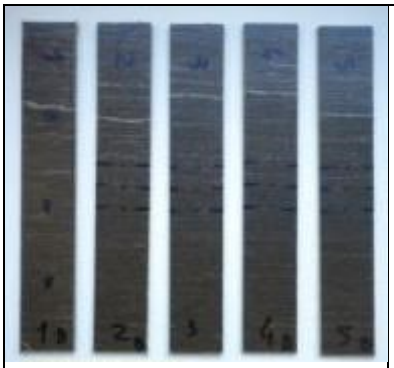

Neat flax/PET 40%, off-axis angle 90°

Twisted flax/PET, off-axis angle 90°

Blended flax/PET, off-axis angle 90°

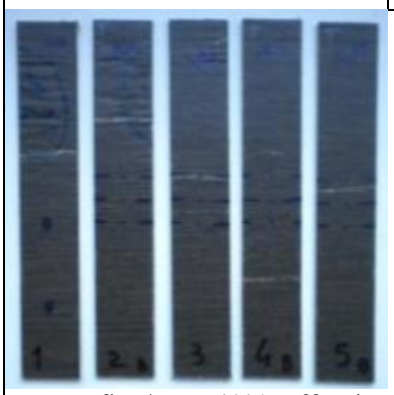

Neat flax/PLA 40%, off-axis angle 90°

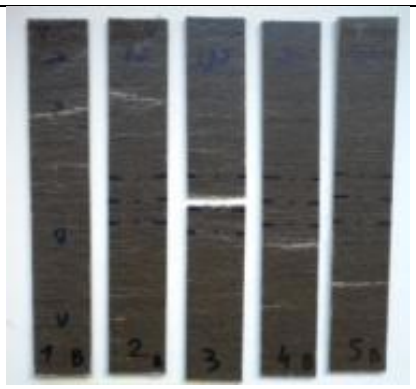

Twisted flax/PLA, off-axis angle 90°

Blended flax/PLA, off-axis angle 90°

6.2.3 Influence of matrix type

a) Volumetric composition

In this section, volume fraction results obtained changing matrix polymer type are reported. The comparison has been carried out considering both the composites made by using neat yarns, and the composites made by using pre-forms.

Type of composite	Theorical Wf	Density (g/cm^3)	Vf	Vm	Vp
Twisted flax/PET	0.411	1.289±0.015	0.342	0.567	0.092
Twisted flax/PLA	0.365	1.313±0.004	0.309	0.673	0.018
Blended flax/PET	0.410	1.174±0.013	0.311	0.517	0.172
Blended flax/PLA	0.339	1.296±0.002	0.283	0.691	0.026
Neat flax/PET 40%	0.383	1.342±0.004	0.332	0.618	0.050
Neat flax/PLA 40%	0.398	1.303±0.003	0.335	0.633	0.033

Table 6.10 List of volume fraction values and estimated fiber weight fraction for composites to evaluate the effect of changing matrix type.

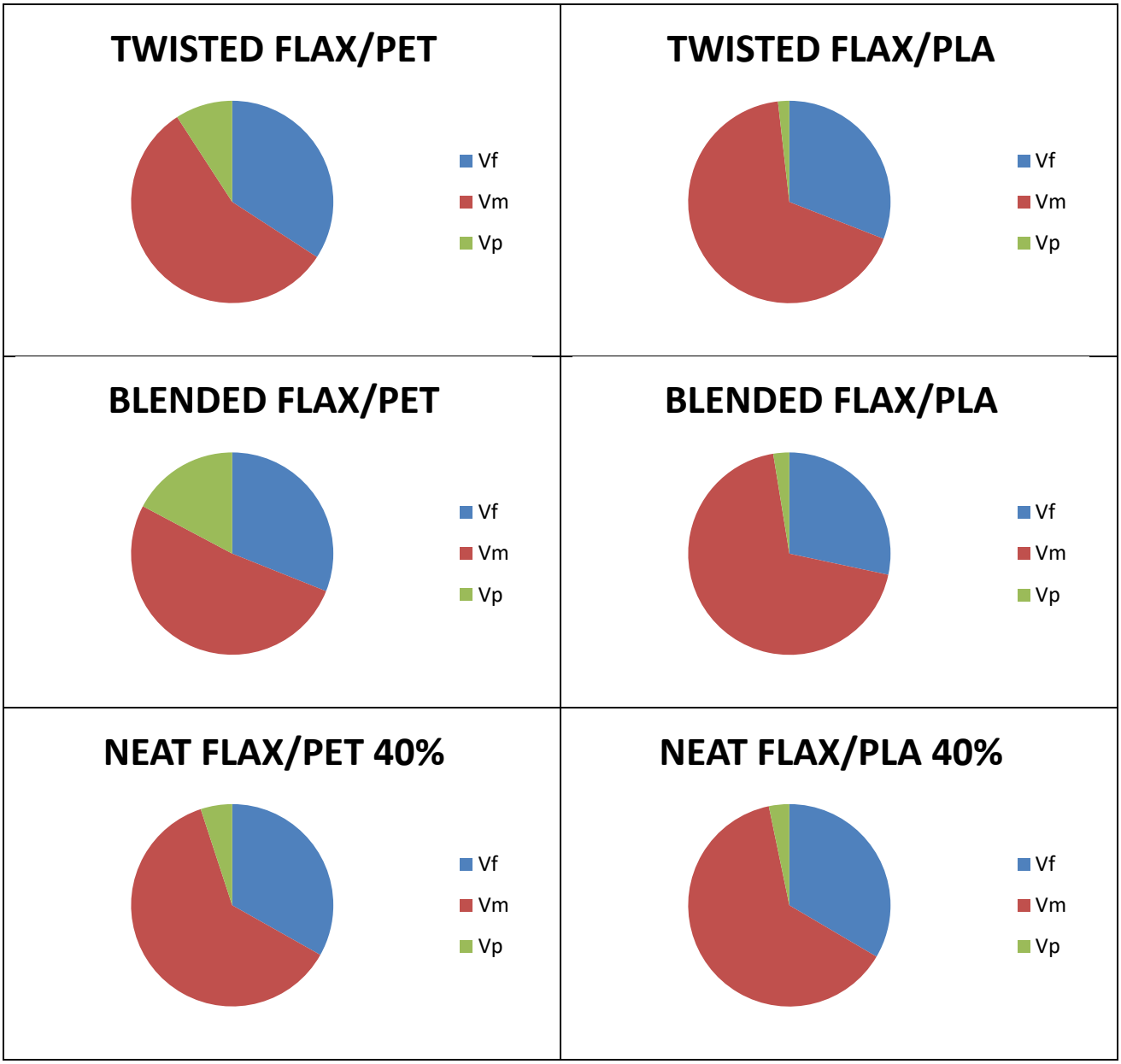

Figure 6.24 Schematic representation of different volume fractions of composite varying the type of matrix.

The results point towards that the porosity volume fraction are higher if PET is used as matrix. In fact it can be observed that for a given type of yarn the amount of porosity is increased, passing from a PLA matrix to a PET matrix. The difference is more marked when pre-forms are used. Especially in the blended yarn case, the percentage of porosity results to be very increased.

b) Mechanical properties

List of tensile test results are reported in the following tables. The data of strain at ultimate stress referred to blended flax/PET composite is missing because a problem with one extensometer occurred during the tensile test.

Off axis angle 0°			
Composite type	**Stiffness**	**Ultimate stress**	**Strain at ultimate stress**
	(GPa)	(MPa)	
Twisted flax/PET	18.4±1.0	171±12	1.512±0.1620
Twisted flax/PLA	15.5±1.6	147±14	1.648±0.1426
Blended flax/PET	10.6±0.8	94±7	2.140±0.1437
Blended flax/PLA	12.2±0.4	109±4	2.063±0.0611
Neat flax/PET 40%	18.6±0.5	183±3	1.636±0.0383
Neat flax/PLA 40%	18.2±0.3	164±12	1.602±0.1436

Table 6.11 List of tensile test results for 0° off-axis angle specimens with different matrix type. Stiffness, ultimate strength and strain at ultimate strength were measured.

Off axis angle 30°			
Composite type	**Stiffness**	**Ultimate stress**	**Strain at ultimate stress**
Twisted flax/PET	7.5±0.3	53±2	1.197±0.1305
Twisted flax/PLA	7.9±0.4	47±3	1.033±0.0523
Blended flax/PET	5.3±0.3	27±2	1.262±0.1328
Blended flax/PLA	8.0±1.4	47±3	
Neat flax/PET 40%	6.9±0.2	49±1	1.036±0.0649
Neat flax/PLA 40%	7.7±0.5	41±3	0.799±0.0577

Table 6.12 List of tensile test results for 30° off-axis angle specimens with different matrix type. Stiffness, ultimate strength and strain at ultimate strength were measured.

Off axis angle 90°			
Composite type	**Stiffness**	**Ultimate stress**	**Strain at ultimate stress**
Twisted flax/PET	3.2±0.2	16±1	1.123±0.1862
Twisted flax/PLA	4.2±0.0	19±1	0.598±0.0347
Blended flax/PET	1.9±0.1	10±0	1.339±0.1205
Blended flax/PLA	4.2±0.1	19±1	0.665±0.0591
Neat flax/PET 40%	3.1±0.3	12±1	0.463±0.0722
Neat flax/PLA 40%	3.8±0.1	13±1	0.478±0.0542

Table 6.13 List of tensile test results for 90° off-axis angle specimens with different matrix type. Stiffness, ultimate strength and strain at ultimate strength were measured.

The results of tensile tests with any off-axis angle, point towards that the PLA matrix give a better behavior than PET matrix, if blended yarns are used as pre-form since both stiffness and ultimate strength have resulted to be higher. The same cannot to be said for twisted yarns and neat yarns, because the properties vary depending on the off-axis angle. With the 0° specimens, PET with twisted pre-form provides a better composite behavior, both for stiffness and strength, whereas with the 30° samples PET offers performance comparable with PLA. Differently, PLA composite with twisted yarns shows higher stiffness and strength if the angle is increased to 90° . Finally if no pre-forms are used, no clear trend of composite behavior have been found using either PLA or PET composites, since the mechanical properties go up and down without a definite law.

c) Microstructure

In this section images taken with electron microscope and optical microscope are reported to investigate any differences in composite microstructure due to the change of matrix type.

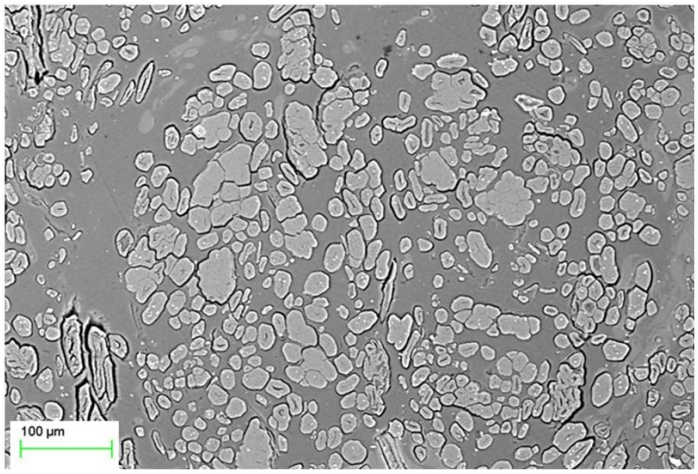

Figure 6.25 ESEM image of blended flax/PET composite cross-section. Scale bar is 100 µm.

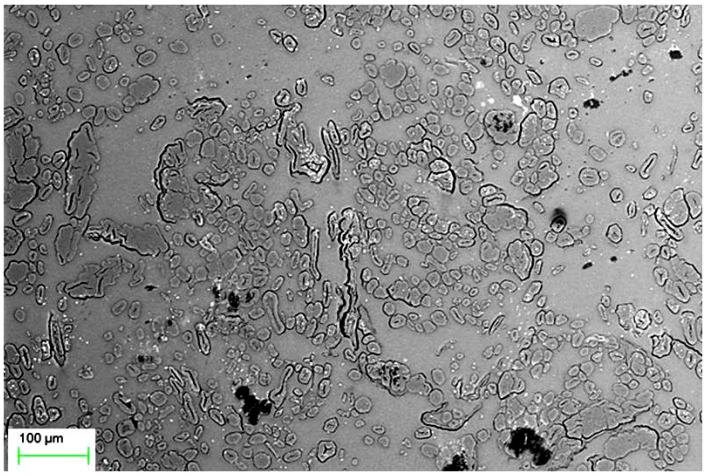

Figure 6.26 ESEM image of blended flax/PLA composite cross section. Scale bar is 100 µm.

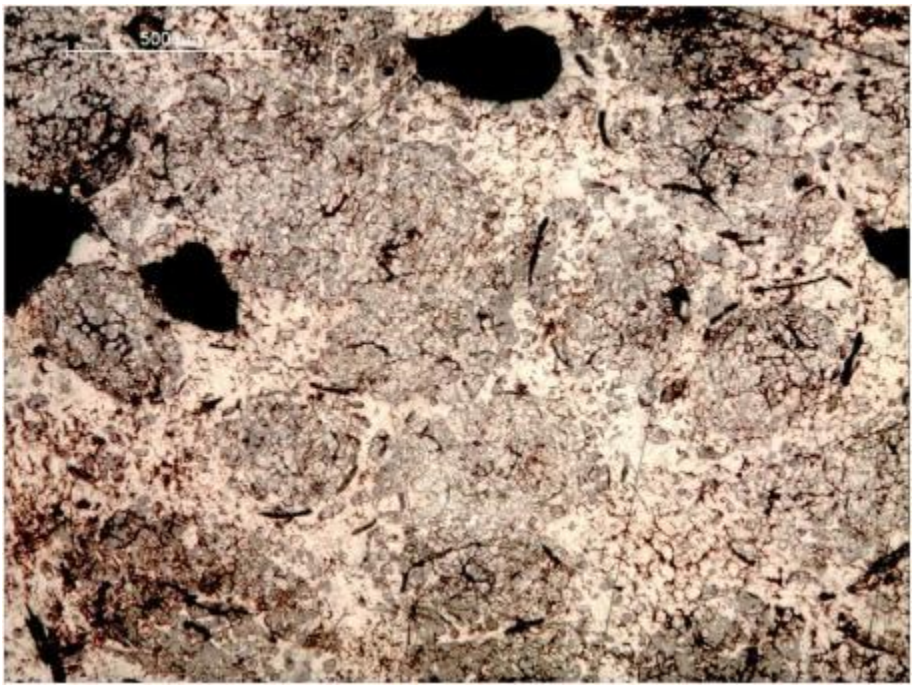

Figure 6.27 OM image of twisted flax/PET composite cross section. Scale bar is 500 µm.

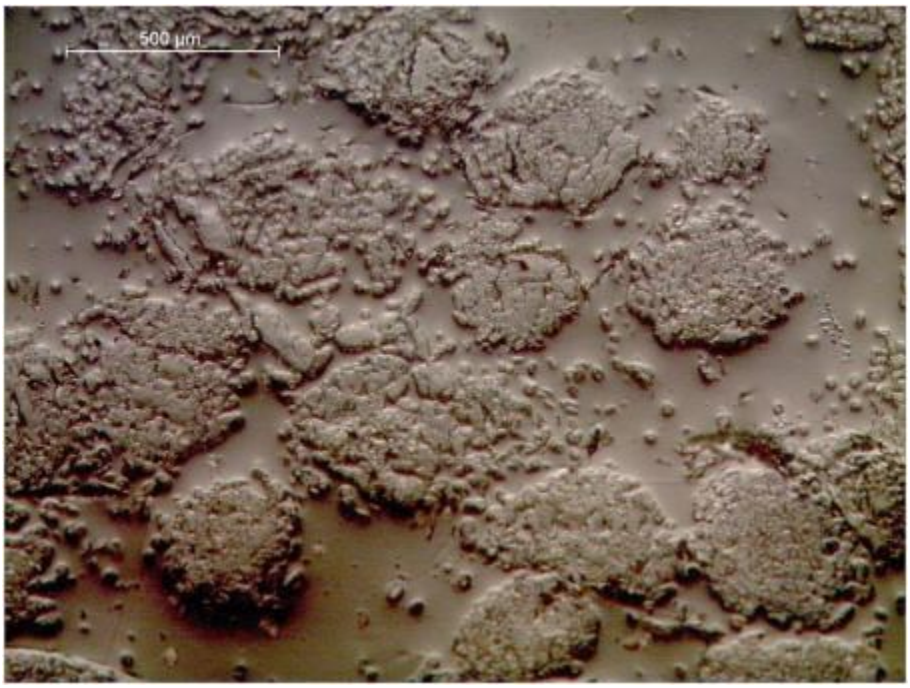

Figure 6.28 OM image of twisted flax/PLA composite cross section. Scale bar is 500 µm.

In all the cases no noteworthy differences of microstructure between PET composites and PLA composite have been noticed, therefore images of composites with neat flax yarns have not been reported.

d) Failure characteristics

0° tests

Analyzing the images of fractured surfaces of samples having 0° off-axis angle, it has been observed that there's a marked resemblance for both PLA and PET composites having neat flax yarns. In fact they exhibit a very similar behavior, even if it has been noted that the breaking surface of PLA samples is a little more indented, with a fracture characterized by the formation of two separated pieces, as it has been seen for twisted and blended yarn composites.

30° tests

In the 30° off-axis angle case, it has been observed that almost all specimens are characterized by a fracture edge oriented at 30°. Therefore it can be inferred that both axial and shear stress are present. Regularity of the fracture sections, with absence of notches, has been observed in most of the samples. Only in the case of PLA composites it has been observed that, even if the fracture edge follows the 30° direction, the shape is a bit more irregular.

90° tests

No substantial differences have been observed changing matrix type. Only in the case of composites with blended yarns it can be noted that the PET samples show a different type of failure with respect to PLA since not in all cases a complete separation in two parts occurred.

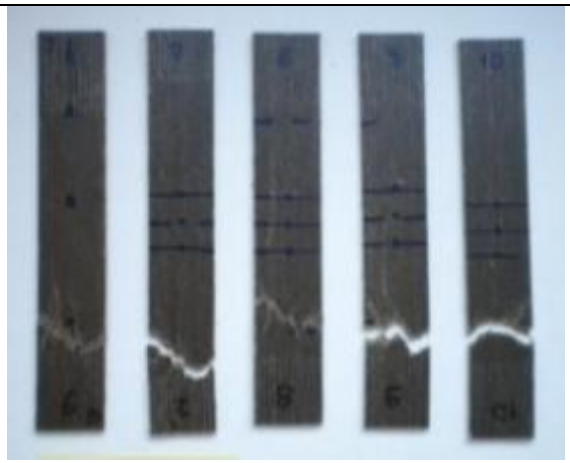

Twisted flax/PET, off-axis angle 0°

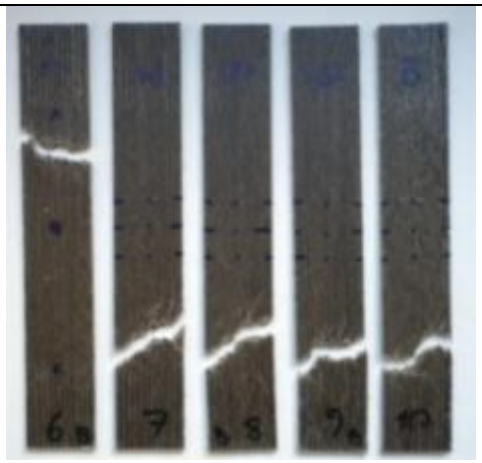

Twisted flax/PLA, off-axis angle 0°

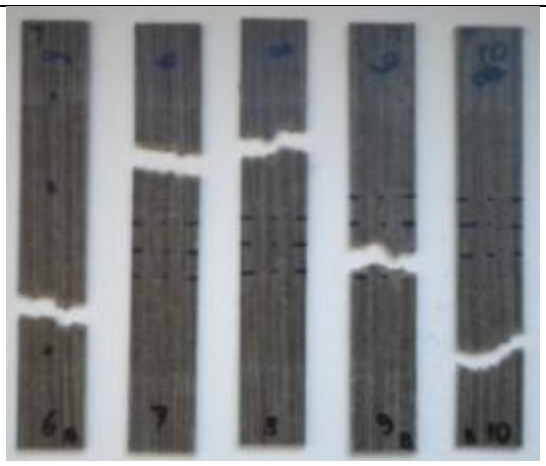

Blended flax/PET, off-axis angle 0°

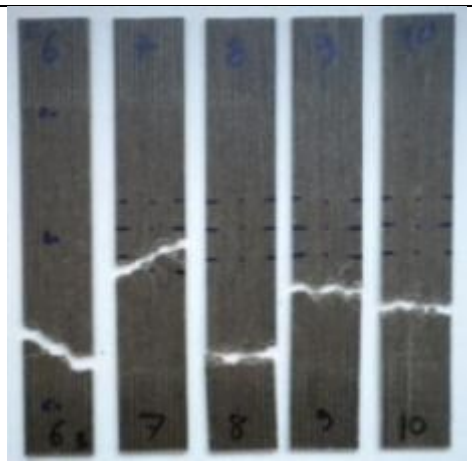

Blended flax/PLA, off-axis angle 0°

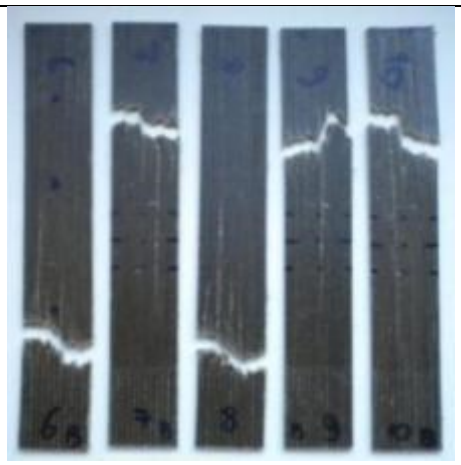

Neat flax/PET 40%, off-axis angle 0°

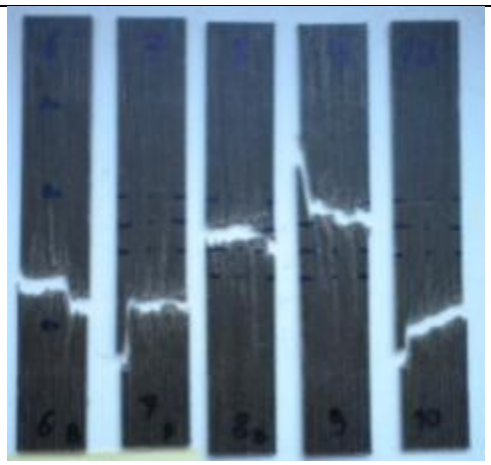

Neat flax/PLA 40%, off-axis angle 0°

Twisted flax/PET, off-axis angle 30°

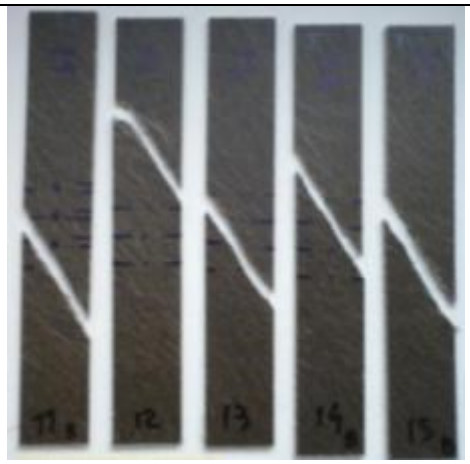

Twisted flax/PLA, off-axis angle 30°

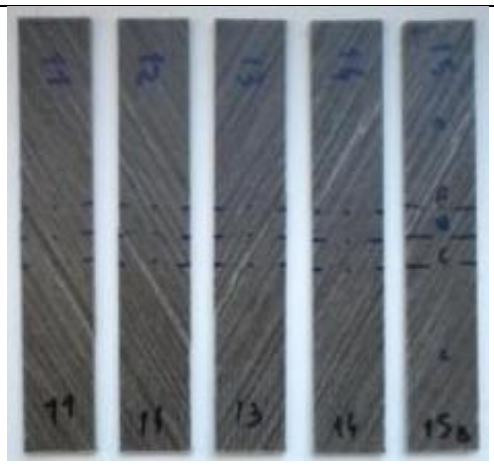

Blended flax/PET, off-axis angle 30°

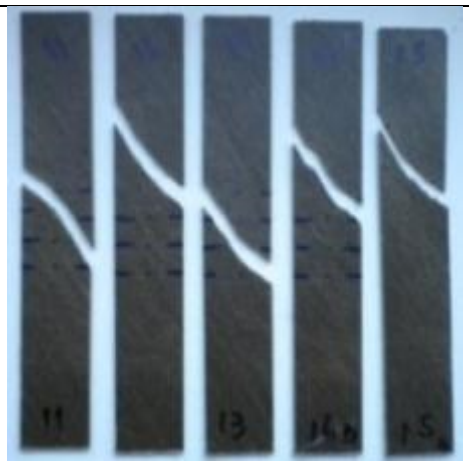

Blended flax/PLA, off-axis angle 30°

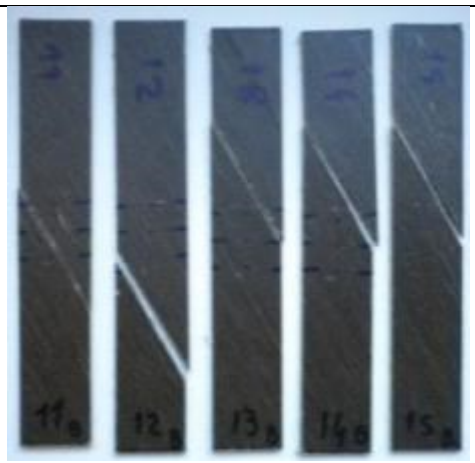

Neat flax/PET 40%, off-axis angle 30°

Neat flax/PLA 40%, off-axis angle 30°

Twisted flax/PET, off-axis angle 90°

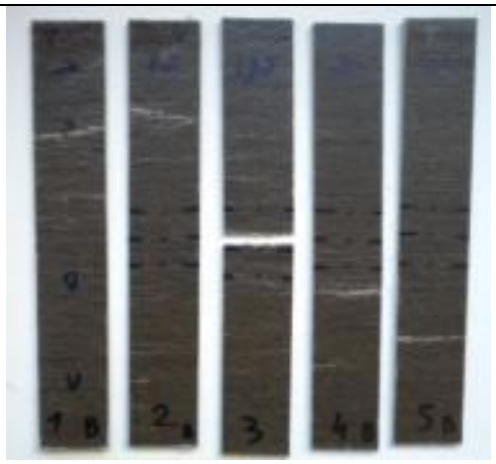

Twisted flax/PLA, off-axis angle 90°

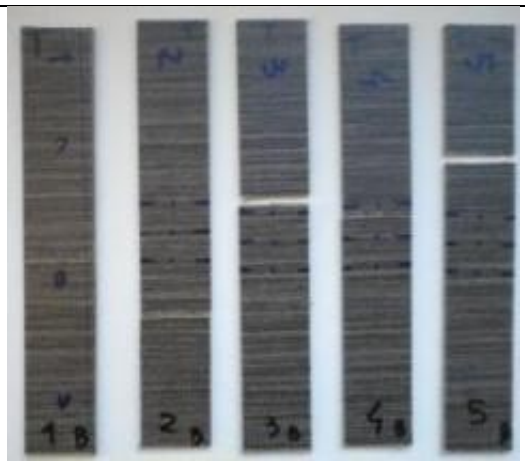

Blended flax/PET, off-axis angle 90°

Blended flax/PLA, off-axis angle 90°

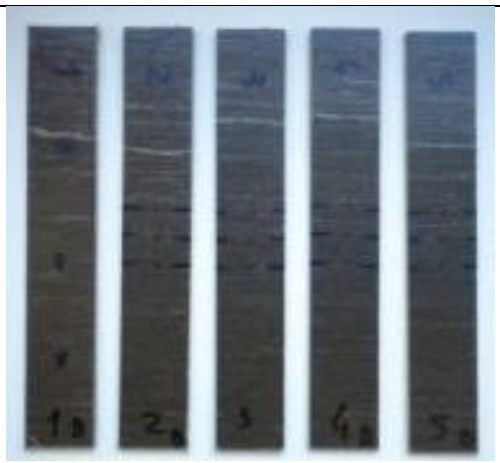

Neat flax/PET 40%, off-axis angle 90°

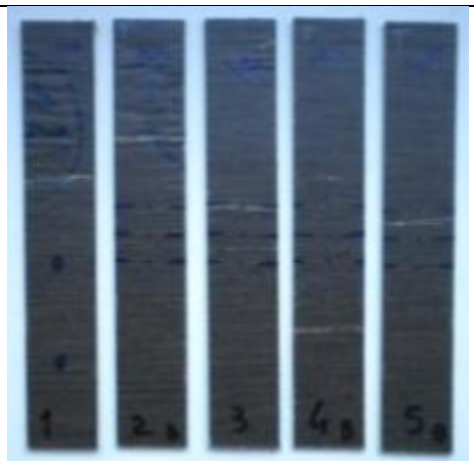

Neat flax/PLA 40%, off-axis angle 90°

6.3 FIBER PROPERTIES ESTIMATION

Once tensile tests had been carried out, and mechanical properties of each composite had been measured, it was attempted to investigate the correlation with flax fiber properties. In the previous studies it has been always assumed that the off-axis angle is referred to the yarn angle but actually, going into more depth, it cannot be said that the off-axis angle of the yarn represents also the inclination of the flax fibers, because it is also biased by the fiber twisting angle, whose effect is not negligible. Therefore it has been tried to correlate the mechanical properties of the composites at the three different off-axis angles (0°, 30° and 90°) with the fiber properties. The analysis has been conducted focusing on both the stiffness and the ultimate strength. Three models have been developed attempting to improve the estimation of composite properties. Once well approximated values had been obtained, fiber stiffness and fiber ultimate strength were back calculated. The main purpose of this analysis is the assessment of a procedure that could help during the design of composite material products, providing a useful tool that, for a given range of required UD fiber composite properties, is able to predict the prerequisites of the fiber reinforcement. To get an idea about the reliability of the modeling results, a confront with the predicted mechanical properties of fibers has been made. This prediction is based on a study of Madsen et.al. [31] which is focused on the effect of processing on fiber bundle strength.

6.3.1 Expected results

The study of the relationship between flax fiber strength and processing might be helpful for the estimation of the theoretical upper limit of fiber mechanical properties. In fact it was found that the trend between strength and the number of processing steps is monotonically decreasing. Each step reduces the fiber bundle strength approximately by 27% [31]. It was demonstrated that both the cellulose content and the crystallinity of cellulose were not consistently affected by mechanical processing. Their values are respectively around 71% and 93% [31]. Therefore the disorder regions (defects) must be correlated with different characteristics as chemical defects or delamination between the layers in the cell wall. [32] [33]. It was found that, assuming a 100% cellulose content, the effective bundle strength of unprocessed fibers is around 1600 MPa. From studies of Bos et al.(2002) one group of flax fiber were hand peeled in order to minimize the weakening effect due to the processing, and showed a strength for single fibers of 1834 MPa [34]. On the other side, when the number of processing steps is above 2, the expected strength falls below 900 MPa. Based on these considerations, an acceptable range for back-calculated ultimate strength of the flax fiber has been supposed to be around 1200/1600 MPa.

6.3.2 Fiber stiffness evaluation procedure

Assuming a state of plane stress, and that tensile properties of flax yarn composites are orthotropic, the tensile stiffness at a given angle to the yarn axis ($E_{c\theta}$) can be estimated as [35]:

$$\frac{1}{E_{c\theta}} = \frac{\cos^4\theta}{E_{c1}} + \frac{\sin^4\theta}{E_{c2}} + \sin^2\theta\cos^2\theta\left(\frac{1}{G_{c12}} - \frac{2\nu_{12}}{E_{c1}}\right) \qquad 6.12$$

where G represents shear stress, ν is Poisson's ratio and the subscripts 1 and 2 are referred to axial direction and transverse direction, respectively. The constant G_{c12}, which represents the shear stiffness of the composites, can be estimated by the semi-empirical expression of Halping and Tsai [36] using the modified equation to consider the porosity effect:

$$G_{c12} = \frac{G_m(1+\xi\eta V_f)}{(1-\eta V_f)(1-V_P)^2} \qquad 6.13$$

where η and G_m are respectively obtained by means of the following formulas, hypothesizing that the matrix properties are isotropic:

$$\eta = \frac{\frac{G_f}{G_m} - 1}{\frac{G_f}{G_m} + \xi} \qquad 6.14$$

$$G_m = \frac{E_m}{2(1+\nu_m)} \qquad 6.15$$

where ξ is a fiber shape factor set equal to 2 by assuming circular fiber cross sections [37] whereas E_m and ν_m represent respectively the stiffness and the Poisson's ratio of the polymer matrix. Based on findings of studies of Madsen [35], PET stiffness was assumed to be equal to 2.7 GPa, while for PLA is was considered to be 3.4 GPa [1]. Previously, ν_m was measured to be 0.4 for neat PET specimens [3], and the same value was assumed to be also a good approximation for PLA samples. From the study by Cichocki and Thomason [38] it was assumed that ν_{c12} is around 0.1 below ν_m thus it was set equal to 0.3, both for PET and PLA composites. Referring to findings of Madsen et al. [35] it was observed that G_f must be at least 8 GPa to fit the experimental data of Hemp/PET

composites. Because of the similarity between hemp fiber and flax fiber, in the present analysis it was also decided to set the value of G_f equal to 8 GPa. Comparing the typical value of G_m (≈1 GPa) with the typical value of G_f (surely higher than 1 GPa), it can be detected that the shear stiffness of the composite (G_{c12}) is primarily governed by the matrix shear stiffness [35].

Once all the foregoing parameters were calculated for each composite, it was attempted to convert the experimental composite stiffness measured at the three off-axis angle (0°, 30° and 90°) into more correct values, considering that the real angle of fibers is different with respect to the yarn angle, because of their twisting angle. In the next sections, the fundamental considerations that represent the framework of the analysis are explained.

O° angle correction

At first, the trend of composite stiffness in function of the yarn angle was plotted, basing on the three experimental points obtained from the three different tensile tests, with 0°, 30° and 90° off-axis angles. So far the fiber angle effect has been neglected in all the previous studies, since it was thought that for small angles the predicted stiffness curve does not change significantly with respect to the intercept at 0°. It can clearly noted that the stiffness measured by the 0° sample tests is actually referred to an angle which is different from zero, and the difference is not negligible. In fact, even if the yarns are parallel to the tensile axis, each single fiber is oriented to the two directions +φ and –φ, where φ is the single fiber angle in respect to the yarn axis. Since the exponent of the trigonometric functions in Equation 6.12 is even, there's not dependency on the angle sign, therefore in this case only the positive value of the angle has been considered. This means that the measured stiffness at the point A in the stiffness-yarn angle plot actually corresponds with the point A' in the stiffness-fiber angle plot (see Figure 6.31 and Figure 6.32) because it is shifted from 0° to 0°+φ. It must be highlighted that in this way, E_{c1} represents now an unknown, differently from the previous studies, and it needs to be investigated and evaluated as fitting parameter from experimental data. The equation for tensile stiffness must be modified because it needs to be referred to the fiber angle φ instead of the yarn angle θ:

$$\frac{1}{E_{c\varphi}} = \frac{\cos^4\varphi}{E_{c1}} + \frac{\sin^4\varphi}{E_{c2}} + \sin^2\varphi\cos^2\varphi\left(\frac{1}{G_{c12}} - \frac{2\nu_{12}}{E_{c1}}\right) \qquad 6.16$$

90° angle correction

Similarly to the 0° degrees case, the point C in the stiffness-yarn angle plot corresponds with the point C' in the stiffness-fiber angle plot (see Figure.6.32). It has been observed that the variation of the stiffness in the two cases is negligible, as in the proximity of 90° the trend of the line is asymptotic, thus it was assumed that E_{c2} has the same value of the stiffness at point C'. In this case, for simplicity, it has been selected 90°-φ as angle instead of taking 90°+φ in order to keep the angle range between 0° and 90°.

30° angle correction

This represents the most complicated case in the analysis, as the experimental stiffness at 30° must be split up into two contributes instead of only one. This occurs because both the angles 30°+φ and 30°-φ need to be considered, therefore it must be understood how to integrate them in the model.

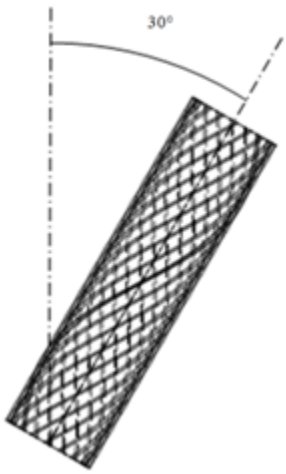

Figure 6.29 Representation of a generic yarn inclined at a 30° with respect to the tensile test axis. It can be clearly observed how the real fiber inclination follow the two direction 30°+φ and 30°-φ.

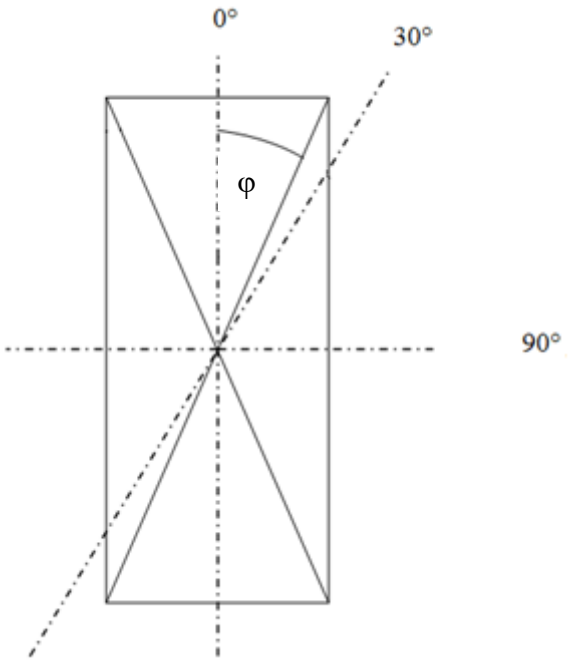

Figure 6.30 Schematization of a generic element of composite. The generic fiber angle φ is indicted, and the three axial test direction (0°,30, and 90°) are depicted. It is possible to see the correlation between the two directions: at 0° the fiber orientation is ±φ, at 30° it is 30°-φ and 30°+φ, at 90° is 90°±φ.

a)First model: average method

Based on the previous considerations it can be observed that at the moment two unknowns are present in the equation 6.16 (E_{c1} and $E_{c\theta}$). It has been attempted to solve the problem handling E_{c1} as a fitting parameter whose value has to be found in order to minimize the sum of the square differences between the experimental stiffness (at 0°, 30° and 90°), and the corresponding values calculated with the equation. The equation was used to evaluate $E_{c\theta}$ at the following angles: 0°+φ , 30°- φ, 30°+φ, and 90°-φ. To make the explanation easier the values of calculated stiffness will be indicated, respectively as: $E_{c\theta}$ (0°+φ), $E_{c\theta}$ (30°-φ), $E_{c\theta}$ (30°+φ) and $E_{c\theta}$ (90°-φ). They are indicated respectively by points A', B_1, B_2 and C'. Referring to the 30° case, it has been hypothesized that the real stiffness value (which has to be compared with the experimental stiffness at 30°), should take in account both the two contributes of $E_{c\theta}$ (30°-φ) and $E_{c\theta}$ (30°+φ). At first it has been chosen to take simply the average of the two values, as it can be seen at point B_{12} in the Figure 6.32, where the method is depicted.

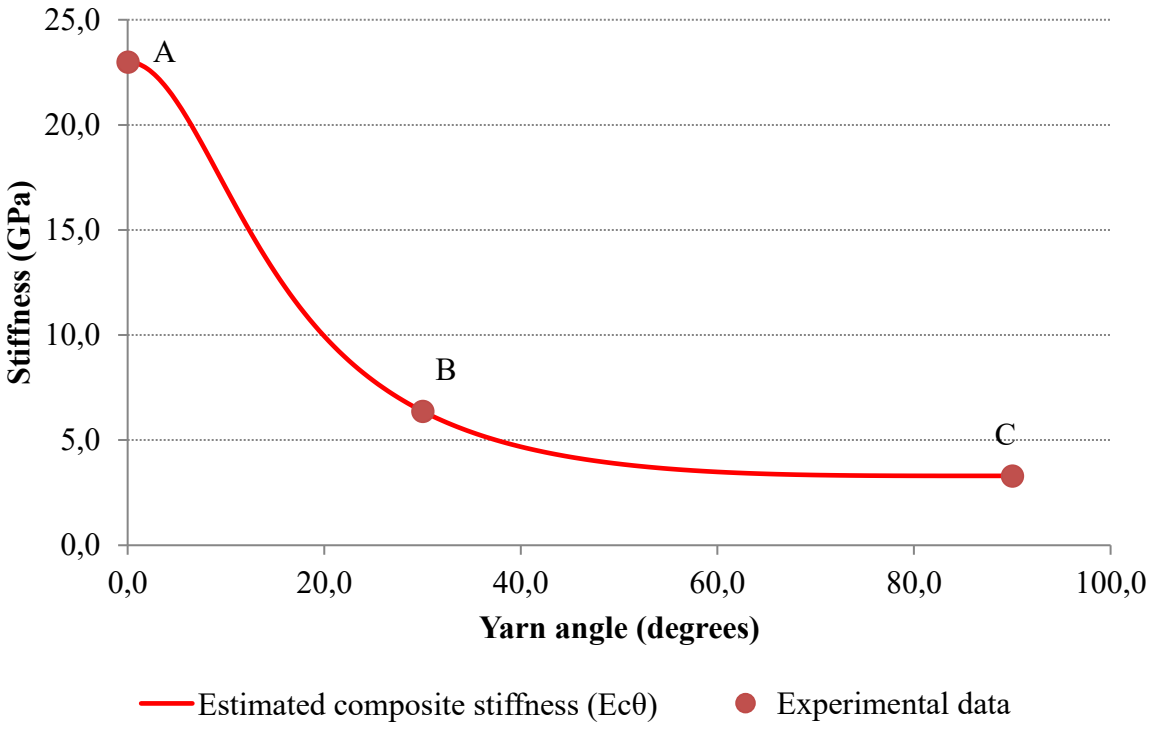

Figure 6.31 Stiffness as a function of yarn angle.

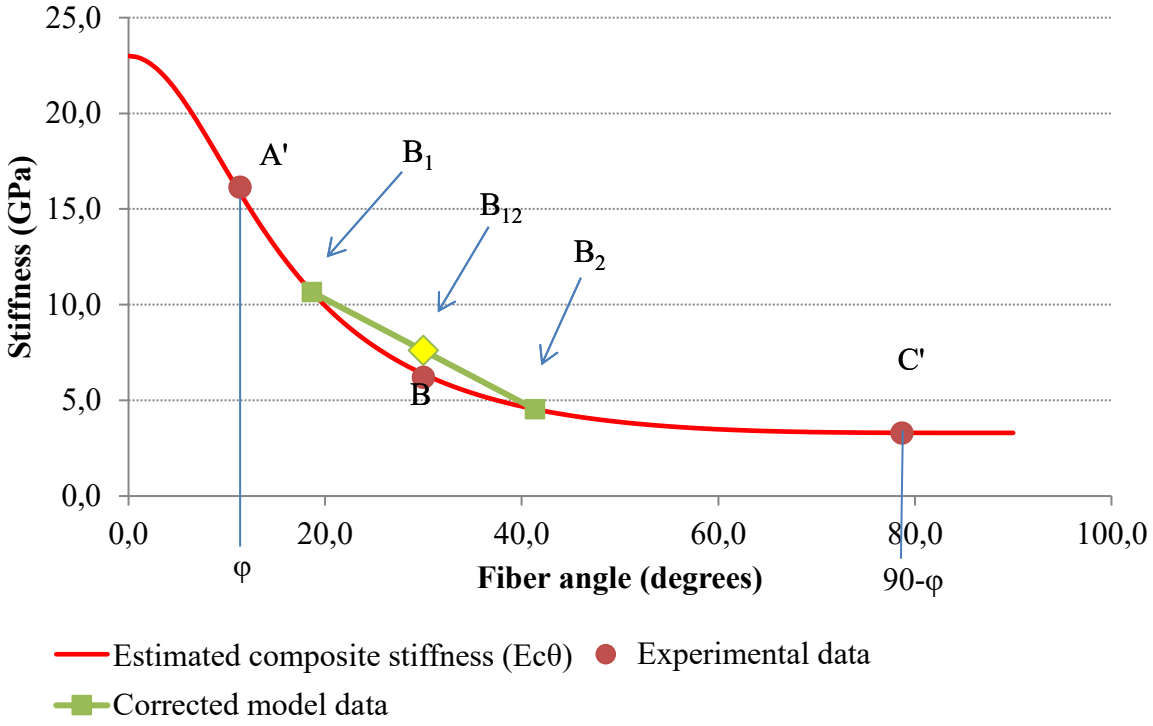

Figure 6.32 Stiffness as a function of fiber angle. φ is the twisting fiber angle. In this example it is equal to 16°, since neat flax fiber yarns are taking into consideration. Point A' is the updated experimental stiffness measured with 0° off-axis angle. Point B' is the updated experimental stiffness measured with 90° off-axis angle. Point B is the experimental stiffness measured with 30° off-axis angle, which has been split into two partial contributions in order to consider the influence of flax fiber twisting angle. Point B_{12} is the average of the two partial stiffness (point B_1 and B_2).

Making essays the E_{c1} value has been modified until the error, evaluated as sum of the square differences as explain above, reached its minimum value. It is important to highlight that the fitting procedure is at moment based on points A', B_{12} and C'. Once the error has been minimized, E_{c1} was used to back calculate the effective fiber stiffness E_{f1} by means of the following equation, derived from a "modified rule of mixtures" model originally described in the study of Madsen and Lilholt [35]:

$$E_{f1} = \frac{E_{c1}\left(1 - V_p\right)^{-2} - V_m E_m}{V_f} \qquad 6.17$$

Initially φ was set equal to the measured twisting flax angle, but going into more depth it has also to be considered that the flax fiber twisting angle φ is not constant since it depends on its radial location in the cross yarn section, therefore this variation needs to be taken in account [3]. Instead of taking the measured value, that is only representative of the external fiber arrangement, it was used a mean value φ_m calculated by the following formula (see appendix A for details):

$$\varphi_{mean} = \varphi_r + \frac{\varphi_r}{\tan^2 \varphi_r} - \frac{1}{\tan \varphi_r} \qquad 6.18$$

b)Second model: rings method

Analyzing the results of the first method, it has been observed that both the estimated composite stiffness and the estimated fiber stiffness, give the impression to be somehow overestimated in almost all cases. This overestimation is thought to be in large extent owing to the average stiffness value calculated between $E_{c\theta}$ (30°-φ) and $E_{c\theta}$ (30°+φ). The observation of the chart stiffness-fiber angle seems to confirm that the stiffness of point B_{12} is too high with respect to the predicted trend, and it can be explained considering that the non-linear trend is deviating too much in respect to the linear trend imposed for the calculation of the average stiffness at 30°. Moreover it has to be considered that the flax fiber twisting angle φ is not constant since it depends on its radial location in the cross yarn section, therefore this variation needs to be taken in account.

It has been tried to sort out the problem firstly working on the mean stiffness evaluation procedure in order to improve the method precision. It has been decided to represent the yarn as a cylinder whose circular section is subdivided into 4 concentric parts, equally displaced along the radius, therefore three ring sections and one central circle were formed. For simplicity in the description reference will be made to 4 rings. The number 4 has been chosen because it has been thought to represent a good compromise between calculation simplicity and method accuracy.

It can clearly noted that for the 0° off-axis angle, the schematic cylinder is vertically positioned, therefore the more inner is the ring, the lower is the corresponding area and the lower is the angle φ in respect to the cylinder axis. In fact in this case the angle between the tensile test axis and the single fiber direction is equal to φ since the cylinder axis is superimposed with the tensile test direction. Differently, for the 90° off-axis angle the cylinder is horizontally lied, therefore the condition is opposite with respect to the previous case, because if φ is lower (i.e. it is closer to the cylinder axis), it means that the angle between the tensile test direction and the single fiber direction is higher. These considerations are necessary in order to evaluate correctly the stiffness, since the tensile test direction has been taken as reference.

The rings method is basically very similar to the previous model, as the same procedure of minimizing the squared differences has been used. The only substantial differences consist in the mean stiffness evaluation, because the variation of φ along the yarn diameter is now considered, and in the analysis of 0° and 90° off axis cases, because instead of calculating only one single stiffness value, it is required to obtain four different values (one for each ring, as it can be seen looking at points A_1', A_2', A_3', A_4' and C_1', C_2', C_3', C_4', respectively). The stiffness values that have to be compared with the experimental data are chosen as before considering that the angle used in equation 6.12 is given by the sum of the flax twisting angle and the off-axis angle, but in this case the fiber angle is not constant, since it varies accordingly with the current section decreasing toward the yarn axis. Consequently, moving from the periphery of the yarn towards its axis, a linear

variation of the fiber angle has been assumed, and for each ring a mean angle value has been considered. By considering the axial-symmetric geometry of the yarn, it can seen that this mean angle is passing through the circle corresponding to the middle radius of the current ring. Therefore, unlike the previous analysis where $E_{c\theta}$ (0°+φ), $E_{c\theta}$ (30°-φ), $E_{c\theta}$ (30°+φ) and $E_{c\theta}$ (90°-φ) were used to back calculate $E_{c1,}$ now in each of these cases φ must be split up in 4 contributes, depending on the 4 different rings. They are indicated respectively as $\varphi_{1,}$ φ_2, φ_3 and φ_4. The average stiffness has been calculated mediating the four stiffness values corresponding to the four rings, considering the relative area of each single ring, by means of the equation:

$$E_{c\varphi m} = \frac{\left(E_{\varphi 1}A_{\varphi 1} + E_{\varphi 2}A_{\varphi 2} + E_{\varphi 3}A_{\varphi 3} + E_{\varphi 4}A_{\varphi 4}\right)}{\left(A_1 + A_2 + A_3 + A_4\right)} \qquad 6.19$$

Finally the stiffness of composite $E_{c1}$was obtained minimizing the sum of the squared differences, and the fiber stiffness E_{f1} was calculated for each composite as it had been done with the previous model. Representation of the individuated points is shown in Figure 6.33.

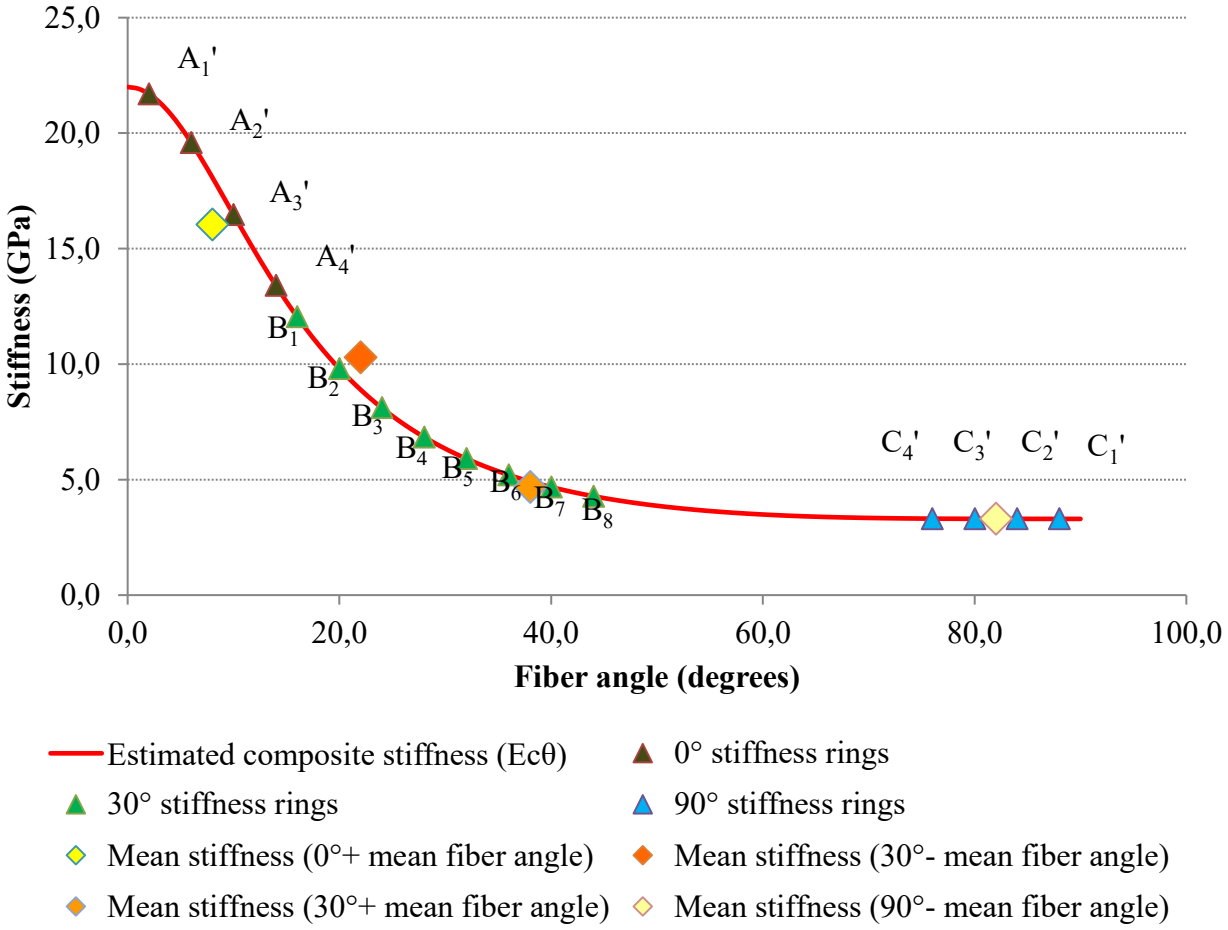

Figure 6.33 Stiffness as a function of fiber angle. Points indicated by A_i' represent the 4 partial stiffness, one for each ring (i.e for each φ value), referred to the 0°off-axis test. Points indicated by C_i' represent the 4 partial stiffness, referred to the 90°off-axis test whereas points indicated by B_i' represent the 8 partial stiffness referred to the 30°off-axis test. In order to have a qualitative representation of the mean stiffness points (indicated with rhomb), they have been plotted considering an average fiber angles, even if these positions are not exactly true since each single mean stiffness is calculated considering the corresponding area.

c)Third model: 16 elements method

The rings method has been furthermore developed as it has been found that the approximation in the stiffness evaluation for the 30° case is still too high. In fact, even if the subdivision into rings demonstrates a more accurate stiffness estimation in respect to the first model, it's nevertheless true that the stiffness variation along a generic ring perimeter is not correctly taken in account.

The most relevant approximation is due to the fact that in each ring the orientation of the fibers in respect to the tensile direction is thought to be constant. Actually, even if the twisting angle is kept constant in the yarn (for a given radial distance), focusing on the angle between fiber and tensile axis, it can be observed that it varies depending on the location along the perimeter. It has been attempted to achieve a better accuracy dividing each ring into 4 equal sectors of a circle. Hence in total 16 elements have been obtained, explaining the reason why of the name "16 elements method"

and for each ring, it is possible to individuate the 4 middle points of the 4 arcs that have been created with the subdivision.

Therefore, in addiction to considering the φ variation along the yarn diameter, the effect of the angle around the yarn axis will also be taken into account. For a given ring (to simplify the explanation reference will be made to the 4th ring) and for the off-axis angle of 30°, it can be said that the angles of the fiber at the middle arc point locations are equal to 30°-φ_4, 30°, 30°+φ_4 and 30°. Furthermore, considering that each arc is referred to a 90° angle around the yarn axis, the fiber angle values at the arc edge locations are: 30°-0.5φ_4, and 30°+0.5φ_4. Basing on these considerations it is possible to correlate one given arc to three angles: the angle at the middle point, and the two angles at the two edges. Keeping on referring to the 4th ring, the values are the following:

sector 1: angle at middle point: 30°+φ_4; angles at edges point: 30°+0.5φ_4, 30°+0.5φ_4

sector 2: angle at middle point: 30°; angles at edges point: 30°+0.5φ_4, 30°-0.5φ_4

sector 3: angle at middle point: 30°-φ_4; angles at edges point: 30°-0.5φ_4, 30°-0.5φ_4

sector 4: angle at middle point: 30°; angles at edges point: 30°+0.5φ4, 30°-0.5φ_4

Schematization of the angle and sector subdivision are depicted in Figure 6.34 and 6.35, respectively.

As it was done with the rings method, subsequently it has been attempted to split the total stiffness at 30° in several partial stiffness contributes and to mediate their values. The most representative angle at which to calculate stiffness changes depending on the sector. It has been decided to use 30° for sectors 2 and 4, since 30° represents the average between the three points 30°-0.5φ_4, 30° and 30°+0.5φ_4. Similarly, for the sector 1 and the sector 3 the angles 30°+0.75φ_4 and 30°-0.75φ_4 have been selected respectively as mean values, as shown Figure 6.36.

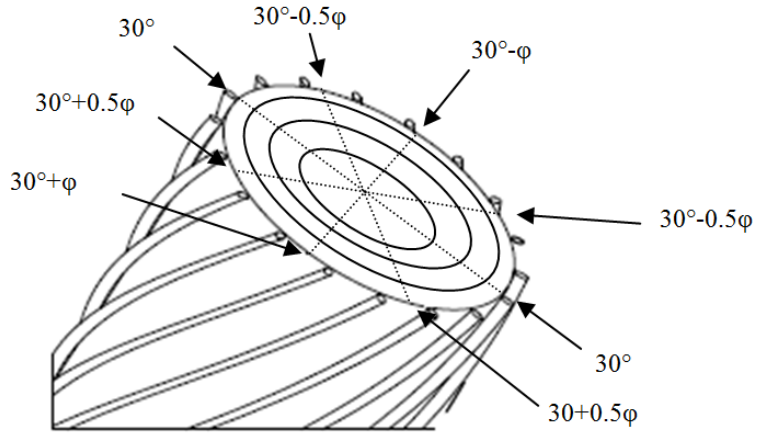

Figure 6.34 Representation of a yarn section inclined with a 30° angle in respect to the tensile axis. Angles used for calculations in the sixteen elements procedure are shown.

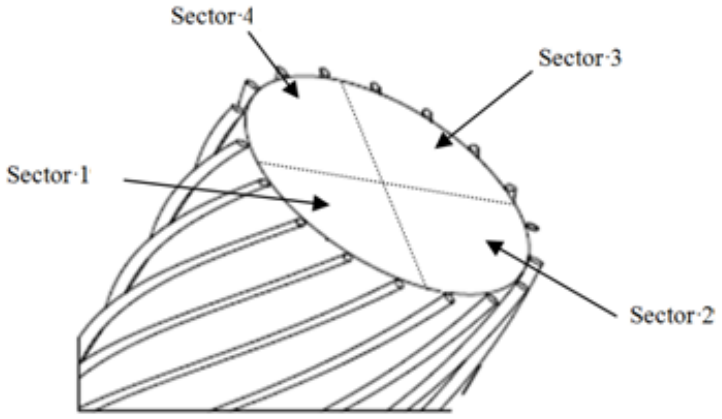

Figure 6.35 Positioning of the 4 sectors of a circle for a generic angle φ.

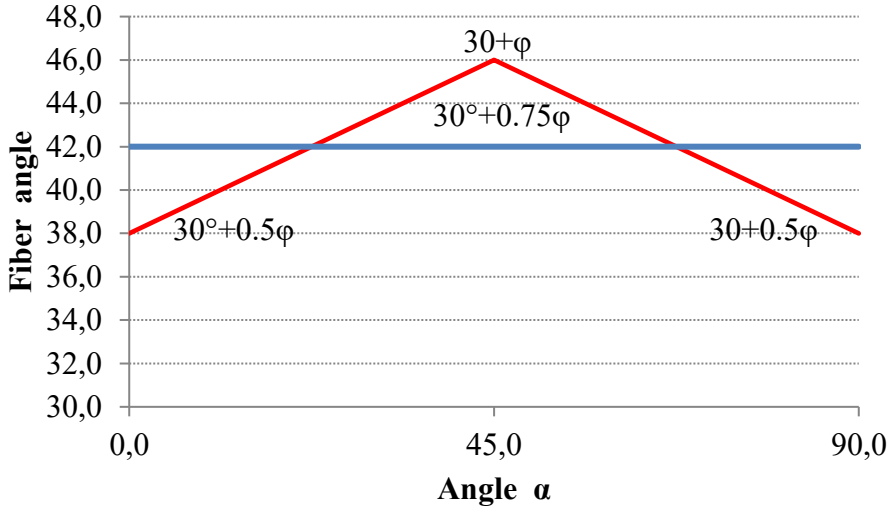

Figure 6.36 Schematic representation of mean angle estimation for 1 for a generic angle φ. Calculation is also suitable for the corresponding sector 3, since the absolute values are the same.

The same procedure has to be repeated with the three more inner rings, considering the variation of φ towards the yarn axis (i.e. substituting φ_4, respectively with φ_3, φ_2, and φ_1). After having calculated the stiffness values for all the combinations of φ and sector types, the total average stiffness is obtained as mean of the 16 partial stiffness contributes. Finally, as done for the previous models, the sum of the square differences between estimated stiffness and experimental stiffness needs to be minimized varying E_{c1}.The found E_{c1} value will be used to back-calculate the fiber stiffness. It must be remembered that for the 0° and the 90° cases, the estimated stiffness is obtained by means of the rings method instead of the 16 elements method. In fact in the first case the tensile axis and the yarn axis are equals therefore there's no need of dividing each ring in different sectors,

while in the second case, the rings method has been chosen for a matter of simplicity, considering the asymptotic trend of stiffness in that off-axis angle range.

Example of model application for fiber stiffness back-calculation

An example of how to apply the 16 elements model for the back calculation of the fiber stiffness is reported in this section. The stiffness values at the three different off-axis angles are available as experimental data.

EXPERIMENTAL DATA		
Stiffness at 0° off-axis angle	**Stiffness at 90° off-axis angle**	**Stiffness at 30° off-axis angle**
(GPa)	(GPa)	(GPa)
16.2	3.3	6.2

The model requires several setting parameters, correlated to the volumetric composition and the type of geometrical subdivisions that has been chosen. In this example, the measured fiber twisting angle is equal to 16°, whereas the external radius is set equal to 200 with a number of section fixed equal to 4. Based on these values, it is possible to calculate the corresponding radius and area of each section. Once the volume fractions of matrix, fiber and porosity have been inserted, the shear stiffness of composite can be obtained. Finally the Poisson's ratio of composite must be assumed, and the mediating factor must be set (in this case equal to 0,75 as explained in Figure 6.36). The composite stiffness along the transverse direction is assumed to be equal to the experimental stiffness measured with the off-axis angle of 90°.

INPUT DATA												
Fiber twisting angle	**External radius**	**N° of section**	**Section radius**	**Section areas**	**Vm**	**Vf**	**Vp**	**Em**	**G_{12}**	**ν_{c12}**	**Med. factor**	**E_{c2}**
(degrees)	(μm)		(μm)	(μm^2)				(GPa)				(GPa)
16	200	4	50	7854	0.693	0.279	0.028	2.7	1.6	0.3	0.75	3.3
			100	23562								
			150	39270								
			200	54978								

In the 0° and 90° cases, the model provides a partial stiffness for each ring the yarn section has been divided in. The angle that is used for the stiffness calculation is the mean angle of each single ring. Based on the obtained stiffness values and the corresponding ring areas, by means of the equation 6.19 a mean stiffness value is got. This value must be compared to the corresponding experimental stiffness.

MODEL DATA						
0° case	**Mean angle in current section**	**Partial stiffness**	**Mean Stiffness**	**Exp. stiffness 0°**	**Squares**	**Error**
	2	21.9	16.2	16.2	5.18E-5	0.161
	6	19.8				
	10	16.6				
	14	13.5				

90° case	**Mean angle in current section**	**Partial stiffness**	**Mean Stiffness**	**Exp. stiffness 90°**	**Squares**	
	88	3.3	3.3	3.3	6.75E-5	
	84	3.3				
	80	3.3				
	76	3.3				

For the 30° case, the model works similarly to the previous cases, the substantial difference consists in the procedure to evaluate the mean stiffness. In fact, it must be considered that each ring is furthermore divided in the 4 sectors. Referring to a generic ring, once the partial stiffness values have been calculated, by means of the equation 6.19 the semi-partial stiffness can be obtained. In the end 4 semi-partial stiffness are got, and mediating them it is possible to determine the mean stiffness that must be compared to the experimental stiffness at the off-axis angle of 30°.

30° case	**Total ring area**	**Quarter of area**	**Mean angle in current section**	**Partial stiffness**	**Semi-partial stiffness**	**Mean Stiffness**	**Squares**	
external ring	54978	13744.5	40.5	4.7	6.9	6.6	**Exp. stiffness 30°**	
			30	6.4			6.2	0.16610
			30	6.4				
			19.5	10.1				
second ring	39270	9817.5	37.5	5.0	6.6			
			30	6.4				
			30	6.4				
			22.5	8.8				
third ring	23562	5890.5	34.5	5.5	6.5			
			30	6.4				
			30	6.4				
			25.5	7.7				
central circle	7854	1963.5	31.5	6.1	6.4			
			30	6.4				
			30	6.4				
			28.5	6.8				

As fitting data, the model has the composite stiffness along the axial direction. This value must be modified until the total error between experimental stiffness and predicted stiffness is minimized. Once the composite axial stiffness has been found, based on it is possible to back-calculate the stiffness of flax fiber by means of the equation 6.17.

FITTING DATA	
E_{c1}	Ef
(GPa)	(GPa)
22.2	75.5

Twisted yarn case

The analysis of the composites made up by twisted yarns is slightly more difficult if compared to the other cases, therefore the 16 elements model was opportunely modified to take in account the twisting effect. It was observed that for the 0° and the 90° cases, the estimated properties of composite are comparable with the experimental data. Focusing on the 0° off-axis tests, calculated stiffness and ultimate strength for twisted flax/PET composite are, respectively, 18.39 GPa and 170.88 MPa, while the corresponding experimental data are 18.41 GPa and 170.84 MPa. Similarly the twisted flax/PLA composite show 15.44 GPa and 147.13 MPa as calculated values, and 15.49 GPa and 146.89 MPa as experimental values.

For the 90° tests, both of the PET and PLA composites exhibit calculated values of stiffness and ultimate strength calculated values very close to the corresponding experimental data, for the asymptotic trend of the curves and their low sensibility to angle variations for angles above 70°.

Based on these observations it has been considered that the 16 elements method provides reasonable comparing values, but it cannot be applied to the 30° case since the influence of the varying fiber angle needs to be taken in account. In fact, as explained in section 6.1, for a given off-axis angle, the twisting yarn angle needs to be considered, and also the twisting flax fiber angle within each twisted yarn. In order to achieve a better approximation, the number of the rings has been increased. Reference to the external ring (with φ_4) will be made, and the twisting yarn angle will be represented by γ to simplify the explanation. For first, concentrating on the 30° off-axis angle, two rings have been assumed to be positioned along two different axis having inclinations of 30°+ γ, and 30°- γ. The first ring has been denoted as ring A, the second as ring B. Considering this geometric schematization, sectors 2 and 4 will be associated to these two angles for all the rings considered, since they are not depending on the radial distance, as it can be observed moving towards the axis (i.e. changing φ value). Stiffness values are calculated on 4 angles for each ring, as for the other composites, but in this case two sectors 1 and two sectors 2 are present since both ring A and ring B have to be considered.

For the ring A the angles chosen are the following:

-sector 1: angle at middle point: $30°+\gamma+\varphi_4$;

-sector 2: angle at middle point: $30°+\gamma$;

-sector 3: angle at middle point: $30°+\gamma-\varphi_4$;

-sector 4: angle at middle point: $30°+\gamma$;

Similarly for the ring B the angles are:

-sector 1: angle at middle point: $30°-\gamma+\varphi_4$;

-sector 2: angle at middle point: $30°-\gamma$;

-sector 3: angle at middle point: $30°-\gamma-\varphi_4$;

-sector 4: angle at middle point: $30°-\gamma$;

As for the other composites, considering the angles at edge points, as average value for sectors 1 and 3 the value 0.75φ was selected. Afterwards the stiffness values have been mediated with the relative quarter of a circle areas, and the same procedure has been repeated with the more inner rings. Finally the final theoretical stiffness has been obtained as average value of all 32 partial contributes.

6.3.3 Fiber ultimate strength evaluation procedure

Similarly to what has been done for stiffness, the composite ultimate strength has been investigated with the aim to evaluate the fiber angle effect, instead of referring only to the yarn angle as it had been done in previous studies. Fundamentally the same approach has been used, basing on the sixteen elements model, hence first of all an equation to predict the ultimate stress of the aligned composites had to be selected. Two models can be used, the maximum stress theory and the Tsai Hill criterion.

The maximum stress theory [39] considers three modes of failure therefore the overall stress trend is obtained by the sum of three curves (one for tensile failure of fibers, one for shear failure parallel with fibers, and one for tensile failure transverse to fibers) as illustrated in Figure 6.37. It has been observed that this criterion is suitable when the independent variable is the yarn angle, since the off-axis angle don't require a further analysis. Conversely in this study the independent variable is represented by the fiber angle, complicating things, as seen in stiffness analysis, hence it might be difficult to evaluate correctly the three sub-curves placement.

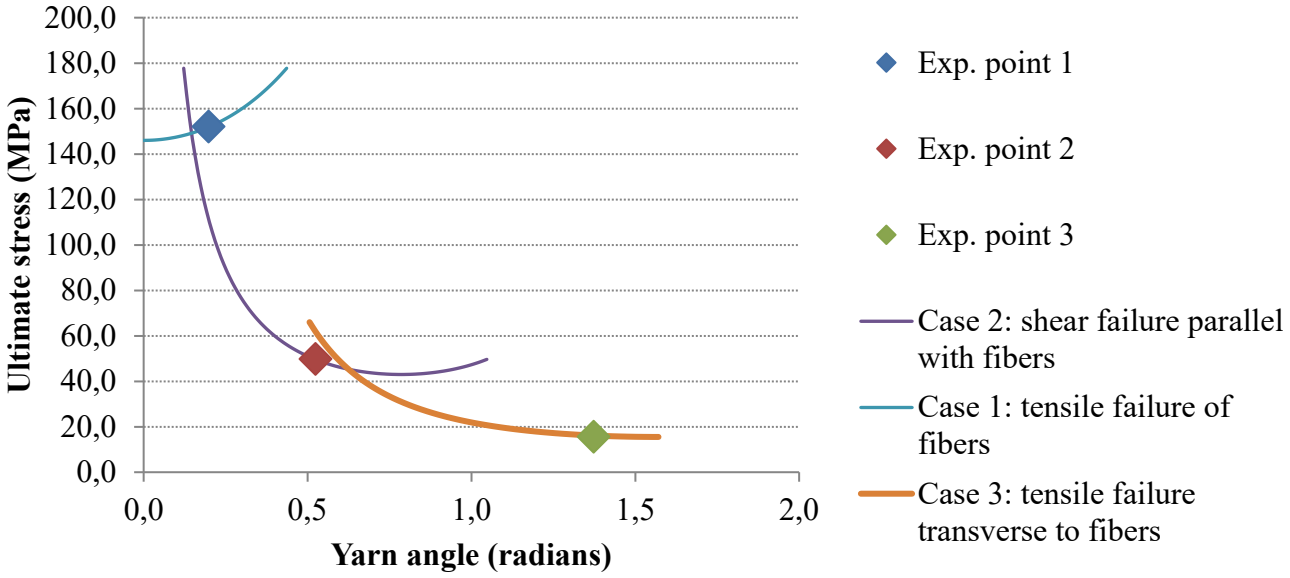

Figure 6.37 Ultimate stress trend predicted by the maximum stress theory using three experimental points at three different off-axis angles.

Basing on these considerations it has been chosen the Tsai-Hill criterion, that provides a single decreasing curve. The equation from the Tsai-Hill criterion [40] is the following:

$$\frac{1}{\sigma_{c\varphi}^2} = \frac{\cos^2(\cos^2\varphi - \sin^2\varphi)}{\sigma_{c1}^2} + \frac{\sin^4\varphi}{\sigma_{c2}^2} + \frac{\cos^2\varphi\sin^2\varphi}{\tau_{c12}^2} \qquad 6.20$$

where τ_{c12} is composite shear stress. From studies of Madsen [35] it was estimated to be in the range of 22-26 MPa for Hemp/PET composites. Since the shear stress of the isotropic PET matrix (τ_m) has been found to be around 18 MPa, it means that the shear stress of the composites is governed by the shear stress of the matrix. The procedure of calculating ultimate stress is very close to the method used for stiffness: using the rings method for both the 0° and the 90° cases, and the 16 elements method for the 30° case, stress values are calculated in order to be compared with the experimental data.

The main difference in respect to the stiffness case, consists in the estimation of the composite shear stress because no accurate values for PLA composites and for composites having either twisted or blended yarns have been found in literature. Thus the minimizing of the square differences sum requires that two fitting parameters (σ_{c1} and τ_{c12}) are handled at the same time. Similarly to what was done for stiffness, it has been assumed that σ_{c2} is equal to the experimental ultimate strength of the 90° samples, because of the asymptotic trend of the predicted stress for fiber angles in the proximity of 90°. Once the best compromise between σ_{c1} and τ_{c12} has been found, the fiber ultimate

stress has been back-calculated by means of the following formula, from a "modified rule of mixtures" model by Madsen and Lilholt [28] :

$$\sigma_{f1} = \frac{\sigma_{c1}(1 - V_P)^{-2} - V_m \sigma_{m^*}}{V_f} \qquad 6.21$$

where σ_m^* is the stress of the matrix at the point of composite ultimate stress and the subscript $_1$ represents the axial direction along the fibers. The applied value of σ_m^* was obtained from the stress-strain curves of neat matrix specimens and was found to be around 46 MPa. [35] Data are referred only to PET specimens therefore the corresponding PLA value was not measured before. In first approximation, considering the similarity between the two polymers, it has been assumed that PLA and PET have the same σ_m^* also because of the weak influence of this parameter on the strength estimation. In fact during the minimization of the square differences for PLA composites it has been tried to modify the PLA value, keeping constant the other parameters and remaining in the range of 30-60 MPa, in order to evaluate its effect in the σ_{c1} estimation, but no relevant changes have been found.

Increasing σ_m^* by 30 MPa, the maximum decrease of σ_{f1} is below 6%, for neat flax/PLA, twisted flax/PLA and blended flax/PLA composites.

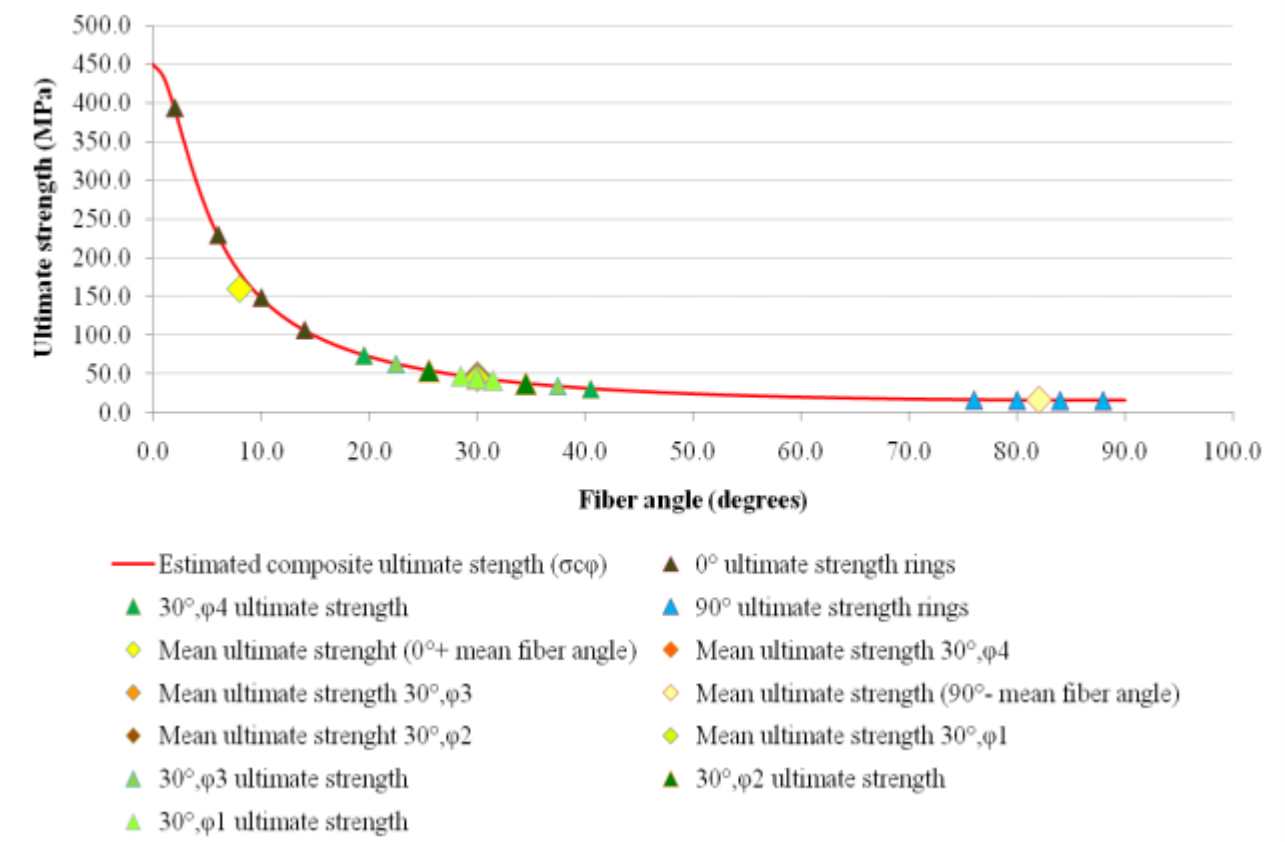

Figure 6.38 Ultimate stress as a function of fiber angle. In order to have a qualitative representation of the mean ultimate strength points (indicated with rhomb), they have been plotted considering an average fiber angles, even if these positions are not exactly true since each strength value is calculated considering the corresponding area.

Off-axis reference test	Angle	Ultimate strength	Mean angle	Mean ultimate strength
(degrees)	(degrees)	(MPa)	(degrees)	
0	2	392.9	8	160.3
	6	229.1		
	10	148.1		
	14	106.2		
90	88	15.5	82	16.0
	84	15.7		
	80	15.9		
	76	16.3		
30(±φ_4)	40.5	30.8	30	48.6
	30	44.7		
	30	44.7		
	19.5	74.3		
30(±φ_3)	37.5	33.9	30	46.6
	30	44.7		
	30	44.7		
	22.5	63.0		
30±(φ_2)	34.5	37.6	30	45.3
	30	44.7		
	30	44.7		
	25.5	54.4		
30±(φ1)	31.5	42.1	30	44.8
	30	44.7		
	30	44.7		
	28.5	47.6		

Table 6.14 Example of calculation data of sixteen elements method.

6.3.4 Results of sixteen elements method

In this section the results of the back-calculation of fiber properties are reported.

Composite type	Ef	Ec1	Em	Used angle
	(GPa)	(GPa)	(GPa)	(degrees)
Neat flax/PET 30%	73	21	2.7	16
Neat flax/PET 40%	81.9	26.4	2.7	16
Neat flax/PET 50%	72.7	28.6	2.7	16
Neat flax/PET 60%	67.9	29.1	2.7	16
Twisted flax/PET	90.2	26.7	2.7	10
Twisted flax/PLA	55.7	18.8	3.4	8
Blended flax/PET	71.4	16.4	2.7	20
Blended flax/PLA	57.3	17.6	3.4	22
Neat flax/PLA 40%	70.3	23.4	3.4	16

Table 6.15 Stiffness results obtained by sixteen elements method. E_{fl} is the back-calculated fiber stiffness, E_{cl} is the axial stiffness of composites, E_m is the stiffness of the matrix, and the angle represents the twisting angle of flax fibers for neat flax/PET (or PLA) composites, of yarns for twisted flax/PET (or PLA) composites and blended flax/PET (or PLA) composites.

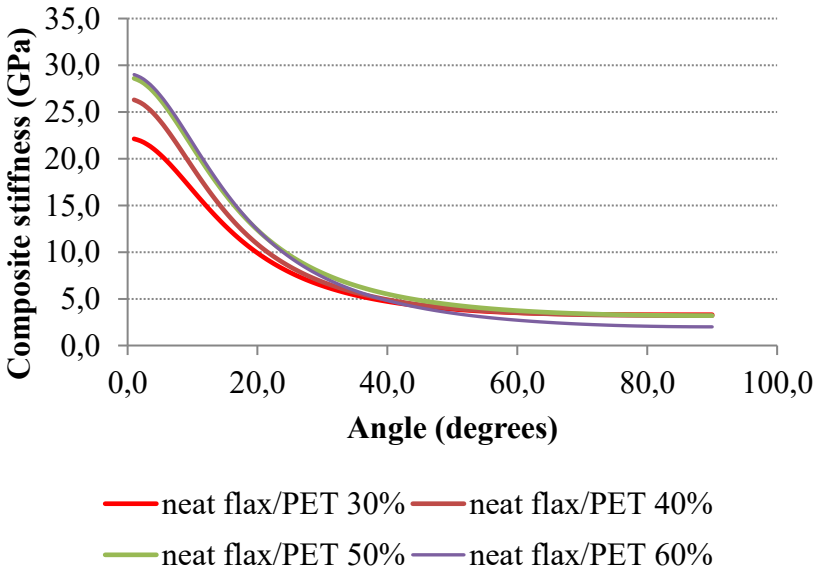

Figure 6.39Plot of different stiffness trend of neat flax/PET composites with increasing the fiber content.

Composite type	τ_{12}	σm^*	σ_{c1}	σf_1
	(MPa)	(MPa)	(MPa)	(MPa)
Neat flax/PET 30%	26	46	450	1592
Neat flax/PET 40%	32	46	640	2055
Neat flax/PET 50%	35	46	780	2018
Neat flax/PET 60%	47	46	1440	2714
Twisted flax/PET	30	46	480	1626
Twisted flax/PLA	24	46	480	1510
Blended flax/PET	20	46	320	1405
Blended flax/PLA	25	46	370	1263
Neat flax/PLA 40%	28	46	540	1637

Table 6.16 Ultimate strength results obtained by sixteen elements method. τ_{12} is the assumed composite shear stress, σ_m^* is the stress of the matrix at the strain of ultimate strength, σ_{c1} is the estimated axial ultimate strength of composite, and σ_{f1} is the back-calculated ultimate strength of the fibers.

6.3.5 Analysis of results

The estimated values of both stiffness and ultimate strength have been analyzed in order to evaluate the reliability of the method used. The investigation is also oriented to finding out the high sensitivity parameters in order to obtain some indications for future developments.

Fiber stiffness results analysis

Theoretically, the values of the back-calculated fiber stiffness should be very close to each other. If so, it will mean that the method works properly, and the parameter correlations have been understood and they have been well approximated. Under a theoretical point of view, all the neat flax/PET composites should be characterized by the same E_f since it is thought to be independent from the V_f variations. Taking a mean value of the fiber stiffness it seems that the procedure is correct since the value 72 GPa is fairly comparable with the flax fiber stiffness range of 50-70 GPa individuated in previous studies [12]. The standard deviation is 11 GPa.

In almost all the cases, the estimated fiber stiffness falls within the reported range except for the neat flax/PET 40% and the twisted flax/PET composites. In both these two cases the stiffness is clearly overestimated. It cannot be said for certainty that in these cases the method does not work correctly. It was supposed that the effect of experimental approximations might have led to an inaccurate estimation of volume fractions, as the other parameters have the same values used for the

other PET composites. However the possibility of a wrong volume fractions evaluation does not seem to be the correct explanation since volume fractions are in agreement with the volumetric interaction model, and this composite, in the ultimate strength analysis doesn't show unexpected results, therefore the reason of this overestimation is still not clear. For the twisted flax/PET composite the reason of the high stiffness is also unclear since, like in the previous case, the ultimate strength analysis does not reveal too deviated results, therefore the initial idea of an incorrect twisting angle measurement have been discarded.

It has been attempted to explain this discrepancy modifying the setting variables used in the method in order to distinguish which parameters whose effect on the stiffness estimation is higher. These variables were evaluated experimentally therefore an intrinsic error of the measurements needs to be taken in account. For instance it was found that the method is not sensitive to yarn diameter because even with a variation of 100% there is no change in estimated composite stiffness and fiber stiffness. Therefore no high accuracy is required during the yarn diameter measuring.

Things change radically focusing on the twisting angle effect since it was found that it has a noteworthy influence on both composite stiffness and fiber stiffness. The higher the angle, the higher the stiffness. The used value of the flax fiber angle is 16°. This value has been obtained as average of all the measures for flax twisting angle, without considering the differences between the measures of flax fiber angle in neat yarns, in blended yarns and in twisted yarns. In fact it has been noted that in the three cases the standard deviations are small enough to assume that the most representative neat flax fiber angle is the mean value of all the measurements. It was found that a variation of 1 degree entails a stiffness variation of 3-5%. It was calculated that, hypothesizing a flax twisting angle of 15° instead of 16°, for neat flax/PET 40% E_{c1} and E_{f1} are, respectively, 25.2 GPa and 79.2 GPa. It was observed that the angle influence is the same in all the composites, except for the PET composites having twisted yarn; in this case the effect is considerably lower, with a stiffness variation below 1% for degree.

It was tried to evaluate also the effect of changing the amount of porosity and it was found that increasing it by 0.001 there is no significant variation stiffness since E_{c1} doesn't change, whereas E_{f1} increase of an amount below 0.3%. The effect seems to be limited even if the porosity variation is brought up to 15%, as the percentage variation of E_{f1} is kept below 3%.

Fiber ultimate strength results analysis

Similar considerations have been done regarding the ultimate strength. In this case the estimation is more difficult as the composites shear stress τ_{12} is also an unknown. At first it was supposed to be included in the range between 22 MPa and 26 MPa, from studies of Madsen [35] thus as initial value 24 MPa was selected. The initial value for σ_{c1} was calculated hypothesizing a σ_{f1} of 1500 MPa, considering the expected properties of fibers [31]. Consequently it has been tried to vary σ_{c1} in order to minimize the sum of the square differences, as it was done for the stiffness calculation, but in this case it must be taken in account that τ_{12} wasn't accurately measured for the composites of this study. It has been noted that the same σ_{f1} could be obtained with different combinations of τ_{12} and σ_{c1} thus it was tried to found the more balanced compromises ,without having not reasonable values of either τ_{12} or σ_{c1}. The mean value of σ_{f1} is 1754 MPa with a standard

deviation of 438 MPa. This value is higher than predicted but it is still comparable with the expected range of 1200-1600 MPa even if more than one case show results which seem to be overestimated.

The mean value of composite shear stress is also high as its mean value of 30 MPa, with standard deviation of 8MPa is clearly out of the predicted range (22-26 MPa). Especially the neat flax/PET 60% composite shows results too high but the reason is still unknown since its ultimate strength deviates too much from the other neat flax/PET composite with lower fiber fraction. Making a comparison with the stiffness results the hypothesis of an incorrect volume fractions evaluation doesn't seem to be realistic, since this composite doesn't show a different behavior in respect to the others.

It has been observed that the back-calculated stiffness of neat flax/PET composites with increasing amount of fibers has an increasing trend too. It is still not clear the reason of this variation, but it is believed that there is no true correlation between the fiber amount in composites and the calculated fiber stiffness.

As it was done for the stiffness analysis, it has been attempted to evaluate the influence of the parameters used in the model calculation. It was found that the yarn diameter does not bias the strength estimation, similarly to the stiffness, whereas the influence of τ_{12} is significant since if it is increased by 1MPa, which corresponds to a percentage variation of 3-4%, σ_{c1} and σ_{fl} decrease by 10-13%. The calculated ultimate strength is also to a great extent affected by the twisting angle. As it was seen for stiffness, the higher the angle, the higher the strength. It was found that if the angle is increased by 1°, σ_{c1} and σ_{fl} can be improved by 30-40%. For instance, taking the neat flax/PET 40% and the neat flax/PET 50% composites, respectively with τ_{12} equal to 32MPa and 35MPa, if the flax fiber twisting angle is increased from 16° to 17°, σ_{c1} and σ_{fl} are respectively 910MPa, 2958MPa and 1490MPa, 3907MPa instead that 640MPa, 2055MPa and 880MPa, 2284MPa.

Finally the influence of the stress of the matrix at the strain of ultimate stress σ_m^* was investigated as no accurate values for PLA were available. Findings from this analysis demonstrate the poor influence of this parameter since it was found that a variation of 20% of σ_m^* don't give noteworthy change of the ultimate strength (σ_{fl} percentage variation is below 2%).

In the σ_{fl} calculation it was also tried to modify the porosity exponent, increasing it from 2 to 3 in order to consider any higher contribute of void spaces in the composite resistance, but not considerable changes were observed since the fiber stiffness variation is below 5%.

Comparison between stiffness and ultimate strength

The normalized stiffness and ultimate strength curves (using the Tsai-Hill criterion) have been plotted in function of the angle over the same char in order to evaluate any trend difference between the two properties. As depicted in Figure 6.40(A) the ultimate strength curve decreases faster than the stiffness one. For a given reduction of 50% it has been seen that the corresponding angle for ultimate strength is very lower in respect to the stiffness. The angle ratio is about 1/3 in fact the values are, respectively, 6° and 18°. Basing on these considerations, it can observed that, for a given

off-axis angle of the experimental test to compare the predicted values with, the ultimate strength is further from the 0° value, in respect with the stiffness, as illustrated in Figure 6.40(B). This means that the off-axis effect for strength is higher than the stiffness one. Therefore the ideal calculation of strength of composites having 0° as fiber angle is more complicated. This argumentation might partially explain the reason why of the overestimation of σ_{c1} and σ_{f1}.

Referring to future studies it could be attempted to prepare sample with off-axis angle slightly lower than 30° in order to get experimental strength data closer to the 0° ideal fiber angle and check if the ultimate strength values result to be less deviated.

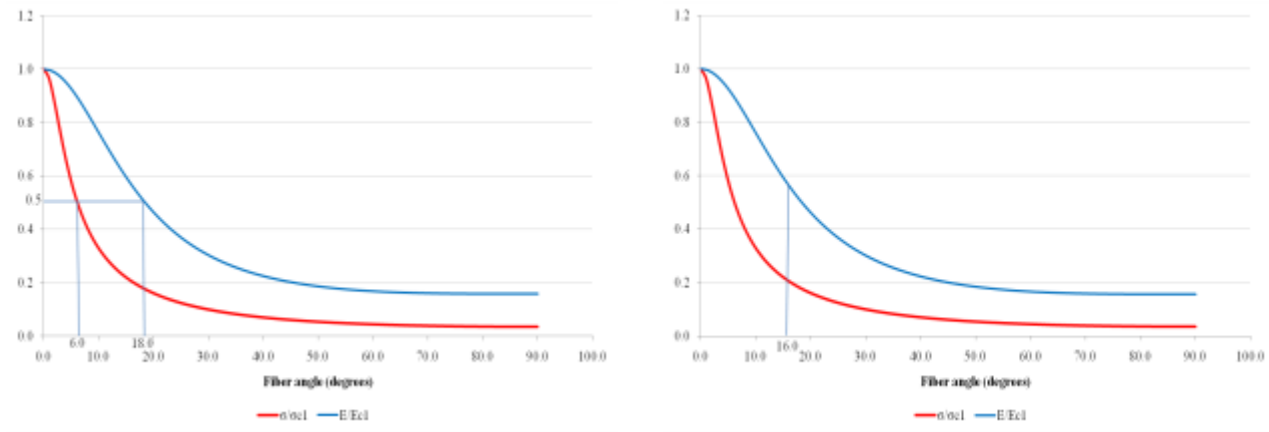

A B

Figure 6.40 Comparison between stiffness trend and ultimate stress trend (predicted by the Tsai-Hill criterion).

6.3.6 16 Elements method considerations

Even if the range of the back-calculated stiffness is deemed acceptable, the ultimate strength seems to be slightly overestimated by the 16 elements method. It is believed that the main problem consists in the relatively high sensibility to the measured fiber twisting angle. A minimal variation of the angle causes a completely different composite properties estimation, therefore it can be inferred that a very accurate angle measurement procedure is required. The microscope analysis should be carried out considering a larger yarn length in order to obtain a very representative survey and minimize the influence of yarn geometry variations. It is thought that a very accurate investigation is necessary, to distinguish the more orderly zone where measure the angle. For the blended yarn case, the twisting angle measurement was difficult because of the presence of very messy and disordered zones. It is inferred that the angle could be not representative of the real fiber disposition along the whole yarn therefore, considering the high sensibility of the model to the angle, it might be that too approximated properties are obtained.

Another problem that has been observed during the angle measurement, especially of the twisted yarns, is the easy untwisting motion of the bundles when they are handled to be observed. Furthermore it has been noted that the twisting angle is very sensitive to the applied tension in fact

if the yarn is slightly pulled, the angle decreases noticeably. Therefore it should be measured with a level of tension which corresponds to the applied stress during the winding process. It is supposed that the best way to achieve reliable information about the real twisting angle consists in the observation of the composite surface, after a grinding treatment.

The possibility of having measured an angle slightly different in respect to the ideal value of 30° during cutting operations has also been hypothesized. In fact it could have influenced the theoretical analysis, since the experimental data of stiffness and ultimate strength are referring to the different angle.

Focusing on the assumptions made as model base, it is clear that the geometrical schematization is very simplified since only 4 rings and 4 sectors of a circle are considered. Therefore the stiffness variation was assumed to be discrete, while actually it varies continuously along the perimeter of each ring and towards the yarn axis, through the different rings. It is though that a finite elements analysis could offer a better approximation, since calculations could be work out basing on a higher number of stiffness values obtained with a tight elements subdivision.

Regarding the PLA composites, it is suggested that other possible improvements in the method could be obtained if τ_{12} and E_m were accurately measured in order to limit the variability range.Furthermore it must be considered the approximation of the cut and weight phases. Especially during the cutting of the twisted yarns it might be that the tension applied to measure the length is slightly different to the tension applied in the winding process therefore, considering the easy un-twisting effect, it might be that the cut length is a little different from the real one, giving a further error in the linear density measurement. These approximations could have change somewhat the estimated fiber weight fraction, influencing negatively the subsequent model estimations.

7 CONCLUSIONS

7.1 STRUCTURE OF YARNS

In addition to the neat flax yarns, two different pre-forms (twisted and blended yarns) were used in composite manufacturing to evaluate if the idea of mixing together plant fibers and matrix polymer in one single yarn is promising. Twisting angles and diameters of the different yarns were measured.

Referring to the twisted case, the structure is S-twist and the yarn twisting angles, with PET and PLA matrix, are 10° and 8° respectively. Referring to the blended yarns, the structure is Z-twist and the fiber twisting angles, with PET and PLA matrix, are 20° and 22°, respectively. For neat flax yarns the structure is Z-twist and the fiber twisting angle is 16°.

The twisted yarn diameters, with PET and PLA matrix, are respectively 800 μm and 840 μm. The blended yarn diameters, with PET and PLA matrix, are 610 μm and 640 μm ,respectively. The diameter of the neat flax yarn is 390 μm.

7.2 COMPOSITE PROPERTIES

Volumetric composition, mechanical properties, microstructure and failure characteristics of all composites have been analyzed trying to evaluate the effect of fiber content (30, 40, 50, and 60%), the effect of type of composite pre-forms (twisted and blended yarns) and the effect of matrix type (PET and PLA).

Volumetric composition has been analyzed by observing the experimental results and comparing them with the predictions of the volumetric interaction model.

Microstructure has been studied by analyzing both electron microscope and optical microscope images.

The tensile properties (stiffness and ultimate strength) of composites were investigated by using specimens with yarns oriented at 0°, 30° and 90°.

The failure behavior of the composites was studied making a qualitative analysis based on the images of fractured surfaces of the testing samples.

7.2.1 Influence of fiber content

The influence of fiber content was investigated. Four different neat flax yarn composites with a matrix of PET were made with increasing fiber weight fraction. The results point towards that the higher the fiber volume fraction, the higher the amount of porosity. The estimated volume fractions have been compared with the results of a volumetric interaction model and a rules-of-mixture model. V_{fmax} was set equal to 0.51 and the calculated value of W_{ftrens} is 0.58. Experimental values of densities and composite stiffness (obtained by the sixteen elements method) have been also compared with the model predictions. All data exhibit a good agreement with the model results.

Referring to an off-axis angle of 0°, for composites with fiber volume fraction in the range 0.28-0.48, stiffness is in the range 16-21 GPa and ultimate strength is in the range 150-220 MPa. For a given composite, as the off-axis angle increases, the tensile properties decrease. With an angle of 90° stiffness in the range 2-3 GPa while ultimate strength is in the range 6-16 MPa. It was found that the higher is the fiber content, the higher are the composite properties (both stiffness and ultimate strength), with an off-axis angle of 0°. In the present study all the composites probably have a fiber content which is below the transition point, so no decay of stiffness and ultimate strength have been observed. The making of a further composite with an higher fiber content would have helped for the transition point estimation. With the off-axis angle of 30° the ultimate strength trend is the opposite with respect to the 0° case, since values are 49 MPa and 25 MPa for the 30% flax/PET composite and the 60% flax/PET composite, respectively. With off-axis angle of 90° the trend is the higher is the fiber content, the lower are the mechanical properties. Stiffness is 3.3 GPa and 2 GPa for the 30% flax/PET composite and the 60% flax/PET composite, respectively. Ultimate strength is 16 MPa and 6 MPa for the 30% flax/PET composite and the 60% flax/PET composite, respectively.

Microscope images show the relatively uniform distribution of flax yarn bundles within the matrix and the growing number of flax fiber bundles in the four composites with increasing fiber content.

With the off-axis angles of 0° and 90°, the composites show a delineated transversal fractured section, with the off-axis angle of 30° the fractured section is 30° oriented. In the case of the composite with the higher fiber amount several cracking surfaces has been observed along the yarn direction, and no breaking into two separated parts occurred.

7.2.2 Influence of fiber/matrix microstructure (pre-forms)

One of the most important objectives of the present study is represented by the assessment of UD composite properties using pre-forms (twisted and blended yarns) as reinforcement, instead of using simple flax yarns. As term of comparison to evaluate the effect of twisting and blending, the neat flax/polymer 40% composite was chosen, since it is characterized by a fiber volume fraction which is close to the composites made with pre-forms.

The analysis of volumetric composition has not provided any clear indications about the pre-forms effect since the results change depending on the matrix type, making it difficult to assess the effective contribution of twisted and blended yarns.

Observing the general trend of tensile test results, it can be affirmed that the blended yarns lead to lower composite mechanical properties. Referring to an off-axis angle of 0°, for composites with blended yarns stiffness is in the range 10-12 GPa and ultimate strength is in the range 90-110 MPa. The corresponding values of stiffness and ultimate strength for the neat flax composites, are in the range 18-19 GPa and 160-180MPa.

It is believed that properties are lower than composites with neat flax yarns because of the poor fiber orientation in the blended yarn. In fact, by means of microscope analysis the presence of several messy zones containing many entangled fibers has been observed. More practice needs to be done in the yarn manufacturing to reduce the formation of these messy parts. No marked bundle profiles have been observed in electron microscope and optical microscope images of cross-sections of blended yarn composites, since the fibers seem to be chaotically dispersed in the polymeric phase.

Differently, it cannot be stated that the twisted yarns provide a notable improvement of composite properties, since no marked differences have been observed with respect to composite with neat flax yarns. Referring to an off-axis angle of 0°, for composites with twisted yarns, stiffness is in the range 16-18 GPa and ultimate strength is in the range 150-170 MPa.

By means of electron microscope and optical microscope observations of composite cross-sections it has been observed that twisted yarns seem to cause a high fiber dispersion in the matrix part. In fact it is more difficult to see marked contours of yarns, with respect to neat flax yarn composites whose reinforcement bundle contours are well defined.

It is thought that the twisted yarns could offer a good potential alternative in composite processing, since suppliers can furnish yarns already twisted with a wanted fiber fraction. One possibility that might be considered to improve the twisted yarn effect on composite properties consists in twisting the polymer yarns around the flax yarns, instead that twisting flax yarns around the matrix, since the reinforcement alignment could be improved. However, more investigations are needed to elucidate the possible improvement given by using this type of perform.

No noteworthy differences in the failure behavior have been observed between the different pre-forms. The only observations refer to a sort of concavity exhibited in the blended flax/PLA with an off-axis angle of 30°, and to the fact that fracture into two separated parts occurred in all the specimens with the off-axis angle of 90°.

7.2.3 Influence of matrix type

The volumetric composition results point towards that the porosity volume fractions are higher if PET is used as matrix. Especially in the blended yarn case, the percentage of porosity results to be very increase.

It has been found that the tensile properties of the composites are only to a lesser extent affected by the matrix type, since no considerable variations were observed between the corresponding PET and PLA composites. With an off-axis angle of 0°, considering only twisted and neat yarns cases, the PET matrix composite stiffness is in the range 18-19 GPa, while the PLA matrix composite stiffness is in the range of 16-18 GPa, the PET matrix composite ultimate strength is in the range 170-180 MPA, whereas the PLA matrix composite ultimate strength is in the range 150-160 MPA.

Altogether, even if PLA composite properties are a little lower than PET composite, the results point towards that the PLA could represent an effective alternative to PET, especially in a ecological point of view, as completely biodegradable composites having competitive performances would be made.

In all the cases no noteworthy differences of microstructure between PET composites and PLA composites have been noticed.

Observing the images of the fractured surfaces, it can be inferred that the change of matrix type does not imply substantial differences in the failure behavior. The only relevant aspect consists in the not straight profile of the fractured surfaces of PLA specimens (with the off-axis angle of 30°), and the clear breaking of the PLA specimens (with an off-axis angle of 90°) into two separate pieces.

7.3 FIBER PROPERTIES BACK-CALCULATION

Experimental data of composite mechanical properties were used as base to develop a micro-mechanical model which calculates the effective stiffness and strength of the flax fibers used.

The model considers that the real fiber angle is different with respect to the yarn angle because of the twisting effect. Therefore the off-axis angle of specimens do not represent correctly the fibers inclination in the composite. By means of a geometrical approximated model the differences between the theoretical composite properties, expressed as a function of the fiber angle, and the experimental data were minimized, back calculating the effective properties of flax fibers.

The mean value of the back-calculated flax fiber stiffness was found to be 72 GPa. This is in agreement with the values obtained by previous studies (50-70 GPa). It has been observed that in the case of composites made up by twisted yarns, the back-calculated fiber stiffness deviates from the average stiffness value. More investigations are needed to find a better fitted geometrical model for the twisted yarns.

The mean value of the back-calculated fiber strength was found to be 1700 GPa. It seems to be slightly overestimated since the expected range hypothesized basing on previous studies is 1200-1500 MPa. It is thought that this discrepancies are due to the high sensibility of the model to the twisting angle (experimentally determined by means of microscope analysis) and to the approximation of the geometrical simplified structure of yarns. More investigations are needed to be done, with a high accuracy of the mean twisting angle measurements. A good method might consist in analyzing the twisting angle by means of microscope observation of polished sample surfaces.

It is believed that a substantial improvement of the micro-mechanical method potential could be obtained increasing the number of the geometrical elements used for calculations. The current method is based on 16 geometrical elements, therefore a FEM analysis with an increased number of elements could offer a more precise estimation of fiber properties.

Referring to future studies it could be attempted to prepare sample with off-axis angle slightly lower than 30° in order to get experimental strength data closer to the 0° ideal fiber angle and check if the ultimate strength values result to be less deviated.

REFERENCES

[1] Selin J.F. Oksman K.,. Norwegian University of Science and Technology, Fortum Oil and Gas, Trondheim (Norway), Porvoo (Finland), ch. 10, pp. 150-163.

[2] Robinson R., *The great book of hemp*, Main, Ed. USA: Park Street Press.

[3] Madsen B., *Properties of Plant Fiber Yarn Polymer Composites*. Roskilde, Denmark: Technical University of denmark, 2004.

[4] Anders Thygesen, Hans Lilholt Bo Madsen, "Plant fiber composites- porosity and volumetric interaction," *ScienceDirect*, pp. 1584-1599, 2006.

[5] Marsh G., "Composites that grow in fields," *Reinforced plastics*, pp. 16-22, November 2008.

[6] Sperber V.E. and Faruk O Bledzky A.K., "Natural and wood fiber reinforcement in polymers," *Rapra Review Reports*, vol. 13, no. 8.

[7] Wynne A., *Textiles*. Oxford, 1997.

[8] Perry D.R., "Identification of textile materials," The textile institute, Manchester UK, 1985.

[9] Chate A., Bledzky A.K. Gassan J., "Calculation of elastic properties of natural fibers," *Journal of Material Science*, vol. 36, pp. 3715-3720.

[10] Mark R.E., Hanna R.B. Anagnost S.E., "Variation of microfibril angle within individual tracheids," *Wood and Fiber Science*, vol. 34, pp. 337-349.

[11] Lawther J.M. Lilholt H., "Natural organic fibers," vol. 1, pp. 303-325.

[12] Zhang M.Q., Rong M.Z., Shi G.and Yang G.C. Lu X.,., 2003, pp. 367-379.

[13] Emile S.Greenhalgh, *Failure analysis and fractography of polymer composites*.: CRC Press LLC.

[14] Lilholt Hans Madsen Bo, "Composite materials and fibers," Riso national laboratory for sustainable energy (DTU), Roskilde , 2009.

[15] Schloesser T.P.,. Ulm, Germany: Research Center, ch. 15, pp. 276-283.

[16] http://Ralph-dte.eu,., january 2011.

[17] www.ogigia.com,., January 2011.

[18] http://tangledwing.wordpress.com, *January 2011*.

[19] www.rossignol.com,., January 2011.

[20] www.naturalhomemagazine.com,., January 2011.

[21] www.addax.com,., November 2010.

[22] Munksgaard J., "Garnfremstilling. In Textilbogen ," Hanbog i Textil Varekundskab, Copenaghen (Denmark), 1961.

[23] Macmillan NH. Kelly A., *Strong solids*. Oford, UK: University press, 1986.

[24] Thygesen A., "Properties of hemp fiber polymer composites-an optimization of fiber properties using novel defibration methods and detailed fiber characterization," University, The Royal Veterinary snd Agricultural, 2005.

[25] Lilholt H. Madsen Bo, "Compaction of plant fibers assemblies in relation to compoite fabrication," Sustainable natural and polymeric composites, Riso National Laboratory, Roskilde (Denmark), 2002.

[26] Lilholt H. Toftegaard H., "Effective stiffness and strength of flax fibers derived from short laminates," Sustainable natural and polymeric composites, Riso National and polymeric composites, Roskilde (Denmark), 2002.

[27] Lilholt H. Madsen B, "Physical and mechanical properties of uniodirectional fiber composites-an evaluation of the influence of porosity," Comp Sci Tech, 2003.

[28] Liang E. Tucker CL., "Stiffness prediction for unidirectional short-fiber composites," Comp Sci Tech, 1999.

[29] Thygesen Anders, Lilholt Hans Madsen B., "Porosity and stiffness," Materials Research Division, Biosystems Division, Riso National Laboratory for sustainable energy, Roskilde (Denmark), 2009.

[30] Thomsen A.B., Lilholt H., Thygesen A. Madsen B., "Cellulosic fibers: effect of processing on fiber bundle strength," Biosystem division, Material research division, Riso National

Laboratory for Sustainable Energy, Roskilde (Denmark),.

[31] L.G., Hoffmeyer, P. Thysegen, "Image analysis for the quantification of dislocations in hemp fibers," 2005.

[32] Bilde Sorensen J. Hoffmeyer P Thygesen L.G., "Visualisation od fislocations in hemp fibers: A comparison between scanning electron microscopy (SEM) and polarized light microscopy," 2006.

[33] Van den Oever, M.J.A.,Peters, O.C.J.J. Bos H.L., "Tensile and compressive properties of flax fibers for natural fiber reinforced composites," 2002.

[34] Hoffmeyer P., Lilholt H. Madsen B., "Hemp yarn reinforced composies II Tensile properties," Material Research Department, Department of Civil Engineering, Riso National Laboratory, Technical University of Denmark, Roskilde (Denmark), Lyngby (Denmark),.

[35] Tsai SW. Halpin JC, "Enrironmental factors in composite design," Air Force Materials Laboratory Technical Report, 1967.

[36] Kardos JL. Halpin JC, "The Halpin-Tsai equations," Polym Eng Sci, 1976.

[37] Thomason JL Cichocki FR, "Thermoplastic anisotropy of a natural fiber," Comp Sci Tech, 2002.

[38] Liu TS. Stowell EZ., "On the mechanical behaviour of fiber-reinforced crystalline materials," J Mech Phys Solids, 1961,.

[39] Tsai SW. Azzi VD., "Anisotropic strength of composites," Exp Mech, 195.

[40] Klein W., "The Technology of short-staple spinning 2nd edition," The Textile Institute, Manchester UK,.

[41] Hoffmeyer P., Thomsen A.B., Lilholt H. Madsen B., "Hemp yarn reinforced composites - I Yarn characteristics ," Material Research Department, Department of Civil Engineering, Byosystems Department, Riso National Laboratory, DTU, Roskilde (Denmark), Lyngby (Denmark), 2007.

[42] Hahn H.T. Tsai S.W., "Introduction to composite materials," Technomic Publishing Company, Connecticut USA, 1980.

[43] Barkas W.W, "The swelling of wood under stress. A discussion of its hygroscopic, elastic and plastic properties.," Department of Scientific and Industrial Research, Forest Products Research Laboratory, USA, 1949.

[44] Skaar C., "Wood in wood," Syracuse University Press, New York , 1972.

[45] Siau J.F., "Wood: influence of moisture on physical properties," Department of Wood Science and Forest Products, Virginia Polytechnic Institute and State University USA,.

[46] Chawla K.K, ch. 3, p. 56.

APPENDIX A:MEAN TWISTING ANGLE ESTIMATION

Assuming that the yarns used in this study have been twisted by means of ring spinning process, the twisting angle distribution along the diameter was studied. During the twining operations the fibers, initially parallel to each other, are twisted around the yarn axis make the bundle assume a helical structure. It was found that this operation cause the variation of the twisting angle of a given fiber since it depends on its radial location [9]. Therefore it can be inferred that at the periphery of the yarn the fiber twisting angle is larger than in the inner part. By means on a mathematical demonstration the overall mean fiber angle, indicated as $\theta_{mean,}$ has been found to be only a function of the fiber twisting angle at the yarn surface, indicated as $\theta_{r.}$

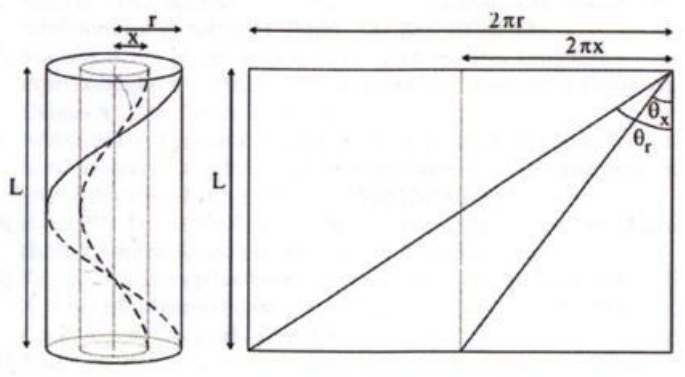

Figure 0.1 Twisted fiber structure in a ring spun yarn.

The basic assumptions of the analytic estimation are the following: [41]

1) The cross section of the yarn is circular
2) The fiber distribution is uniform in the bundle cross section
3) The radial location of a given fiber is fixed therefore it cannot move along the radial direction
4) The twisting fiber patterns are geodetic
5) The length of the fibers in the yarn direction of a single twist (L) doesn't change because all the fibers are concurrently twinned around the bundle axis.

The length of a single twist (L) can be calculated as:

$$L = \left(\frac{\rho_{lf} \pi}{10^7 \rho_f V_f} \right)^{\frac{1}{2}} \frac{2}{\tan \theta_r} \qquad 0.1$$

Where ρ_{lf} is the fiber linear density (tex), ρ_f is the fiber density (g/cm^3), and V_f is the fiber volume fraction.

If the volume fraction is unknown, the following equation can be used:

$$V_f = \frac{\rho_{lf}}{10 \pi r^2 \rho_f} \qquad 0.2$$

Where r represent the yarn radius

Once L has been calculated, the twisting number can be also obtained as 1/L

Basing on the 5th assumption, the twisting angle (θ_x) at a given radial location x can be obtained in the following way:

$$\tan \theta_x = \frac{2\pi x}{L} \Rightarrow \theta_x = \tan^{-1} \frac{2\pi x}{L} \qquad 0.3$$

Multiplying the twisting angle at the given location x with the ratio $2\pi x dx/\pi r^2$,it is possible to obtain the mean angle by the integral equation:

$$\theta_{mean} = \int_0^r \frac{2\pi x}{\pi r^2} \tan^{-1} \frac{2\pi x}{L} dx \qquad 0.4$$

The integral is solved by means of the steps reported in succession:

$$\theta_{mean} = \int_0^r \frac{2\pi x}{\pi r^2} \tan^{-1}\frac{2\pi x}{L} dx = \frac{2}{r^2}\int_0^r x \tan^{-1}\frac{2\pi x}{L} dx \qquad 0.5$$

$$\Rightarrow \theta_{mean} = \frac{2}{r^2}\left(\left[\frac{1}{2}x^2 \tan^{-1}\frac{2\pi x}{L}\right]_0^r - \int_0^r \frac{1}{2}x^2 \frac{1}{1+\left(\frac{2\pi x}{L}\right)^2}\frac{2\pi}{L} dx\right) \qquad 0.6$$

$$\Rightarrow \theta_{mean} = \frac{2}{r^2}\left(\left[\frac{1}{2}x^2 \tan^{-1}\frac{2\pi x}{L}\right]_0^r - \int_0^r \frac{x^2 L\pi}{L^2 + 4\pi^2 x^2} dx\right) \qquad 0.7$$

$$\Rightarrow \theta_{mean} = \frac{2}{r^2}\left(\left[\frac{1}{2}x^2 \tan^{-1}\frac{2\pi x}{L}\right]_0^r - \frac{L\pi}{4\pi^2}\int_0^r \frac{x^2}{\frac{L^2}{4\pi^2} + x}\right) \qquad 0.8$$

$$\Rightarrow \theta_{mean} = \frac{2}{r^2}\left(\left[\frac{1}{2}x^2 \tan^{-1}\frac{2\pi x}{L}\right]_0^r - \frac{L}{4\pi}\left[x - \frac{L}{2\pi}\tan^{-1}\frac{2\pi x}{L}\right]_0^r\right) \qquad 0.9$$

$$\Rightarrow \theta_{mean} = \frac{2}{r^2}\left(\left[\frac{1}{2}x^2 \tan^{-1}\frac{2\pi x}{L}\right]_0^r - \frac{L}{4\pi}\left[x - \frac{L}{2\pi}\tan^{-1}\frac{2\pi x}{L}\right]_0^r\right) \qquad 0.10$$

$$\Rightarrow \theta_{mean} = \frac{2}{r^2}\left(\frac{1}{2}r^2 \tan^{-1}\frac{2\pi r}{L} - \left(\frac{L}{4\pi}\left(r - \frac{L}{2\pi}\tan^{-1}\frac{2\pi r}{L}\right)\right)\right) \qquad 0.11$$

$$\Rightarrow \theta_{mean} = \tan^{-1}\frac{2\pi r}{L} - \frac{L}{2\pi r} + \frac{L^2}{4\pi^2 r^2}\tan^{-1}\frac{2\pi r}{L} \qquad 0.12$$

The following equations are used as support in resolution of the last equation.

$$\frac{d}{dx}\tan^{-1} u = \frac{1}{1+u^2}\frac{du}{dx} \qquad 0.13$$

$$\int \frac{x^2}{x^2+a^2}dx = x - a\tan^{-1}\frac{x}{a} \qquad 0.14$$

If equation 0.3 is inserted in the last formula it is possible to eliminate the parameters L and r, demonstrating how the mean angle is only function of the angle at the periphery of the yarn.

$$\theta_{mean} = \theta_r + \frac{\theta_r}{\tan^2\theta_r} - \frac{1}{\tan\theta_r} \qquad 0.15$$

APPENDIX B: FICKIAN MODEL AND RESULTS

To make it possible to assess water adsorption behavior of the made composites, the Fickian diffusion model was used since it's suitable for samples having low ratio between thickness and the planar dimensions (length and width). The model predicts the degree of water saturation as a function of time and assumes that the water diffusion occurs only in a single direction. The basic equation is the following:

$$\frac{U_{RH}(t)}{U_{RH}} = 1 - \frac{8}{\pi^2}\sum_{i=0}^{\infty}\frac{1}{(2i+1)^2}\exp\left(-\frac{(2i+1)^2\pi^2 Dt}{(2d)^2}\right) \qquad 0.1$$

where $U_{RH(t)}$ and U_{RH} represent respectively the unsatured water content as a function of time and the satured water content in equilibrium with the surroundings, the parameter D is the diffusion coefficient (m^2/s) whereas the parameter d represents the diffusion distance (m) therefore it is assumed to be half the sheet thickness. All the samples have been put in a climate chamber having a temperature of 23°C and have been weighed regularly with intervals of about one day.

The relative water content U(t) was calculated with the following formula:

$$U(t) = \frac{m(t) - m_0}{m_0}100 \qquad 0.2$$

where m(t) is the specimen weight at time t and m_o is the initial specimen weight.

Since the diffusion coefficient is typically the only unknown parameter, it can be adjusted to fit the model to the experimental data. However in this study it was estimated choosing two corresponding values of U(t) and time t in the initial linear region in the following way [42]:

$$D = \frac{\pi}{16}\left(\frac{U(t_2) - U(t_1)}{\sqrt{t_2} - \sqrt{t_1}}\right)^2 \frac{(2d)^2}{U_{RH}{}^2} \qquad 0.3$$

Once the coefficient diffusion had been calculated, and the satured water content at equilibrium condition had been read as asymptotic trend of experimental data plot, the unsatured water content was estimated using equation 0.1.

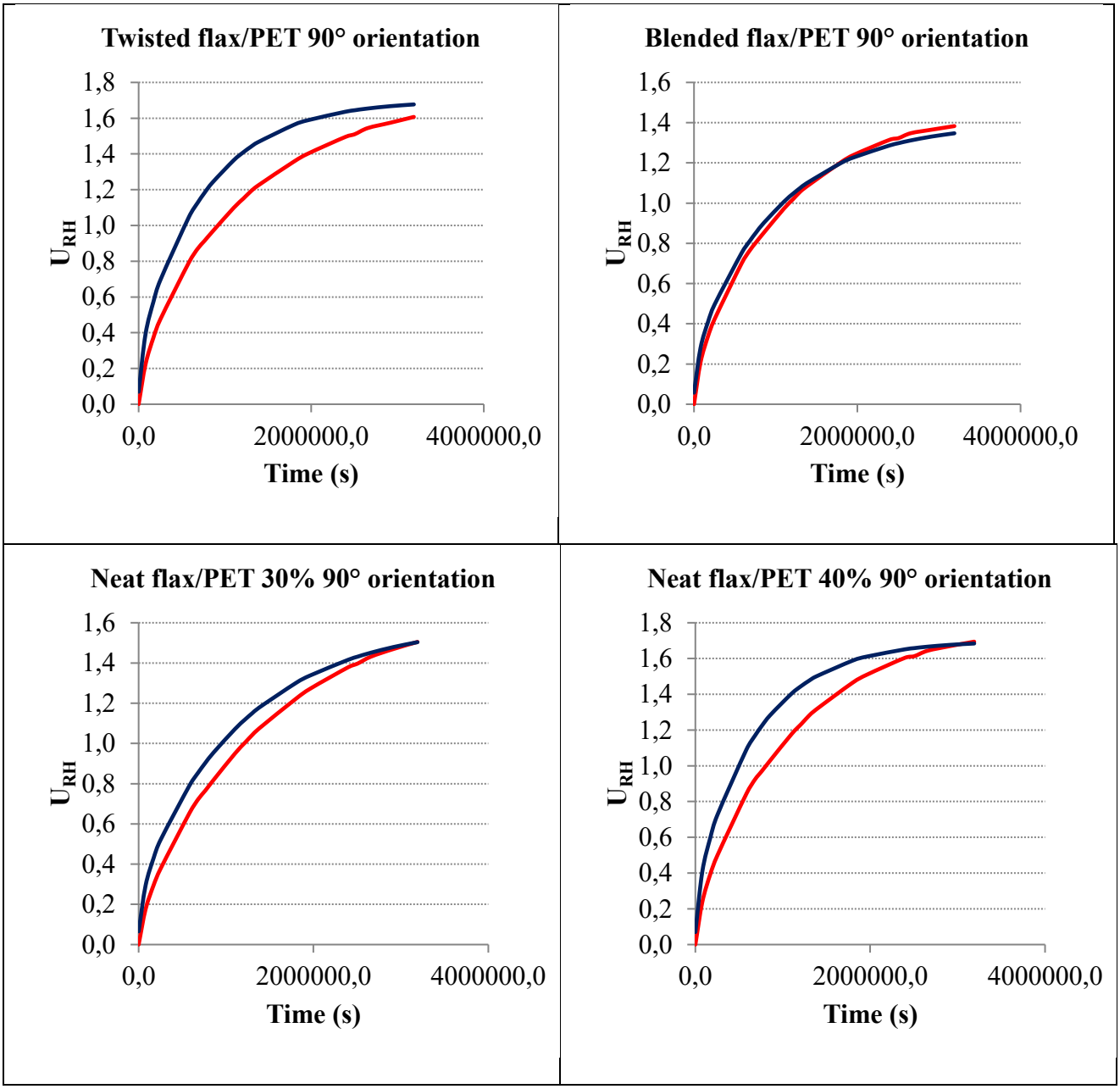

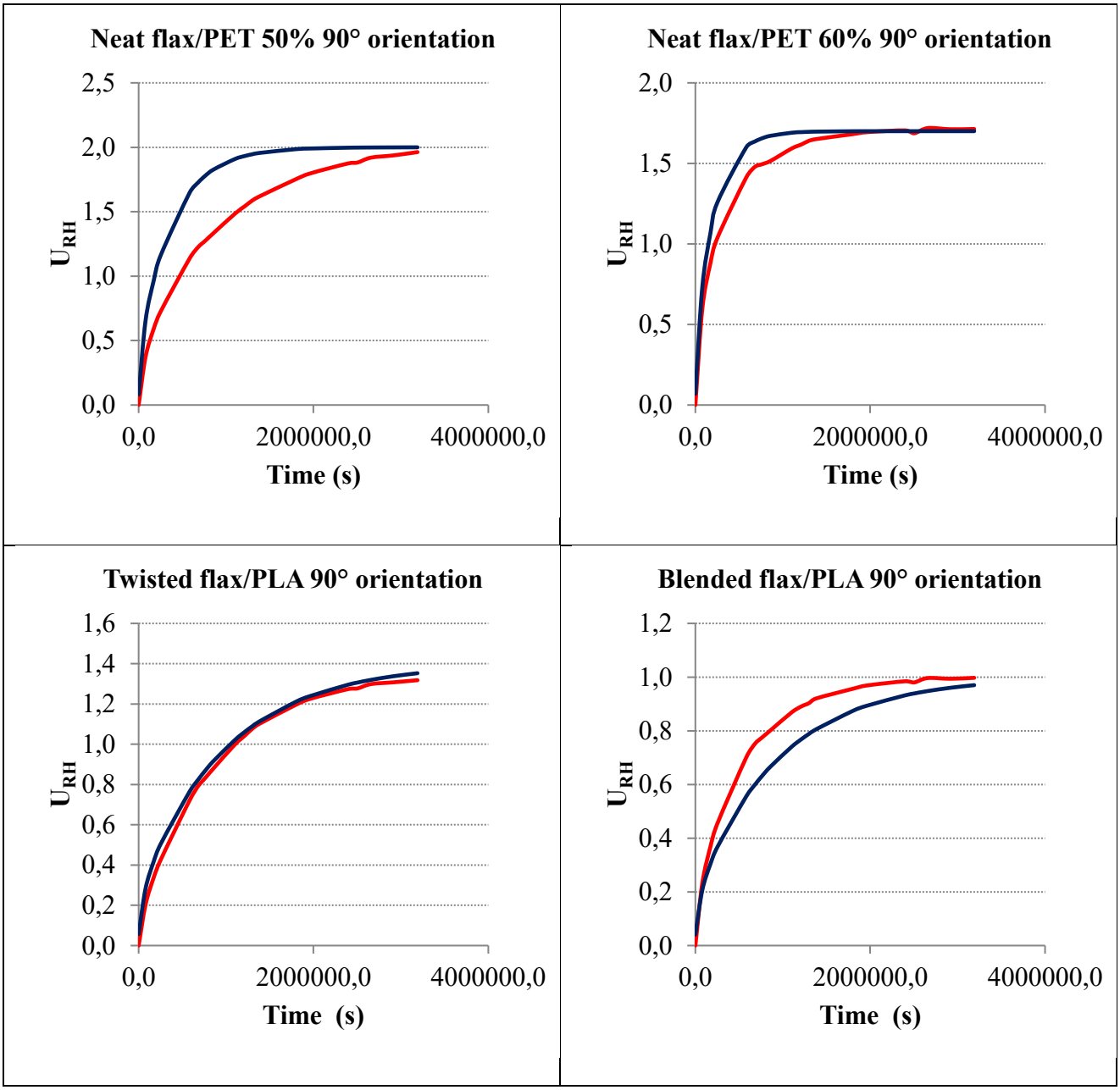
Neat flax/PET 50% 90° orientation
2,5
2,0
1,5
1,0
0,5
0,0
U_{RH}
0,0
2000000,0
4000000,0
Time (s)
Neat flax/PET 60% 90° orientation
2,0
1,5
1,0
0,5
0,0
U_{RH}
0,0
2000000,0
4000000,0
Time (s)
Twisted flax/PLA 90° orientation
1,6
1,4
1,2
1,0
0,8
0,6
0,4
0,2
0,0
U_{RH}
0,0
2000000,0
4000000,0
Time (s)
Blended flax/PLA 90° orientation
1,2
1,0
0,8
0,6
0,4
0,2
0,0
U_{RH}
0,0
2000000,0
4000000,0
Time (s)

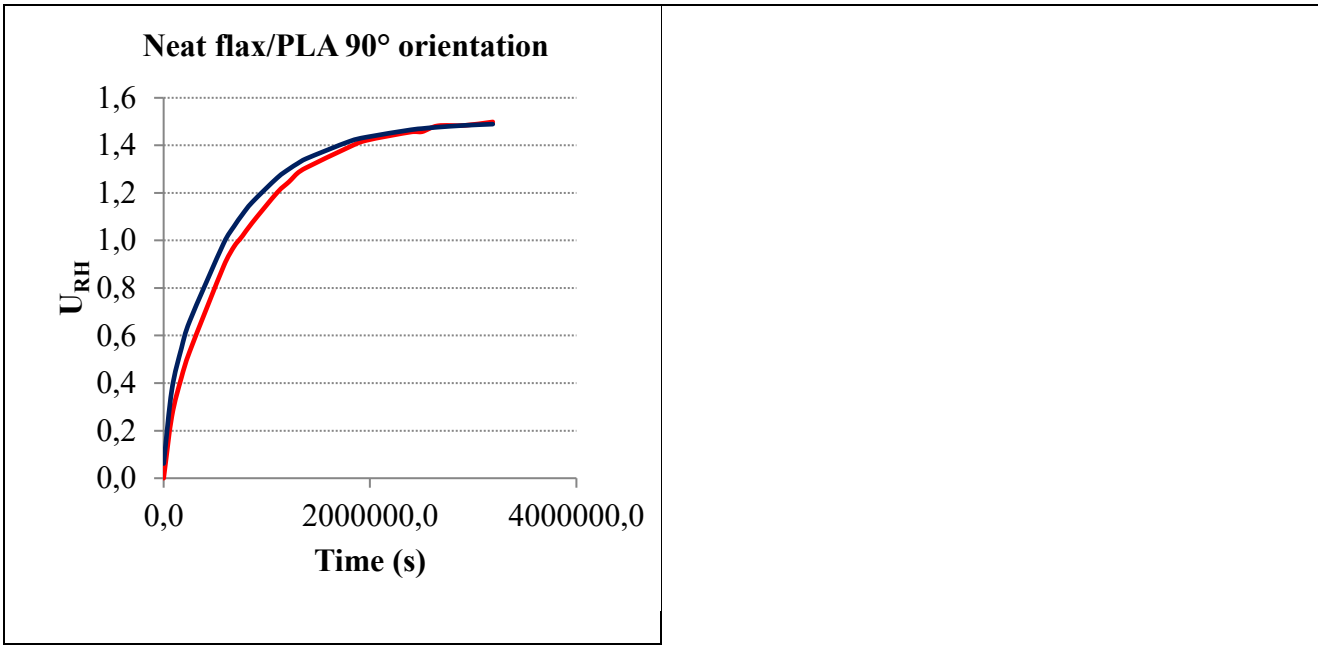

Figure 0.1 Trends of experimental data (red lines) and model estimation (blue lines) for 90° yarn orientation.

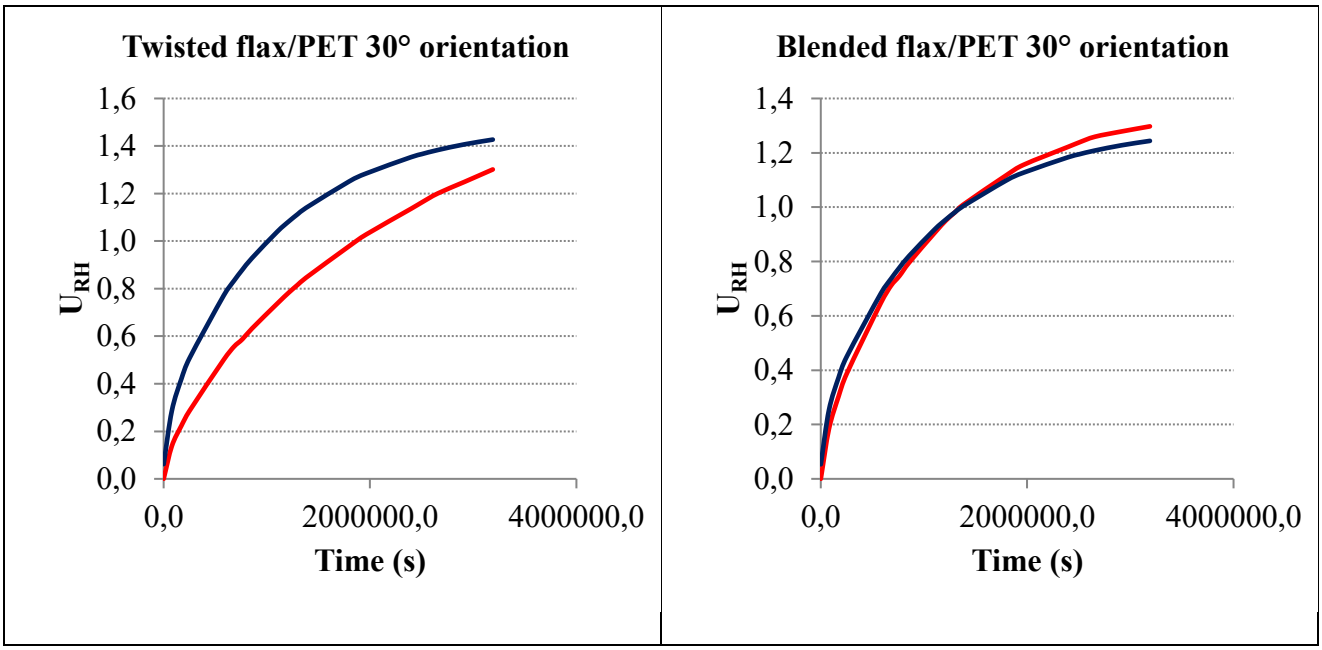

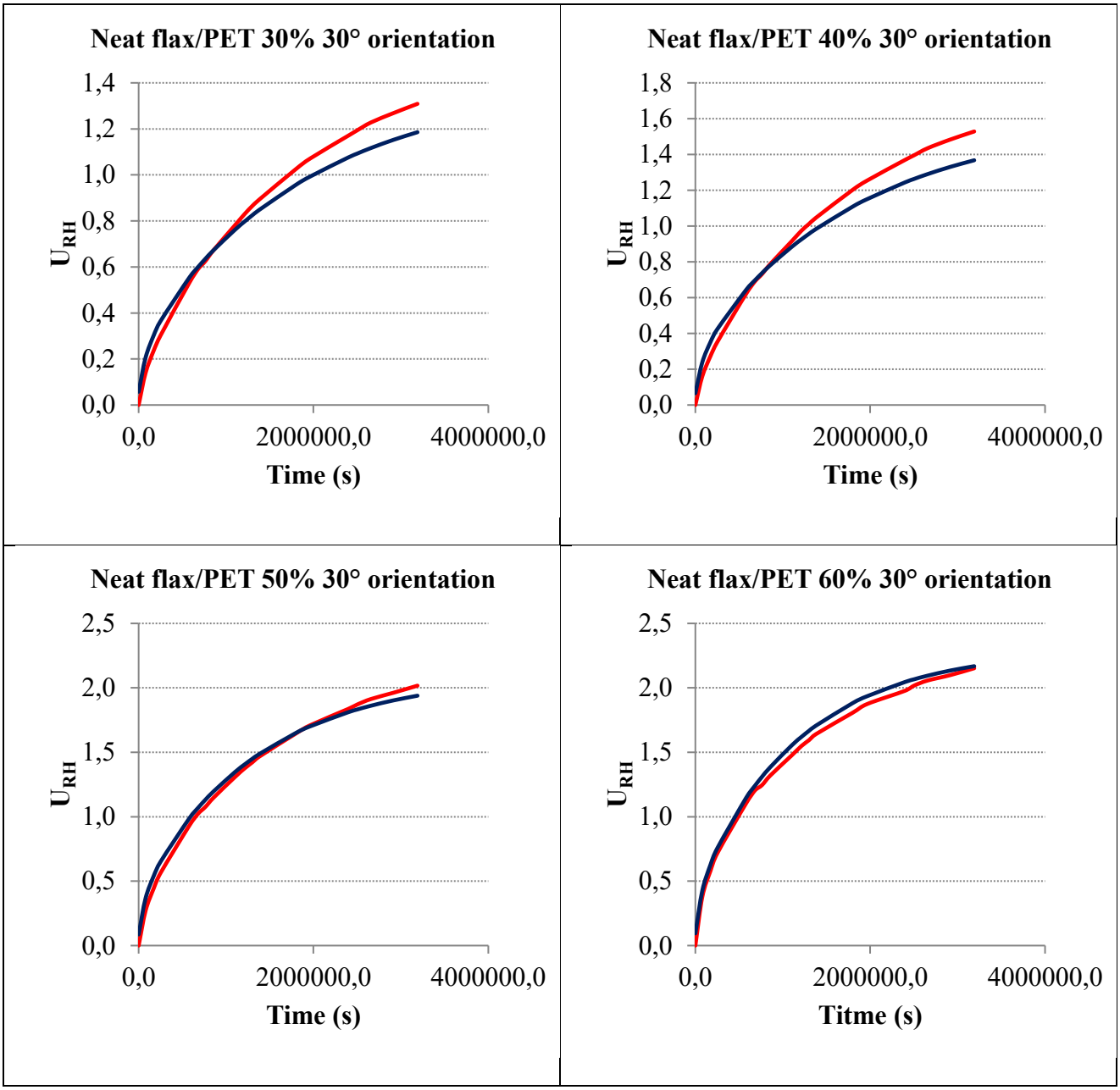
Neat flax/PET 30% 30° orientation
1,4
1,2
1,0
0,8
0,6
0,4
0,2
0,0
U_RH
0,0
2000000,0
4000000,0
Time (s)
Neat flax/PET 40% 30° orientation
1,8
1,6
1,4
1,2
1,0
0,8
0,6
0,4
0,2
0,0
U_RH
0,0
2000000,0
4000000,0
Time (s)
Neat flax/PET 50% 30° orientation
2,5
2,0
1,5
1,0
0,5
0,0
U_RH
0,0
2000000,0
4000000,0
Time (s)
Neat flax/PET 60% 30° orientation
2,5
2,0
1,5
1,0
0,5
0,0
U_RH
0,0
2000000,0
4000000,0
Titme (s)

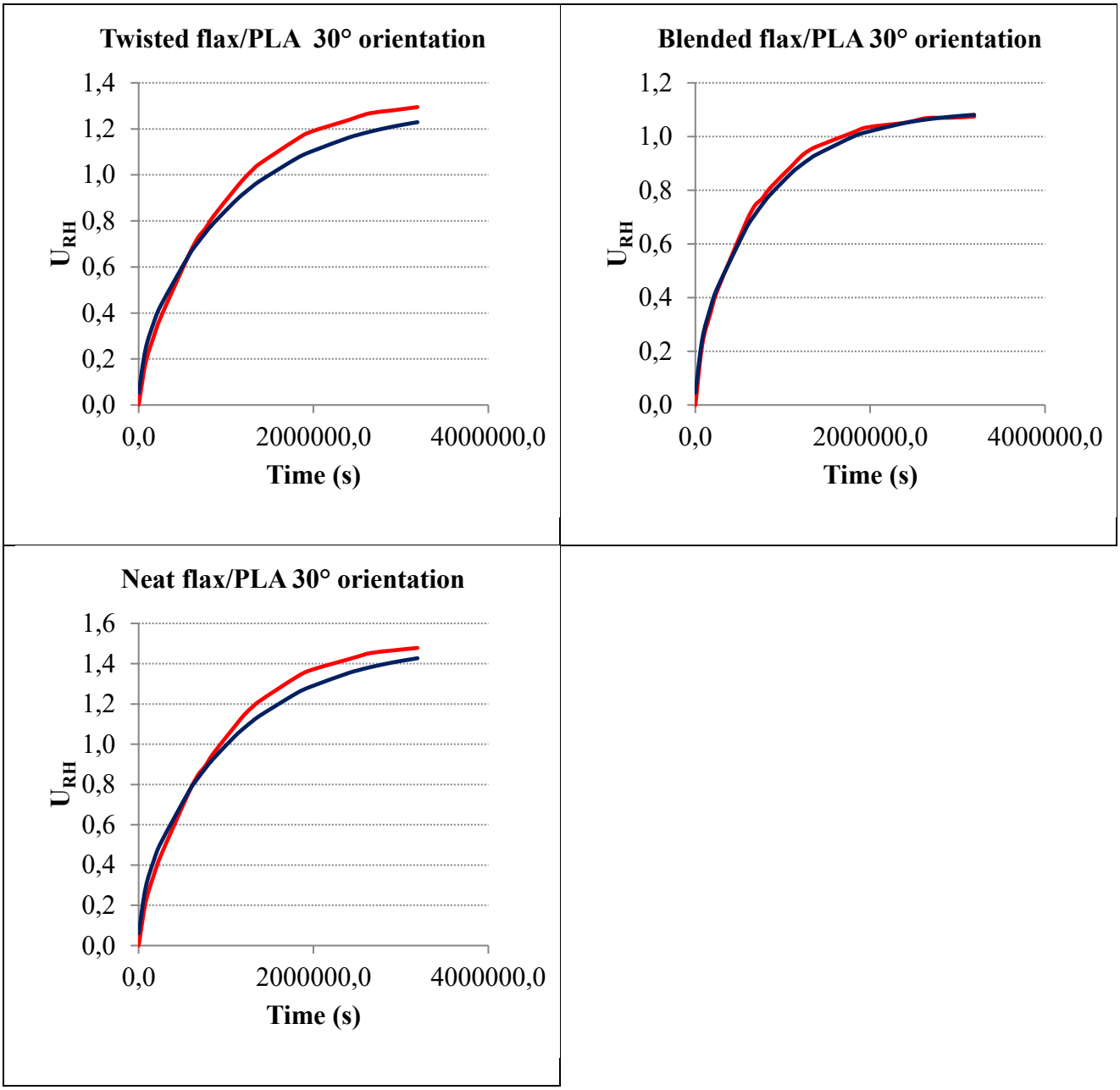

Figure 0.2 Trends of experimental data (red lines) and model estimation (blue lines) for 30° yarn orientation.

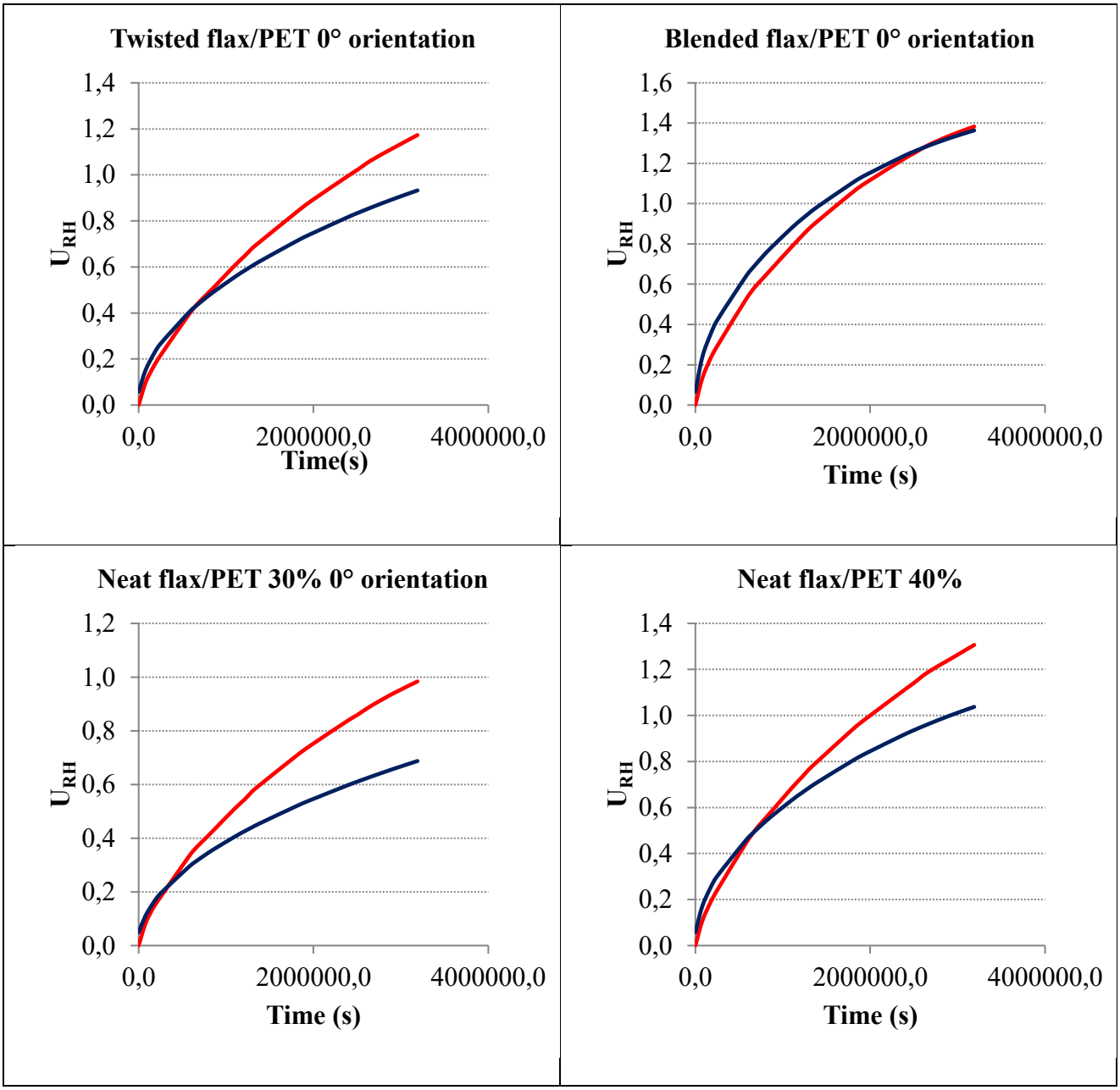
Twisted flax/PET 0° orientation
1,4
1,2
1,0
0,8
0,6
0,4
0,2
0,0
U_RH
0,0
2000000,0
4000000,0
Time(s)
Blended flax/PET 0° orientation
1,6
1,4
1,2
1,0
0,8
0,6
0,4
0,2
0,0
U_RH
0,0
2000000,0
4000000,0
Time (s)
Neat flax/PET 30% 0° orientation
1,2
1,0
0,8
0,6
0,4
0,2
0,0
U_RH
0,0
2000000,0
4000000,0
Time (s)
Neat flax/PET 40%
1,4
1,2
1,0
0,8
0,6
0,4
0,2
0,0
U_RH
0,0
2000000,0
4000000,0
Time (s)

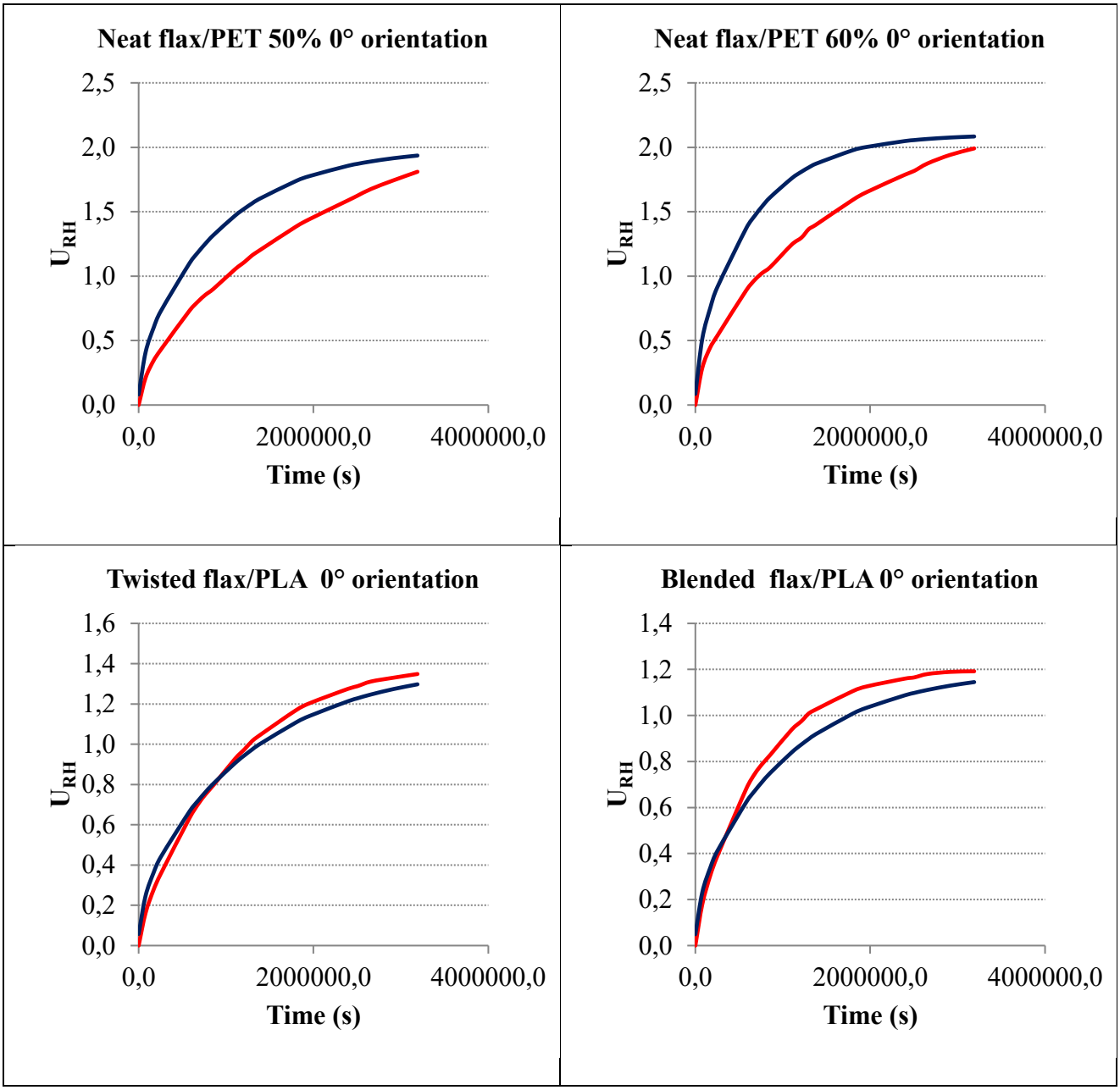
Neat flax/PET 50% 0° orientation
2,5
2,0
1,5
1,0
0,5
0,0
U_RH
0,0
2000000,0
4000000,0
Time (s)
Neat flax/PET 60% 0° orientation
2,5
2,0
1,5
1,0
0,5
0,0
U_RH
0,0
2000000,0
4000000,0
Time (s)
Twisted flax/PLA 0° orientation
1,6
1,4
1,2
1,0
0,8
0,6
0,4
0,2
0,0
U_RH
0,0
2000000,0
4000000,0
Time (s)
Blended flax/PLA 0° orientation
1,4
1,2
1,0
0,8
0,6
0,4
0,2
0,0
U_RH
0,0
2000000,0
4000000,0
Time (s)

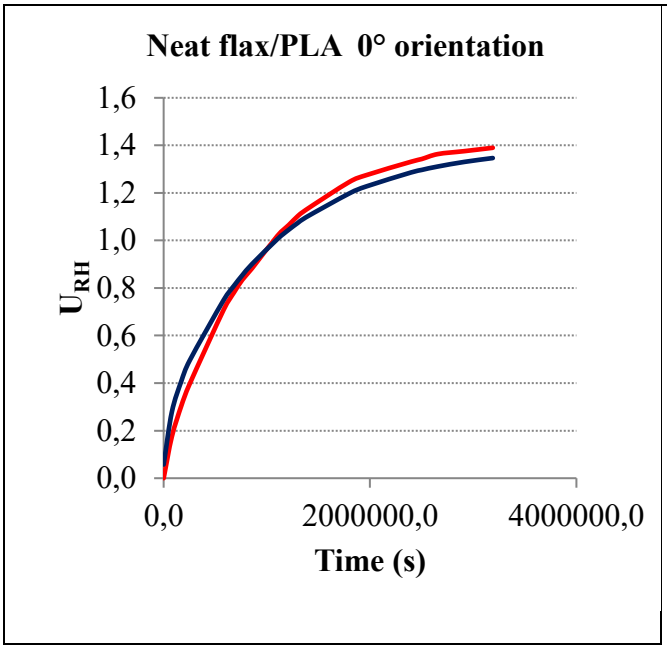

Figure 0.3 Trends of experimental data (red lines) and model estimation (blue lines) for 0° yarn orientation.

Type of composite	Orientation	Diffusion coefficient	Orientation	Diffusion coefficient	Orientation	Diffusion coefficient
	(degrees)	(m^2/s)	(degrees)	(m^2/s)	(degrees)	(m^2/s)
Twisted flax/PET	0	1.76E-13	30	2.42E-13	90	8.11E-13
Blended flax/PET	0	3.38E-13	30	5.82E-13	90	6.08E-13
Neat flax/PET 30%	0	1.27E-13	30	3.30E-13	90	5.15E-13
Neat flax/PET 40%	0	2.26E-13	30	3.41E-13	90	8.83E-13
Neat flax/PET 50%	0	6.41E-13	30	4.68E-13	90	1.65E-12
Neat flax/PET 60%	0	9.23E-13	30	5.25E-13	90	2.85E-12
Twisted flax/PLA	0	4.77E-13	30	5.35E-13	90	6.30E-13
Blended flax/PLA	0	5.70E-13	30	7.65E-13	90	6.54E-13
Neat flax/PLA 40%	0	6.06E-13	30	5.58E-13	90	9.41E-13

Table 0.1 List of diffusion coefficients for all the composites.

Observing Table 0.1 it can clearly noted the general trend that the higher is the orientation angle, the higher is the diffusion coefficient, thus the faster is the moisture absorption. It is believed that this is due to the variation of fiber length within the different type of samples. In fact the humidity requires more time to diffuse along the fibers of the 0° specimens, rather than along the width of the 90° specimens, where the fiber length is lower. Therefore it can be inferred that the type of diffusion is function of the yarns orientation within the samples, as it is shown by the overall trend of the charts. It has been also seen that for a given angle the diffusion coefficient increases depending on the fiber volume fractions. Analyzing the neat flax/PET composites this trend is particularly evident with the 0° and 30° cases, whereas it is no possible to individuate it in the 90° case, since values are not clearly ordered.